VERLAG DER TECHNISCHEN UNIVERSITÄT GRAZ

Matthias Landgraf

Smart data for sustainable Railway Asset Management

Railway Track: Assessment - Aggregation - Asset Management

RR 3

MONOGRAPHIC SERIES TU GRAZ
RAILWAY RESEARCH

Matthias Landgraf

Smart data for sustainable Railway Asset Management

Railway Track: Assessment - Aggregation - Asset Management

Monographic Series TU Graz

Railway Research RR

Series Editor

Univ.-Prof. Dipl.-Ing. Dr.techn. Peter Veit

Monographic Series TU Graz

Railway Research **Volume 3**

Matthias Landgraf

Smart data for sustainable Railway Asset Management

Railway Track: Assessment - Aggregation - Asset Management

This work is based on the PhD thesis “Zustandsbeschreibung des Fahrwegs der Eisenbahn - Von der Messdatenanalyse zum Anlagenmanagement”, presented at Graz University of Technology; submitted to the Faculty of Civil Engineering, in 2016
Assessor A (internal) Peter Veit (Graz University of Technology)
Assessor B (external) Stephan Freudenstein (Technische Universität München)

© 2018 Verlag der Technischen Universität Graz

Cover photo	Stefan Marschnig
Layout	Christina Fraueneder, TU Graz
	Stefan Schleich, TU Graz
Print	Medienfabrik Graz | mfg.at

Verlag der Technischen Universität Graz
www.ub.tugraz.at/Verlag

Print
ISBN 978-3-85125-569-0

E-Book
ISBN 978-3-85125-570-6
DOI 10.3217/978-3-85125-569-0

https://creativecommons.org/licenses/by/4.0/

Vorwort zur Schriftenreihe
Railway Research

Das Institut für Eisenbahnwesen und Verkehrswirtschaft der Technischen Universität Graz beschäftigt sich als Institut der Fakultät für Bauingenieurwissenschaften mit der Eisenbahninfrastruktur, und zwar den bautechnischen Fragen des Errichtens des Fahrwegs, des Betrieb der Strecken und damit eng verknüpft seiner Wartung und Instandsetzung. Damit sind sämtliche für eine Betrachtung des gesamten Lebenszyklus der Infrastruktur erforderlichen Bausteine abgedeckt.
Das Einbeziehen wirtschaftlicher Bewertungen der Lebenszyklen erlaubt den Schwerpunkt „Nachhaltigkeit" umfassend in technischer, betrieblicher und wirtschaftlicher Sicht abzudecken.
Die Forschungsfragen betreffen dabei das Gleislageverhalten, mit der Zielsetzung dieses prognostizierbar zu machen und damit die Voraussetzung für präventive Instandhaltung zu schaffen.
Die Forschung des Instituts in betrieblicher Hinsicht umfasst Fahrplangestaltung und eine auf Nachfrageprognosen aufbauende Netzentwicklung sowie Auswirkungen unterschiedlicher Verfügbarkeiten. Alle diese Themen werden im Forschungsbereich Life Cycle Management einer umfassenden wirtschaftlichen Bewertung zugeführt.
Mit diesem Ansatz versucht das Institut für Eisenbahnwesen und Verkehrswirtschaft seinem Anspruch das System Eisenbahn in Forschung und Lehre zu vertreten gerecht zu werden.

Smart Data for Sustainable Railway Asset Management
Durch die Digitalisierung des Fahrwegs der Eisenbahn steht eine wachsende Menge an Daten zur Verfügung. Messdaten stellen für sich jedoch keine Information dar, sie sind Momentaufnahmen und somit für das Asset Management kaum verwendbar. Präventive Instandhaltung erfordert Trendanalysen. Im Band 2 dieser Schriftenreihe wurde bereits die zwischen 2011 und 2014 entwickelte Fraktalanalyse der vertikalen Gleisgeometrie vorgestellt. Der aktuellen Band beschreibt die notwendigen Schritte diese Analyse im Anlagenmanagement anzuwenden. Dazu gehören Validierung und Definition von Grenzwerten. Validierung stützt sich auf netzweite und spezifische Vergleiche mit bestehenden Verfahren. Die Korrelation dieser Ergebnisse und das Analysieren älterer Messdaten erlauben Trendanalysen und damit die Festlegung von Grenzwerten. Die Prognosefähigkeit der Entwicklung der Schotterbettverschmutzung und des Unterbaus zu einem sehr frühen Zeitpunkt der Fehlerentwicklung konnte nachgewiesen werden. Damit ist ein spezifisches Eingreifen frühzeitig und somit kostengünstig möglich. Die Bedeutung dieses Ergebnisses ist besonders hervorzuheben, da für diese Bereiche derzeit noch keine (netzweiten) Daten zur Verfügung stehen, obwohl die Lebenszyklus-kosten massiv von Unterbau und Schotter determiniert werden.

Peter Veit

Preface

First and foremost, I would like to express my sincerest gratitude to my wife Marie and my family for their untiring support, love and motivation. I would like to thank you above all for your understanding in those times, when I was composing this work and carrying out the research and projects linked to it instead of being at home.

I would like to thank Peter Veit, Stefan Marschnig and all my colleagues at the institute for all their help and support. Because of you, our university is such a great place to work. Our long, productive and sometimes challenging discussions were of great value to my research.

Furthermore, I want to thank my project partners all over the world, especially the ones from Austrian and Swiss Federal Railways. The validation and application of my research would not have been possible without our fruitful collaboration.

Abstract

Cost pressure forces infrastructure managers to work sustainably and efficiently. Therefore, track engineers face increasing difficulty to carry out necessary measures owing to budget restrictions. Consequently, they should be supported in prioritising. This requires an objective tool enabling proper condition monitoring as well as component-specific, preventive maintenance and renewal planning. Hence, the right measures are to be executed at the right time.

This dissertation deals with a description of the railway track condition. A bottom-up approach provides an in-depth assessment of track using a variety of measurement signals and an aggregated component-specific assessment. Since the approach is based on well positioned measurement signals, it is valid for monitoring specific track sections as well as whole networks. Innovative analyses of various measurement signals form a sound basis to grasp their characteristics enabling a component specific condition evaluation of railway track. The use of historical measurement data allows for an analysis of track behaviour over time. A thorough validation process, including on-site inspections and excavations, shows that the presented approach is able to evaluate the actual condition of railway track.

The assessment of the specific components condition can be used for timely maintenance as well as renewal planning. Based on correlation analyses, the component specific evaluations are aggregated into one holistic quality figure. This enables asset managers to monitor the asset condition network-wide as well as to predict future budget demands.

Kurzfassung

Anlagenmanagement für Eisenbahninfrastrukturunternehmen bedeutet, möglichst effizient mit immer knapper werdenden budgetären Ressourcen umzugehen. Dementsprechend essentiell gestaltet sich die Fragestellung nach dem Zustand der zu verwaltenden Anlagen.

Die hier entwickelte Methodik ermöglicht eine messdatengestützte und komponentenspezifische Zustandsbeschreibung des Eisenbahnfahrwegs. Aufgrund der Evaluierung der Komponenten Schwelle und Schotter kann eine notwendige Gleiserneuerungsmenge ermittelt werden. Die Komponentenbeurteilung des Unterbaus erlaubt darüber hinaus, bereits frühzeitig jenen Anteil der Reinvestitionsmaßnahmen abzuschätzen, welcher zusätzlich einer Unterbausanierung bedarf. Darauf basierend kann eine langfristige Planung des Mitteleinsatzes etabliert werden. Die erarbeitete Methodik ermöglicht dem Infrastrukturbetreiber die Evaluierung des Netzzustandes, wobei die Auswirkungen unterschiedlicher Investitionsstrategien analysiert werden können.

Verwendet werden dabei vorrangig Anlageninformationen und Messdaten, welche in einer an der TU Graz entwickelten Datenbank für rund 4000 Streckenkilometer der Österreichischen Bundesbahnen mit Zeitreihen seit 2001 vorliegen. Des Weiteren konnten auch vereinzelte Streckenabschnitte aus der Schweiz sowie den USA für Korrelationsanalysen herangezogen werden.

Die Erarbeitung der vorgestellten Methodik beinhaltet in einem ersten Schritt die Erarbeitung innovativer Messparameter. Diese werden aus verschiedenen Roh-Messsignalen sowie unterschiedlichen Messsystemen gewonnen, um die Charakteristika einzelner Signale besser fassen zu können. Jene Parameter werden einem eingehenden Validierungsprozess unterzogen. Anschließend wird diese Vielzahl an automatisiert messbaren Parametern fundiert zu je einer Zustandszahl für die Komponenten Schwelle, Schotter und Unterbau aggregiert.

Darüber hinaus wird im Rahmen der Arbeit aufgezeigt, welchen Nutzen die vorgestellte Methodik für das Anlagenmanagement eines Eisenbahninfrastrukturbetreibers bringen kann. Einerseits im Rahmen einer netzweiten, gebiets-, strecken- oder querschnittspezifischen Zustandsbeschreibung, welche die vergangene sowie zukünftige Entwicklung des Streckennetzes beschreibt. Andererseits wird es ermöglicht, komponentenspezifische Instandhaltungsmaßnahmen sowie benötigte Erneuerungsmengen zu definieren.

Table of Contents

1 Introduction

The operation of railway infrastructure requires major capital investment. ÖBB Infrastruktur AG, for instance, invested 611.4 million euros in renewal and expansion and 493.3 million euros in maintenance of their assets in 2014 alone [ÖBB Infrastruktur AG 2015]. An essential part of the duties of a railway infrastructure manager is establishing a balanced maintenance and reinvestment strategy, as well as the related efficient use of tied capital. This is to mitigate potential safety risks, as well as to ensure compliance with availability targets and handle the ever-increasing cost pressures. This area of responsibility is summarised by the phrase *asset management*.

The focus of the present work is on the management of the asset track. The key parameters for asset management are capacity, residual value and quality/condition of the assets (Figure 1). These three parameters have significant mutual interplay, particularly when it comes to railway infrastructure.

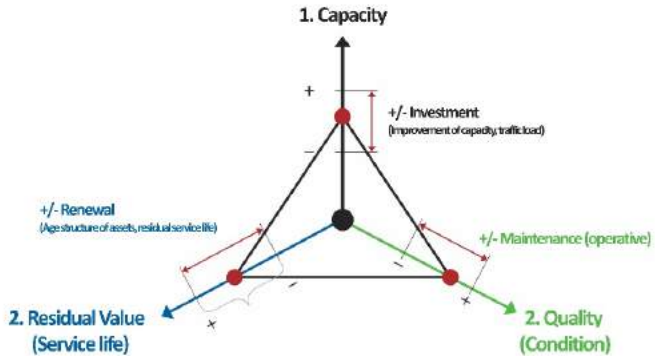

Figure 1 Key parameters of asset management [according to Balfour Beatty Rail 2010]

In particular, the term capacity describes the current performance of assets, which is largely a function of their availability. The latter is determined by the quality or condition of the asset. Quality refers to the deviation of the asset condition from its optimal initial quality. Once the deviation exceeds a predefined limit, maintenance activities are required to reinstate the quality of the asset to the target condition. The availability of the asset is reduced by maintenance works, since the track cannot be used for operations during such works, or only at reduced speed. However, if maintenance works are omitted or performed too late, the speed on the track section is reduced for a longer period. If this measure also proves insufficient to ensure safe railway operation, the section may even be closed pending adequate reinstatement. Since such measures have significant adverse effects on availability, the following requirement for asset management follows: Maintenance and repair works are to be conducted as rarely and as late as possible, but with sufficient frequency to ensure adequate and sustainable quality levels.

However, capacity may also refer to future required performance capabilities, requiring construction of adequately dimensioned assets. The dimensioning or rather the design of the assets affects the parameter of residual value in two ways: On the one hand, systems are generally (expected) to have a longer service life with higher initial build quality. On the other hand, however, the assets are subject to more wear and tear with increasing loads; in rail transport, this is mainly a function of the type, number and weight of trains.

Finally, the parameters of quality and residual value are subject to certain essential dependencies. In principle, the residual value of an asset may be estimated at the beginning of its service life, provided that the estimate is based on sound knowledge of the asset in question. In this context, however, it is vital to discern the defining boundary conditions for the assets, such as build materials, anticipated loads and topographic features. In the scope of railway infrastructure asset management, strategic expected useful lives are determined for this purpose (see 2.2). These estimates are based on the average behaviour of all track sections subject to the same boundary conditions within a network. However, individual sections may display strongly diverging behaviour; it is thus essential to consider the current quality of the individual sections. Poor quality in recent assets automatically implies a reduced expected service life (residual value), whereas individual cases of excellent quality in older assets compared to the average expectation indicate markedly improved residual value. Moreover, the adequate capture of the current condition (quality) is the only means for establishing a sustainable maintenance regime, which ensures the highest possible service life of the built asset.

Establishing an automated condition monitoring of the quality of railway infrastructure is a further aim of the present work. The goal is to formulate a component-specific evaluation

of the condition, which could make a significant contribution to maintenance and renewal planning for railway infrastructure. Furthermore, the work strives to link the above-mentioned notions of residual value and quality (Figure 1) to enable a condition evaluation of the "substantial quality" based on measured data. This is partly to ensure a description of current quality, but also to facilitate estimates of the residual service life of individual components.

Objectives and approach

The main objective of this research thus lies in detecting the actual wear of railway infrastructure components, namely those of relevance for renewal measures, and thus the residual value: sleeper, ballast and substructure (see 2.1). In addition to the component-specific condition evaluation, a holistic quality figure is also to be developed as a descriptor for the infrastructure, which, even though being of limited informative value, may be of use for network-wide comparisons and developments. The achievement of these objectives requires treatment of a wide range of issues. The following issues thus pave the way to the goal, as well as forming the basis of the present research.

- Does measurement data analysis theoretically permit detection of the condition of individual components from existing, automated and measured signals? (See Chapter 3)
- Are the individual formulated methods of condition evaluation capable of recognising the real condition of the parameters under evaluation? (See Chapter 4)
- Do these detection methods, with their specific characteristics, produce a consistent condition evaluation for the individual infrastructure components? (See Chapter 5)
- Is the establishment of a component-specific condition evaluation feasible on the basis of the assessed detection types or rather novel methods of analysis? (See Section 6.2)
- Is the aggregation of this component-specific condition evaluation sense into holistic quality figures for the infrastructure (excl. rails) feasible? (See Section 6.2.4)
- (How) could such a condition evaluation be sensibly applied in railway infrastructure asset management? (See Chapter 7)

Answering the above questions requires in-depth analysis of measured data, as well as the formulation of innovative statistical figures to develop a better understanding of the characteristics of the measured data. The evaluation parameters thus established are then validated and cross-correlated. Both component-specific and holistic quality figures for the infrastructure will then be aggregated on the basis of the information derived in this manner (Figure 2).

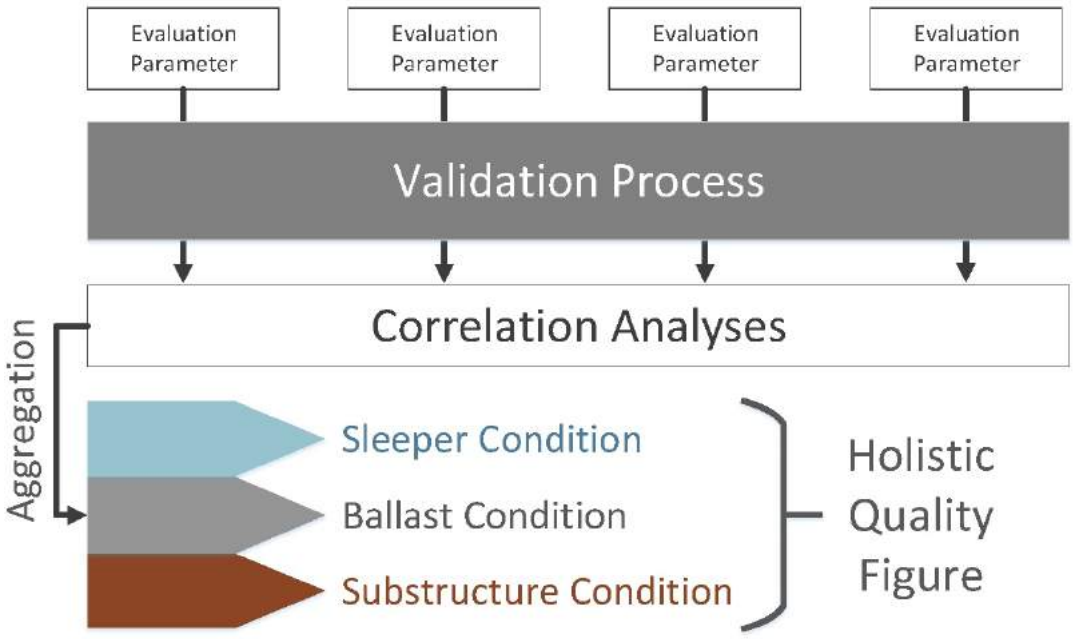

Figure 2 Approach

2

Railway Infrastructure – Foundations and Documentation

Railway infrastructure is characterised by special boundary conditions, since the transfer of loads takes place by way of a range of components, which are subject to significant reciprocal effects. Moreover, the required load transfer is always (and mainly negatively) affected by external boundary conditions. This renders the documentation of the widest possible range of such conditions all the more necessary, along with ensuring evaluation of the condition of the assets by objective and automated measurements.

1.1 The components of railway infrastructure

The above-mentioned load transfer is based on the principle of transferring the major wheel loads, which are applied point by point to the subsoil via a widening surface. At the contact point between wheel and rail, a force of approximately 30,000 N/cm² is applied on a surface of approximately 3 cm² (Hertz area). This force ultimately is to be distributed to around 10,000 cm² at the track substructure level by way of an optimised railway configuration, thereby reducing it to around 6 N/cm². The principal components in this context are the rails, sleeper and ballast. The uppermost layer of the subsoil must be frequently processed to prevent overloading; the substructure component is thus an important element in the load transfer [Kohler 2002].

The present research is concerned with the condition evaluation of these components, with the exception of the rail. The necessary delimitation of the research topic aside, this is

owed to the fact that this component, in spite of being responsible for a substantial portion of the maintenance budget, seldom triggers track renewal measures due to its condition. Furthermore, damage to the rail, such as surface defects and wear, can be considered as more or less isolated from the overall system, since the rails can typically be replaced independently of the rest of the system. A more detailed assessment of this interaction is only necessary in cases of increased loads caused by the condition of the rail surface (eg. rail contact fatigue). Due to this fact measured signals relating to the component rail are not taken into account within this work.

1.2 Documentation and storage of asset information

On the one hand, measurement data is delivering an increasingly precise description of track behaviour; on the other, the demands on data management are growing proportionally. For this reason, the TUG database [Holzfeind & Hummitzsch 2008] was developed in close cooperation between the Austrian Federal Railways (ÖBB) and the Institute of Railway Engineering and Transport Economy (TU Graz) (Figure 3). All available information for cross-sections every five metres is linked therein. The coverage extends to around 4,000 km of the Austrian main network (TUG network), whereby each cross-section contains all system information, (raw) measurement signals, as well as the resulting quality signals.

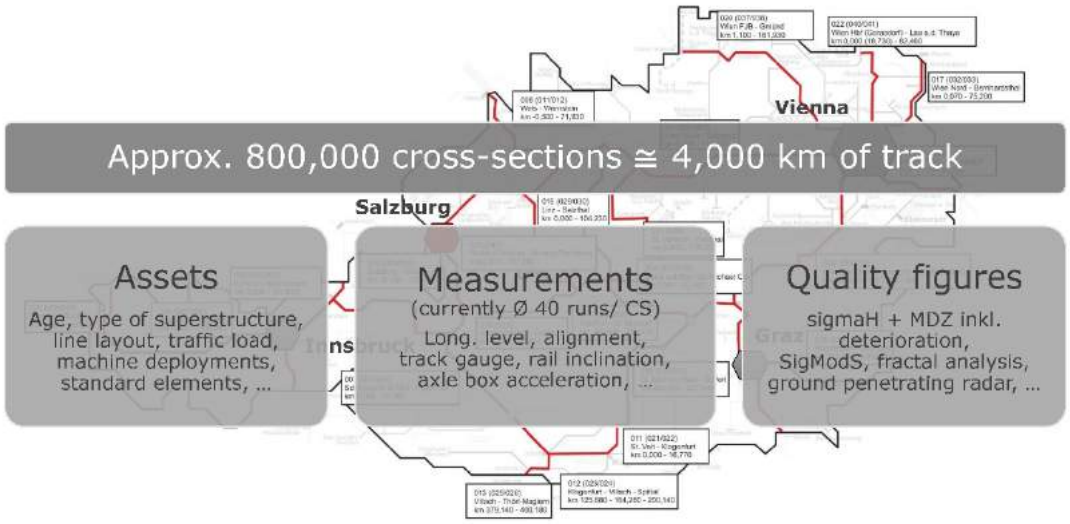

Figure 3 Overview TUG database

The system information for the individual tracks is particularly described by the superstructure configuration (sleeper type, rail profile, rail quality), traffic load, and routing. The variation in these characteristics results in differences in service life and maintenance intervals, and resulting significant variations in life cycles, or rather life-cycle costs, for the various sections. A specific version of the distinguishing features of the tracks as described above is referred to as a standard element in this context (Figure 4). The Institute of

Railway Engineering and Transport Economy at TU Graz, in cooperation with the ÖBB, has developed duty cycles for any combination of parameters, and thus for all standard elements [Veit 2002].

Südbahn 2	600<R<1000																	
Gross Tons per Day, Track	Profile	Steel Grade	Substructure			Sleeper												
45.000 - 70.000	60E1	260	good			Concrete												
Maintenance Measure	Service Life	30,0	0	1	2	3	4	5	6	7	.....	22	23	24	25	26	27	28	29
Renewal		1,0	1								.....								
Tamping	all x years	3,0	1			1			1		.....			1			1		
Grinding	Number	1,0									.....								
Grinding RCF	Number	6,0				1				1	.....		1				1		
Rail Exchange	Number	0,0									.....								
Rail pad exchange	Number	0,0									.....								
Small maintenance	Number	30,0	0,5	0,5	0,5	0,5	0,5	0,5	0,5	0,5	.....	1,5	1,5	1,5	1,5	1,5	1,5	1,5	1,5

Figure 4 Example of a standard element

These standard elements include technical expertise, statistically-supported assumptions regarding strategic service life, as well as the average of maintenance activities required across all tracks with certain boundary conditions. Standard elements thus permit network-wide analysis and strategy formulation. As mentioned above, the application to specific route sections is not feasible, since the standard elements merely describe average behaviour; individual track sections, however, may be subject to considerable variations due to a wide range of factors.

Accordingly, the area of track geometry research was also intensified to develop an improved description of the behaviour of specific sections. Previous research primarily concerns the degradation behaviour of the track geometry and the formulation of new analysis types for an improved evaluation of track behaviour [Hummitzsch 2009; Holzfeind 2009; Hansmann 2015]. Moreover, this knowledge has been linked to economic considerations [Enzi 2011] so as to determine a technically and economically optimised reinvestment schedule for major projects. The structure of the track geometry database is less geared towards the presentation of all values and the observance of safety limits; rather, the objective is the filtering, processing, classification and consolidation of the track data in the sense of a holistic condition evaluation.

Naturally, the degradation behaviour of the infrastructure is also particularly affected by the introduced loads. To this end, the database also has cross-section specific exposure information in the form of gross tonnes per day and track, which appear to be a useful approximation to describe the static load on the line. However, widely divergent, dynamic stresses to the track system from vehicle-specific speeds and different types of vehicles are not considered. This is partly due to the lack of continuous network-wide information to describe these effects, and partly due to a need to simplify the problem for the intended use in this work.

Economic, demographic and political factors cause certain changes in loads over the life cycle of a track system. However, consideration of previously introduced loads beyond track load and current loads requires determination of the cumulative load since track installation. For this purpose, the Institute [Hansmann 2015] analysed the track loads from 1971 to 2013 [Federal Ministry of Science and Transport from 1971 to 2001; ÖBB Holding AG in 2016; Röhsler]. As a result, a methodology to determine the cross-sectional specific cumulative load in gross tons was formulated. The frequency distribution of these cross-sections (Figure 5) shows that there is a drop in the cross-section figure from around 500 million gross tons (MGT) per day and track. Consequently, trend analysis based on cumulative load in the present work is conducted up to that load level.

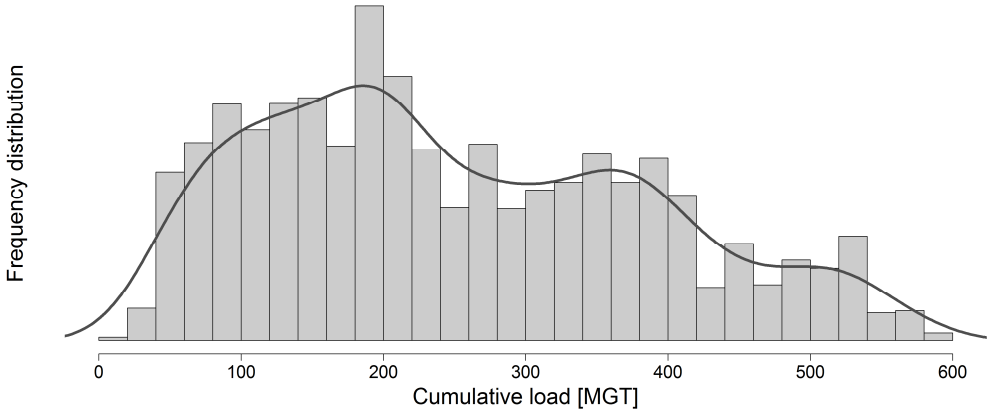

Figure 5 Distribution of cumulative load

The identification of network-wide behaviour patterns in the scope of track geometry analyses commonly requires restrictions to the data population. The general behaviour of the railway infrastructure may be heavily influenced by specific infrastructure components (eg. bridges, switches); evaluations are thus subject to scattering, with a risk of mapping unrealistic behaviour. Accordingly, the TUG database attribute "valid length" permits exclusion of those effects from consideration. In addition to the beginning and end of machine deployments, valid length also considers radius, load class, rail shape, sleeper type, station areas, junctions, bridges, crossings and tunnel sections. Where such data filtering was applied for analyses conducted in the scope of the present study, this is explicitly stated.

1.3 Superstructure types in the rail network

Different superstructure types affect the infrastructure behaviour, and, particularly, wear to ballast and substructure. The rail network of the Austrian Federal Railways (ÖBB) is currently predominantly equipped with a concrete sleeper superstructure (Figure 6), which was installed in the 1970s, gradually replacing the hitherto dominant wooden sleepers.

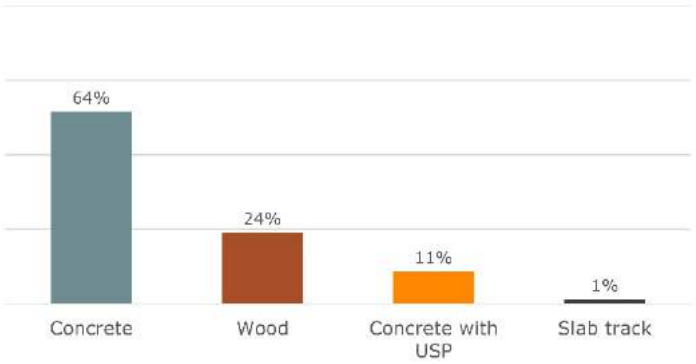

Figure 6 Current distribution of sleeper types in the TUG database network

In the last 15 years, the use of sleepers equipped with under sleeper pads (USP) has, however, increased substantially. Following installation of this technology in several test sections, concrete sleepers with pads have been becoming ubiquitous in Austria since 2005, and are now installed in around 70% of annual sleeper installations (Figure 7). At this time, as many as 11% of installed concrete sleepers throughout the TUG network are equipped with an elastic pad (Figure 6). This is equipped with an elastic layer less than one centimetre in thickness on the underside of the concrete sleeper, which is either glued on after installation or pre-installed in the manufacturing process of the sleeper. The elastic properties of the sleeper allow for continuous and largely permanent embedding of ballast into the elastic material of the pads. This results in an increase in contact area and a significant reduction in pressure on the adjacent ballast layer [Freudenstein et al. 2011; Berghold 2016].

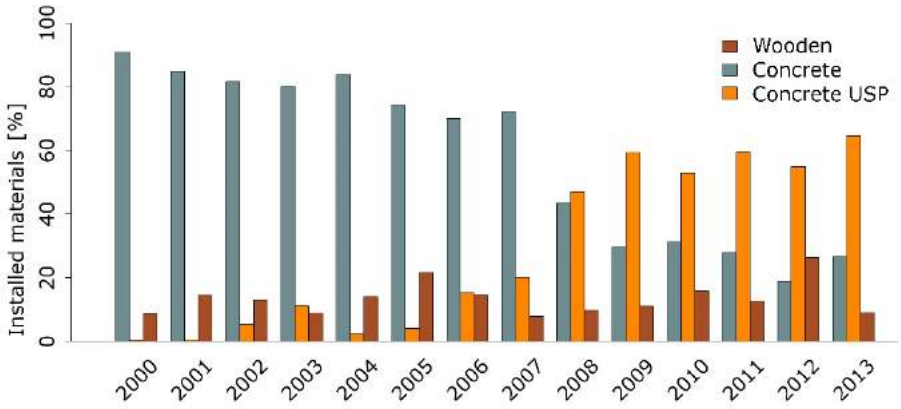

Figure 7 Distribution of annually installed sleeper types

The installation of wooden sleeper tracks has remained reasonably constant. This is due to the fact that this track type is still being installed in curve sections (partially with rail joints), tunnel areas with ballasted track and track sections with highly varying loading capacity patterns, and/or suboptimal ballast bed thickness.

This innovation in superstructure strategy is naturally also apparent from the age distribution of the different sleeper types (Figure 8). While tracks with wooden sleepers with an average installation year of 1989 display the highest superstructure age and a right-skewed distribution, the average year of installation for concrete sleepers now present in the network is 1995. The concrete sleepers have an average track age of five years, with a strong left-skewed distribution. This must also be considered in the further course of this study in the scope of investigating the quality behaviour of the various sleeper types.

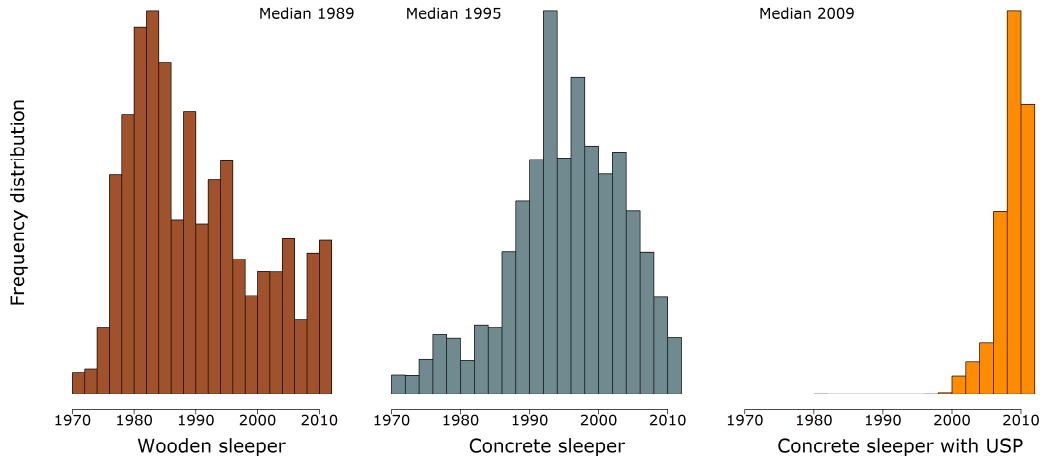

Figure 8 Age distribution in the TUG network by sleeper type

Apart from ensuring adequate rail infrastructure maintenance, the asset management of an infrastructure operator is also particularly concerned with its renewal. The condition of

the track sections due for renewal in the medium term is thus of essential importance. This is illustrated in Figure 9 for the track network in the TUG database. The abscissa describes the number of cross-sections present in the network, while the ordinate shows the remaining service life as a percentage. This is based on the current track age, as well as the expected service life of the individual cross-section according to the standard element (see 2.2). As explained above, the service life is a calculated average expected value; for this reason, some cross-sections have a remaining service life of less than 0%. These have already been in the track longer than expected due to apparently optimal boundary conditions. Overall, the age distribution of rail network components is extremely balanced, which is reflected in the average remaining service life of 48%.

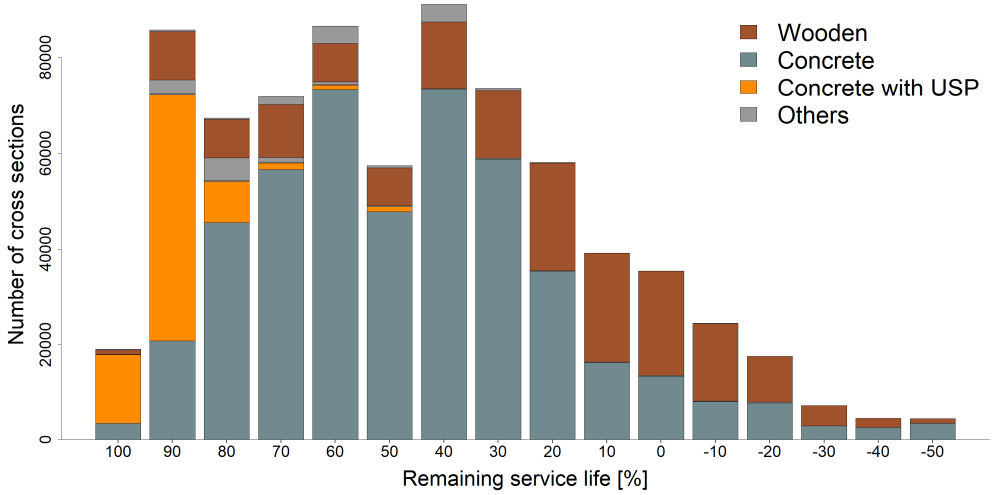

Figure 9 Distribution of remaining strategic service life

Regarding the change in superstructure strategies, one aspect must always be considered. The railway system is characterised by a high service life (usually 30 years or more); as a result, the impact of any strategic action comes to bear years (or decades) later. As mentioned above, concrete sleepers have been increasingly installed in place of wooden sleepers since the 1970s. These conventional concrete sleepers, in turn, have been replaced by concrete sleepers with pads (Figure 7) in the scope of track renewal for nearly ten years. Nonetheless, track sections that are currently at the end of their expected service life are still equipped with a significant proportion of wooden sleepers (Figure 9). This should be considered, since wooden and concrete sleepers have entirely different wear characteristics. Concrete sleepers are characterised by their very strong material, which generally provides for adequate adhesion between rail and sleeper until the end of their service life, and usually without lasting damage to the residual value of sleeper. Due to the lower elasticity of concrete in comparison to wooden sleepers, however, the stress to the ballast bed is higher; this component is thus the dominant factor when it comes to the service life of the track. While wooden sleepers reduce the stress to the ballast bed, the sleepers fail to provide the necessary adhesion between rail and sleeper later in their service life. This is also demonstrated by an evaluation of a total of 110 current Austrian reinvestment projects, which required renewal due to the sleeper condition in 43% of cases (Figure 10). This distribution between the two components that limit service life, ballast and sleeper, accurately reflects the relationship between wood and concrete sleepers that are close to their expected service life (Figure 9).

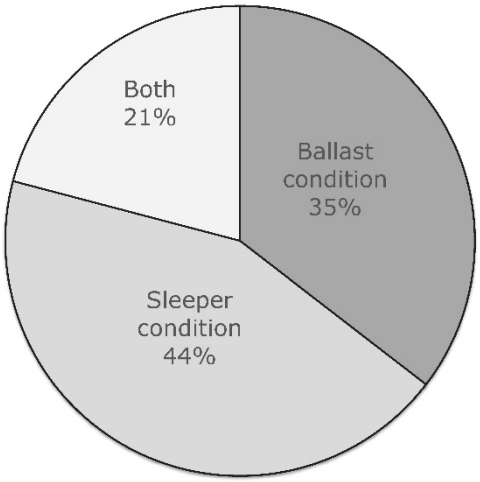

Figure 10 Current triggers for track renewal measures

Railway infrastructure asset management is thus faced with an interesting constellation. On the one hand, the rail network is dominated by superstructure types whose service life largely depends on the condition of ballast bed. On the other hand, there is a considerable proportion of wooden sleepers in the stretches currently up for renewal; in this case the service life is particularly limited by the sleeper condition.

Accordingly, the design of a suitable evaluation methodology for the component-specific infrastructure condition, which is to be discussed in this work, is of essential importance.

3

Railway Infrastructure Condition Evaluation

Precise monitoring, description and documentation of the rails is required to ensure optimal preservation of the railway line; this is to ensure recognition of defects, as well as the planning of suitable solutions. The maintenance works required to remedy a fault may be preventive or reactive in nature. Reactive maintenance is defined as the initiation of measures after the occurrence of a fault, or rather once it has developed to an extent where postponement of measures is no longer feasible for safety reasons. A preventive repair strategy involves the correction of faults before predefined intervention thresholds are breached. This permits the development of strategic, and thus cost-saving maintenance planning. Regardless of the strategy, the regularity and quality of inspections is of enormous importance in ensuring safe operations. The Austrian Federal Railway as one example shows that automatically generated data has been increasingly collected and used in recent years (Figure 11).

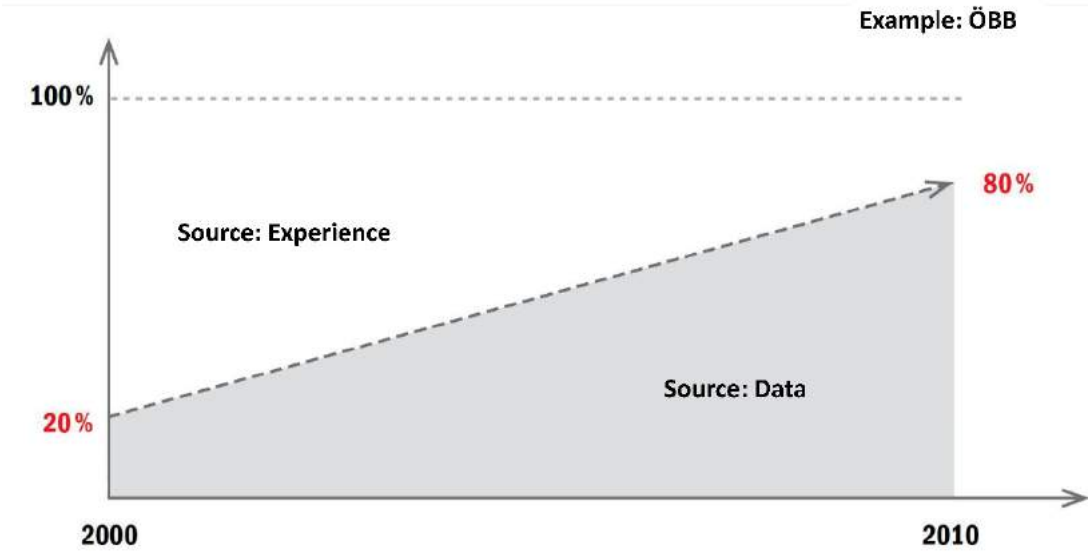

Figure 11 The growing influence of measurement technology in maintenance [according to Auer 2014]

Thanks to their high speed, various measurement vehicles permit regular detection of the entire rail network without disturbance to the rail schedule. Moreover, objective and temporally reproducible measurements are determined, which form the basis of sustainable maintenance and reinvestment planning. For this reason, the condition evaluation in this work is mainly based on such measurement systems, while maintaining the need for further inspection and investigation methods (route inspection, geotechnical studies, etc.). The latter evaluation methods are primarily used for validation of the condition evaluation methods presented here.

The railway infrastructure companies cooperating within the framework of the present work perform infrastructure condition evaluation with a range of tools (Figure 12). The main differences between these methods mainly relate to two aspects: (1) the degree of automation and (2) the detection rate. The higher the degree of automation, the more objective and therefore person-independent the detection method. High acquisition speed enables an evaluation of the entire route network without detrimental effects on ongoing railway operations. Also, faster travel across the entire network translates to more regular network-wide detection. This results in more effective time series analyses, and thus measure planning.

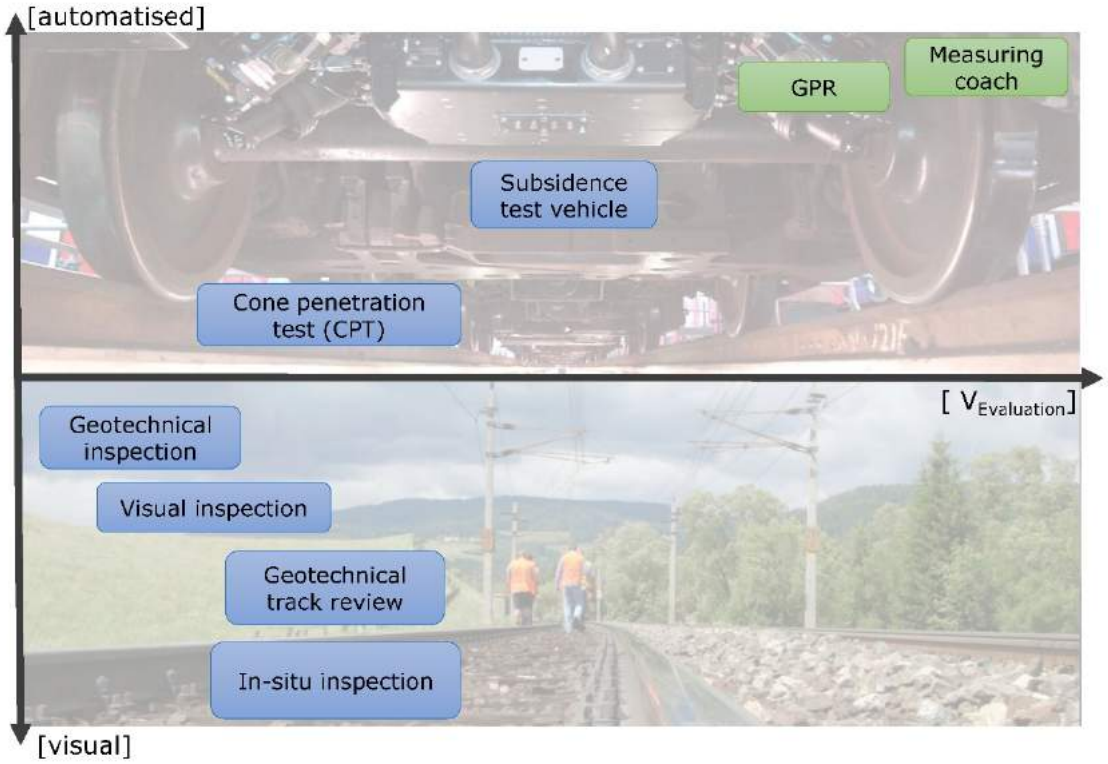

Figure 12 Discussed infrastructure condition evaluation tools

The present work categorises the tools for condition evaluation into three basic areas: The establishment of a network-wide condition evaluation primarily requires (1) track geometry vehicles and (2) ground-penetrating radar (Figure 12, highlighted in green); in the context of the validation process, (3) further detection methods are taken into account.

The latter are mainly selective detection methods, each capable of assessing specific components of railway track (e.g. ballast sampling, loading capacity of the substructure). However, these methods cannot be employed on a network-wide basis, and certainly not at the frequency required for an adequate time series. This raises the following question, which will be the subject of the present chapter:

- Does measurement data analysis permit detection of the condition of individual components from existing, automated and measured signals?

3.1 The track geometry vehicle

Since the end of World War II, when a former saloon vehicle was converted into a measurement vehicle, track geometry detection in Austria has been automatic and rail-based. Currently, measuring speeds up to 250 km/h are feasible. Track geometry measurement is defined by international standards [EN 13848-1 2009], and is principally composed of the following parameters (Figure 13):

- Track position: Level and alignment
- Gauge
- Cant, and derived twist

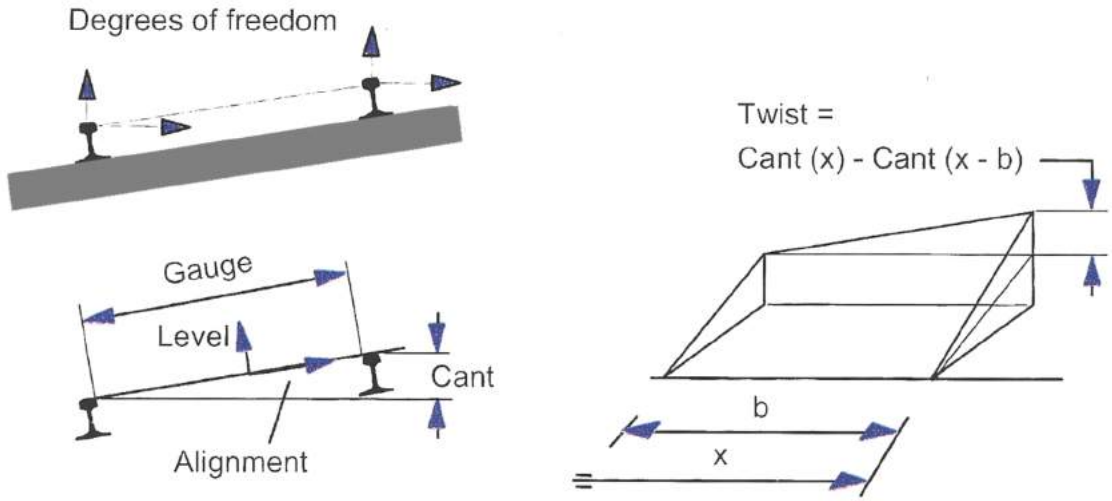

Figure 13 Parameters of track geometry [Esveld 2001]

The gauge, like the exact rail profile geometry and rail inclination, is detected by laser-based optical measurement systems at precisely 14 mm below the rail level, and stated in millimetres [EN 13848-1 2009]. The parameter cant is measured by a fibre optic gyroscope, as well as the exact position of the two rails relative to each other (see 3.1.1). Further measuring systems for monitoring of the structure gauge, contact line, rail surface, axle bearing acceleration and thermographic detection, have recently been developed for installation in self-propelled or tractive track geometry vehicles.

3.1.1 Track geometry

Track geometry, and particularly the vertical aspect, is one of the most important measurement signals in the rail sector. Tamping operations, and especially ballast cleaning and associated renewal activities are planned on the basis of this signal. In the present work, the vertical aspect of the track geometry plays a central role for this reason.

3.1.1.1 Measurement of vertical track geometry

Depending on the measuring vehicle generation and operator, the track geometry may be determined by two main systems: the chord and inertial measurement methods.

For the inertial measurement principle, the actual measurement is performed on a measuring frame that carries an inertial measurement unit (IMU) in addition to the two optical gauge measurement systems (Dual OGMS). The metrological design of the IMU includes accelerometers, as well as rotary encoders for measuring the angle change. The twofold integration of the measured accelerations provides the position of the measurement transducer relative to the inertial coordinate system [Oberweiler 1987]. An additional measurement of the distance between the transducer and the rail yields an exact position of the track in space. This is achieved by mounting the aforementioned measuring frame to the axle bearings of the bogie, which ensures that the sensors are constantly aligned in parallel to the rail surface. The resulting spatial curve permits mapping of track geometry irregularities with a wavelength of more than 150 m.

The chord measurement method is based on measuring the distance between axle and track at the middle of three vehicle axes, while a chord is stretched across the two outer axles. The continuous performance of this measurement provides the relative track geometry based on the chord alignment (position of the vehicle) and the distance to the rail, without a minimum speed requirement. However, a major disadvantage arises due to the fact that the real, true-to-shape track geometry is distorted with respect to amplitude and phase. This distortion is a factor of chord length (base length) and pitch. If the chord pitch is asymmetric, the measurement result is also dependent on the direction of measurement [Wolter et al. 2013]. A transfer function is derived on the basis of known centre distance values, which permits conversion of measured amplitudes to true amplitudes. The centre distances of the three axes should be arranged asymmetrically, since specific wavelengths cannot be detected at all otherwise, and therefore also cannot be converted into a true-to-shape track position by way of the known transfer function [Rießberger 1975].

A European standard [EN 13848-2 2004] with a focus on these issues was formulated to ensure equivalence of employed measurement methods and identical filter transfer functions, as well as comparability of the output and data formats. Ultimately, the outcome of any measurement is only sufficiently defined by additional indication of the measurement uncertainties, which are also subject to international regulations [ENV 13005 1999].

3.1.1.2 Analysis and condition evaluation of track geometry in Austria

The track geometry information delivered by track geometry vehicles is internationally standardised, and thus contains the same raw data (depending on the range of installed measuring equipment). However, in addition to data processing (stationing, filtering), there are various approaches to measurement-based condition evaluation and maintenance planning.

In Austria, the ÖBB developed the "New Austrian Track Analysing System" (NATAS) more than ten years ago, which includes a holistic view of all relevant measured data and infrastructure information. The output consists of four sheets per five kilometre stretch, containing the measured track geometry values and rail condition, as well as the associated intervention thresholds for many sections. Information on machine deployments of the last 15 years, as well as routing, superstructure type and installation year is also included. Figure 14 shows a sample NATAS sheet for track geometry analysis.

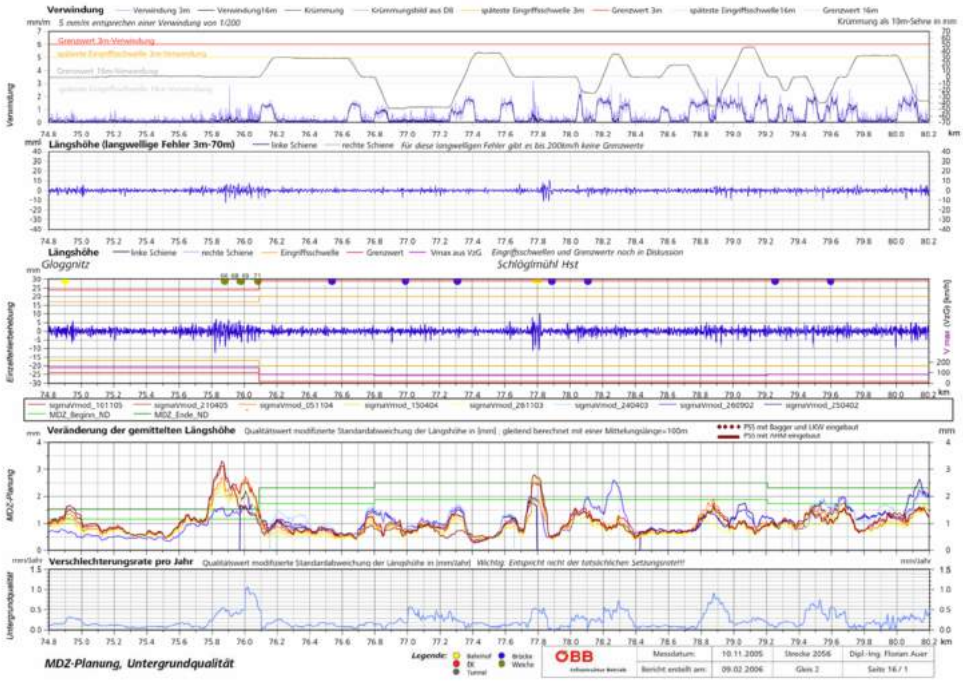

Figure 14 Track geometry analysis of the Austrian Federal Railways [Auer 2010]

This tool allows for the graphical comparison of the amplitudes of all measurement signals with the specific threshold levels. Specially defined attention (AL) and intervention (IL) levels are to prevent violation of the safety-critical immediate action level (IAL) [EN 13848-5 2008]. Consequently, the system is a vital tool in terms of maintenance and infrastructure measures for safe operation of the Austrian railways. However, when it comes to reinvestment and maintenance plans at the national level, its limits become apparent: since the information on each track section is available as a printed sheet, individual values cannot be filtered or classed on a network-wide basis. For this reason, neither network-wide, automated planning of maintenance and renewal measures, nor a holistic infrastructure condition evaluation are yet feasible.

3.1.1.3 Conventional track geometry within the TUG database

The filtering and classification of all measurement and quality signals for the entire route network is possible with the above-mentioned TUG-database (Figure 3). The available data on vertical track geometry falls into two categories [Auer 2004]:

- The raw data of the longitudinal level signal permits detection of local violations of threshold values during an inspection run with the track measurement coach.
- The average track geometry condition is to be described for a certain section by averaging several measurements over a certain distance.

The quality signal is calculated by formation of discrete or moving averages over a predefined cut-off length (usually 100 m/200 m/500 m). The standard deviation, with a constraint length of 200 m as defined in EN13848-5, is an extension of this calculation; it describes the dispersion of values around their mean, and thus serves as an figure of irregularities in the longitudinal level signal. In addition, it permits analysis of these quality signals with a chronological component. Calculation of a deterioration rate by way of a regression model allows the prediction of future violations of certain thresholds. The TUG database includes the same standard deviation of longitudinal level (sigmaH) that is also used internally by the ÖBB [Auer 2004]. The temporal behaviour of this data (Figure 15) is described by an exponential regression function [Holzfeind & Hummitzsch 2008].

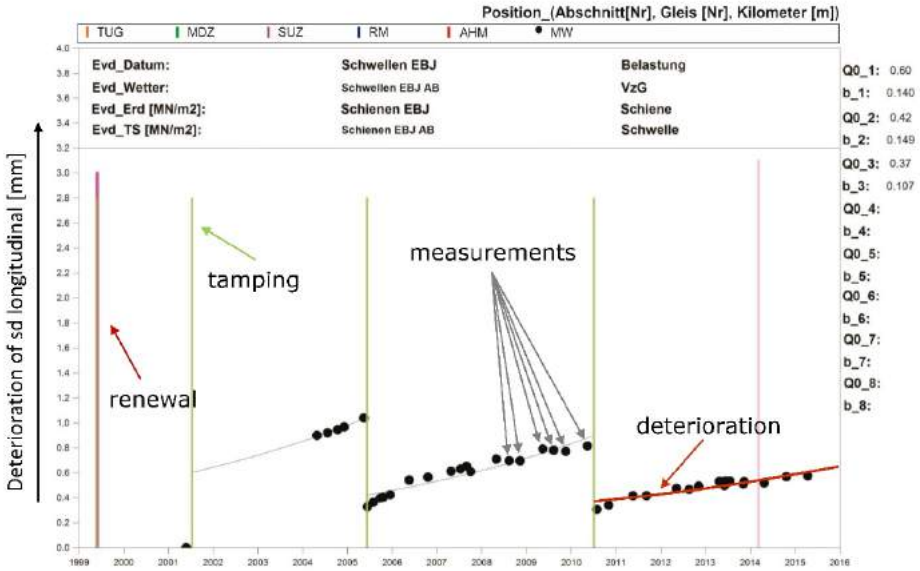

Figure 15 Track geometrical behaviour sigmaH

These measurement and quality signals permit description of track geometry quality for individual points, as well as entire sections. In the linear and exponential approaches, the regression function as calculated from the measurement points is clearly defined by the initial quality and deterioration rate for the range. This permits evaluation of the current condition and prediction of track geometry behaviour.

3.1.2 Fractal analysis of vertical track geometry

The track geometry analysis has always formed the basis for a condition-based planning of measures in the field of railway infrastructure. Different approaches for converting of raw signals from track measurement coach into quality values have been formulated over the years. Statistical quality values provide a description of track geometry, and a representation of its development over time. Early attempts to infer different types of faults were made by way of spectral analysis of track geometry data; however, such attempts were often doomed to fail due to the lack of network-wide evaluation capabilities. Fractal analysis permits examination of track geometry data with respect to different wavelength ranges for the first time, as well as its evaluation with respect to different fault characteristics. This form of analysis was developed more than 40 years ago [Mandelbrot 1967] to describe the jagged coastline of Great Britain. Later, it was used to describe the roughness of granular materials in geology [Hyslip & Vallejo 1997], before its first application in the rail sector as part of research on the American AMTRAK network [Hyslip 2002]. This method permits allocation of track geometry irregularities to the causative wavelength range, and thus assignment of a specific damage type based on the specific fault characteristics of the track geometry data.

3.1.2.1 Methodology

The methodology, as used and implemented by the Institute of Railway Engineering and Transport Economy, as well as the algorithm programmed for fractal analysis of vertical track geometry, were developed in close collaboration with Dr. Fabian Hansmann. Consequently, the present chapter includes results and passages that were previously published [Hansmann 2015; Landgraf 2015; Landgraf et al. 2014; Hansmann & Landgraf 2013]. Text passages with the same wording are marked as such.

The network-wide calculation of fractal analysis takes place continuously for the entire track network with a constraint length of 150 metres. The Modified Divider Length Method [Mandelbrot 1967] employed here requires at least two points for the sufficient description of a wavelength. Since the measurement signal currently available for Austria covers wavelengths of up to 70 m, the aforementioned 150 m constraint length was chosen so as to be able to describe any wavelength. The output of the result takes place as a moving average.

At the beginning of the algorithm, longitudinal level is prepared and analysed in order to distinguish error values. In this context, a data segment consists of 600 individual measurements for each cross-section and measurement run at a selected constraint length of 150 metres, and extends over a section of ± 75 m to the current section under evaluation. The data segment is iteratively subdivided into progressively smaller sections λ, and the associated measuring point Y_i is determined (Figure 16). If the division is located between two actual measurement points, the measured values are interpolated. Thereafter, the lengths of the polygons stretched between the points are determined using the Pythagorean theorem, and summed.

$$L = \sum_{1}^{N} L_i = \sum_{1}^{N} \sqrt{(Y_{i-1} - Y_i)^2 + (\frac{EL}{N})^2}$$

N … Number of divisions
i … Running variable
EL … Length of data segment

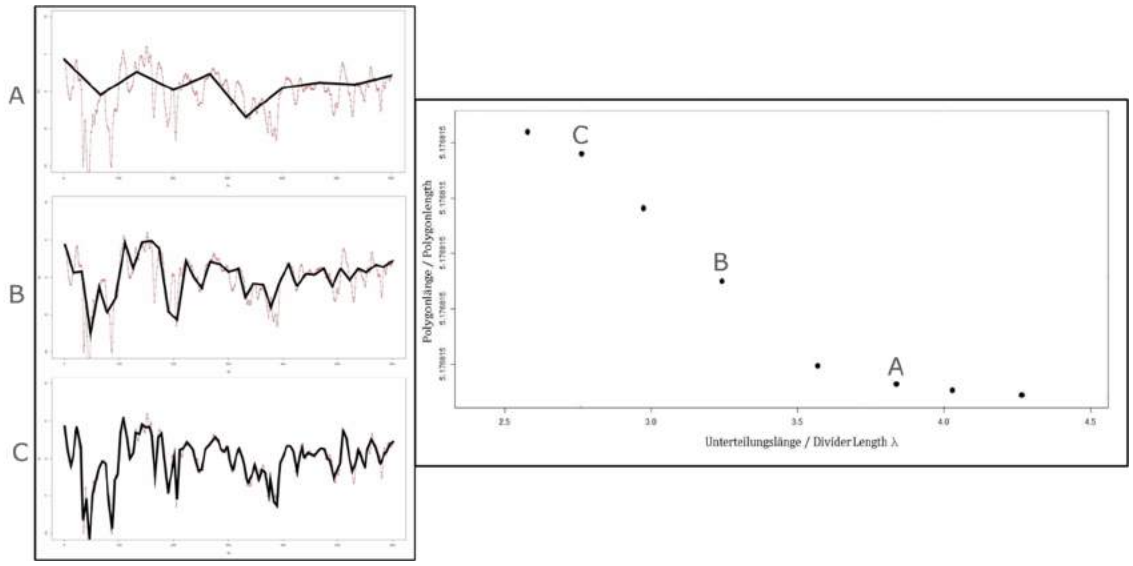

Figure 16 Iteration of sub-division length (left) and creation of Richardson plot (right)

The progressively increasing traverse lengths (ordinates) are subsequently compared to the progressively smaller segment lengths (abscissae) on a logarithmic scale (Richardson plot, Figure 16). The different fractal dimensions are described by a regression line. In this context, the three dimensions represent short-, medium- and long-wave track irregularities, and the slope of the calculated regression line shows the expression of the respective wave range in the data segment.

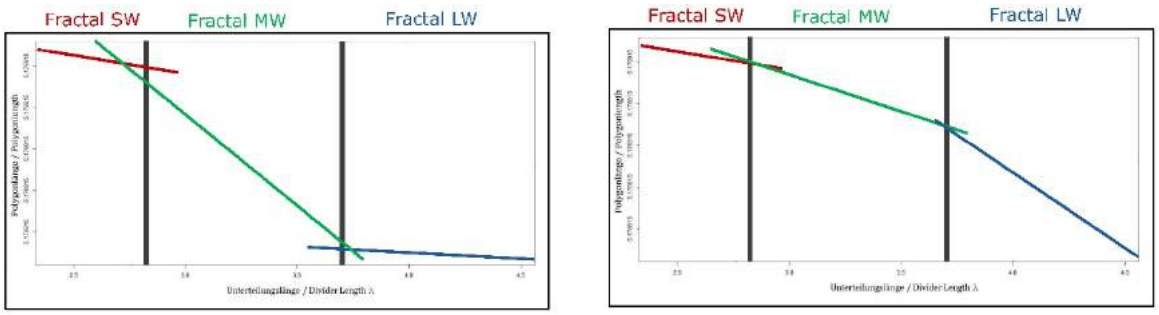

Figure 17 Richardson plot with increased gradient in the medium (left) and long wavelength range (right)

Higher values cause a stronger representation of the observed wave range in the data segment, while lower values describe a weaker expression (Figure 17). This algorithm is applied to the longitudinal level signal of both rails. Due to the negligible difference in results for the individual rails [Hansmann & Landgraf 2013], only the result of the left rail is used. Treatment of a track-specific rather than rail-specific result is required to permit comparison with other measurement and quality signals.

3.1.2.2 Interpretation

In the scope of the method utilised in Austria [Hansmann & Landgraf 2013], irregularities in track geometry are divided into three wavelength ranges on the basis of the so-called Richardson plot (Table 1). The classification of the wavelength ranges is theoretically variable; however, a further sub-division may have a negative impact on the significance of the fractal analysis.

Wavelength range	Description	Designation
λ ≤ 3 m	Short-wave range (SW)	Slope 1
3 m < λ ≤ 25 m	Mid-wave range (MW)	Slope 3
25 m < λ ≤ 70 m	Long-wave range (LW)	Slope 2

Table 1: Differentiation of fractal wavelength ranges

It is assumed that the medium-wave range covers an error characteristic that describes the condition of the ballast bed. The long wave range, in turn, is assumed to be significant when it comes to the lower ballast bed, transition area, or even the substructure condition (Figure 18).

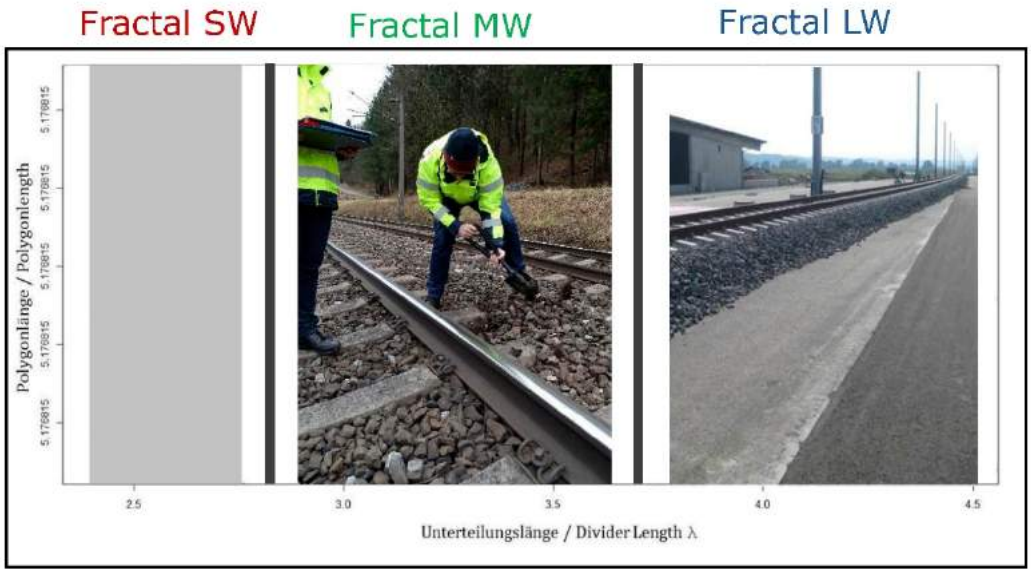

Figure 18 Classification of sectors of the Richardson plot in respect of their significance

These assumptions were already confirmed in the scope of a comprehensive validation process [Hansmann 2015; Landgraf 2015; Landgraf et al. 2014], primarily by comparison with *in-situ* behaviour and stochastic analysis. An extension of the analysis to wavelengths of more than 70 metres would be feasible with the algorithm; however, this is not necessary for typical speed levels in Austria. The wavelength range D3 [EN 13848-5 2008], which was generated for this purpose, focuses on the examination of high-speed lines in excess of 300 km/h. The short wavelength range has not yet been studied in the same

depth, the measurement system noise would most likely be an issue in the relevant wavelength ranges. However, initial attempts have shown that the short-wave range may yield some useful conclusions, especially in the region of interaction between fastening, sleeper and ballast.

3.1.2.3 International comparison of fractal values

One of the questions which inevitably arise in the context of fractal analysis, is the following: Are comparable analytic methods feasible for other measurement methods (chord and inertial measurement methods)? To find an answer to this question, fractal wavelength analysis was applied to measurement data of different infrastructure operators. In addition to the Austrian track network in the TUG database, a route from the network of Swiss Federal Railways SBB (length ~ 55 km) was examined for this purpose; by contrast to the ÖBB, the SBB use a measurement vehicle equipped with chord measuring technology (see 3.1.1). The relevant metrics are based on a relatively new route with very high quality ballast and bituminous formation layer. The superstructure for the entire route is of the same installation year; the route should accordingly be in good condition throughout. In addition, the analyses were performed for the Northeast Corridor of the National Railroad Passenger Corporation Amtrak (length ~ 100 km). This section is in a mediocre condition, and subject to strong scattering of superstructure age. Again, track geometry measurements were performed with a measurement vehicle equipped with chord measurement method technology.

The comparison of evaluation outcomes (Figure 19) demonstrates that the network-wide fractal values in both the medium and long wavelength ranges for the Austrian Federal Railways (ÖBB) correspond very well with US values. This is plausible, since both areas have a comparable age structure, and the populations generally include sections of all ages. Consequently, this confirms that fractal values from both chord and inertial measurements are indeed comparable. However, there are some differences in the short-wavelength range. This may be due to the fact that a certain degree of measurement noise cannot be excluded, particularly in the wavelength range of less than three metres. On the other hand, this is also the wavelength range that could provide an indication of the sleeper condition, or rather the interaction between rail fastening, pad, sleeper and ballast. Accordingly, the differences may also be partially affected by the fact that the standard of installed track materials tends to be very high in Austria, or rather generally in Central Europe.

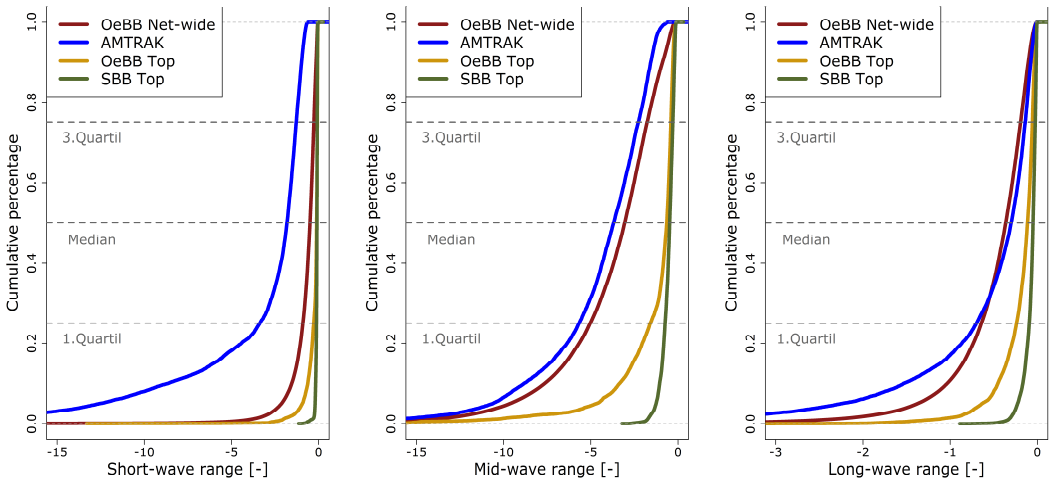

Figure 19 International benchmark of fractal values

As mentioned above, the Swiss stretch is a relatively new track with excellent superstructure and substructure components. For purposes of comparability, sections that meet these criteria reasonably well are also filtered from the Austrian route network. This selection from the Austrian route network refers to sections with an age below 10 years, and which are equipped with concrete sleepers. Generally, Figure 19 shows good comparability of fractal values for *ÖBB Optimum* and *SBB Optimum*. The somewhat lower expression of the Swiss fractal values in the medium wave range is probably due to the siliceous limestone used as railway ballast, which is of above-average quality [Berghold 2016]. The advantages of the Swiss section in the long-wave range result from the aforementioned bituminous formation layer, which just about eliminates mixing of the formation layer with the ballast bed.

3.1.3 Standard deviation of modified gauge (SigModS)

The measurement of the gauge is determined as a deviation from the standard gauge. This deviation must not exceed a value of -10/+ 35 for the most common speed segment (120 km/h < Vmax ≤ 160 km/h) [EN 13848-5 2008]. The standard therefore refers to individual faults on the track. Furthermore, measurement of the deviation from the mean gauge over 100 m is recommended, which is to capture the condition of the track section, allowing safety-critical track cross-sections or sections to be identified. However, the classification of the aforementioned wear behaviour (see 2.1), or the further prediction thereof, is not possible. Detection of this behaviour requires a methodology capable of quantifying the signal noise. However, a simple standard deviation, as used for vertical track position, does not yield a solution for the problem. This is due to the following two peculiarities of this measuring signal: Firstly, this measurement signal is not scattered around a fixed value (e.g. zero line); rather, it can take on values ranging from -10 mm to +35 mm, and even

beyond. Secondly, the track gauge tends to yield higher values in curve sections (Figure 20, above). In some cases, gauge widening is installed deliberately in curve areas for improved curve negotiation. A calculated standard deviation of the track gauge signal (Sigma track gauge) is affected significantly by the long-wave gauge widening. This is particularly evident in the transition zones, which cause a rapid change in the values (Figure 20). The short and medium wavelength noise, which supposedly describes the adhesion between rail fastening and sleeper, as well as the wear of the pad or rather pressing-in of the ribbed base plate is thus not detected, or strongly under-represented.

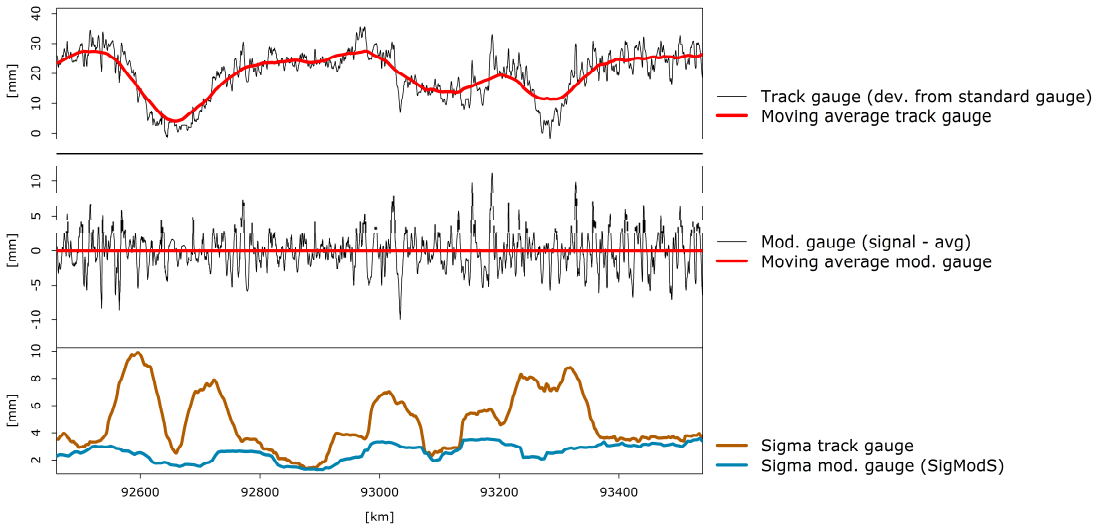

Figure 20 Methodology standard deviation of the modified gauge (SigModS)

This problem is treated by application of a high-pass filter, which lets signal components with frequencies above its cut-off frequency through with minimal attenuation, while components with lower frequencies are attenuated. For this filtering approach, the delta between the raw signal and its moving average is now calculated with a constraint length of 25 m [Hansmann 2015]. This results in a modified gauge signal (mod. gauge), which scatters around the zero line (Figure 20, centre), and no longer responds to long-wave influences. The standard deviation for the modified gauge (SigModS) now shows a completely different picture compared to the standard deviation of the raw signal (Figure 20, below). While the latter is subject to strong scattering, which is largely due to the aforementioned transition zones, the former has a more continuous profile; this is capable of detecting the short and medium wavelength noise of the signal. In long straight sections (eg. 92,800 to 92,900 m or 93,400 m onwards), the values of the two standard deviations tend to converge. This is further confirmation that the standard deviation of the modified gauge signal (SigModS) detects the noise without being affected by long-wave gauge widening resulting from track design or caused by curve areas.

The frequency distribution of this quality signal across the entire route network located in the TUG database is shown in Figure 21. The median evidently takes on a value of around 0.95 mm for all cross-sections. Filtering the valid lengths from this basic dataset, the bar graph shows a reduction of the population to around a third of the values. As already explained (see Figure 6), the cross-sections of valid lengths include homogeneous areas for open track sections. Accordingly, the standard deviation of the modified gauge (SigModS) indicates a better condition for these areas, as indicated by a median of about 0.8 mm SigModS.

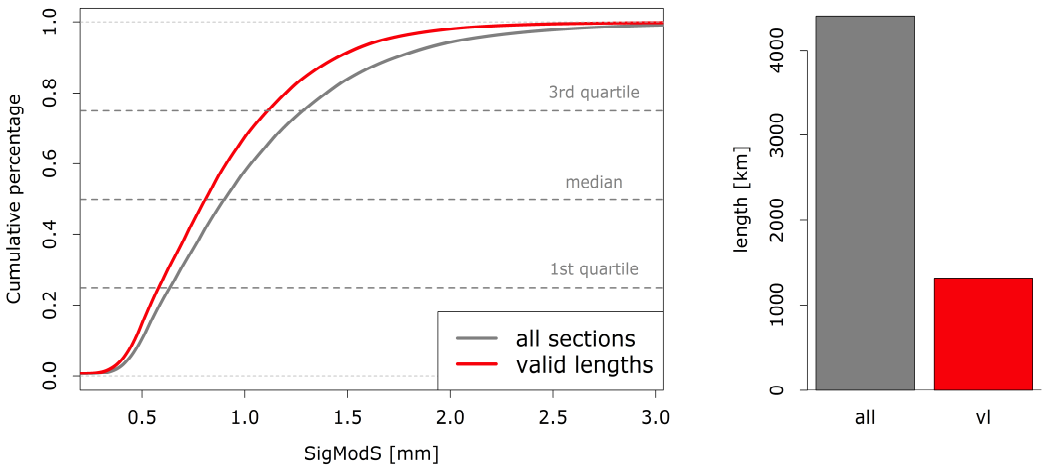

Figure 21 SigModS frequency distribution

The 90% and 95% quantiles of all cross-sections amount to 1.73 mm and 2.07 mm SigModS. Accordingly, poor condition can be presumed for this value range on the basis of this initial statistical analysis.

3.2 Ground-penetrating radar (GPR)

The GPR is a geophysical measuring system that does not entail track geometry measurements; rather the condition of the superstructure and substructure is analysed. Thus, it represents an entirely different measuring principle to the above-described track geometry vehicle. The GPR is both a transmitter and receiver of electromagnetic pulses, which are used to derive the characteristics of different materials from their duration and intensity. Among other applications, ground penetrating radar has been used in resource exploration, pipeline exploration and investigation of air pockets in concrete. This exploration method is being increasingly employed in the railway sector to describe the condition of the infrastructure materials. An important advantage is the measuring speed, which permits exploration of the ground condition at speeds of more than 100 km/h [Eriksen et al. 2006].

3.2.1 Ground Penetrating Radar (GPR) measurement methodology

The emitted electromagnetic pulses are reflected by the various materials at different speeds and strengths, depending on their dielectric constant. The different reflections of an introduced pulse are displayed as a function of time in nanoseconds and amplitude in millivolt. Thereafter, this function is allocated with a specific colour code, creating a radargram from successive individual measurements (Figure 22). This radargram enables the graphical analysis of GPR measurements, which permits the identification of layer boundaries and any fixtures (lines, packing layers, etc.).

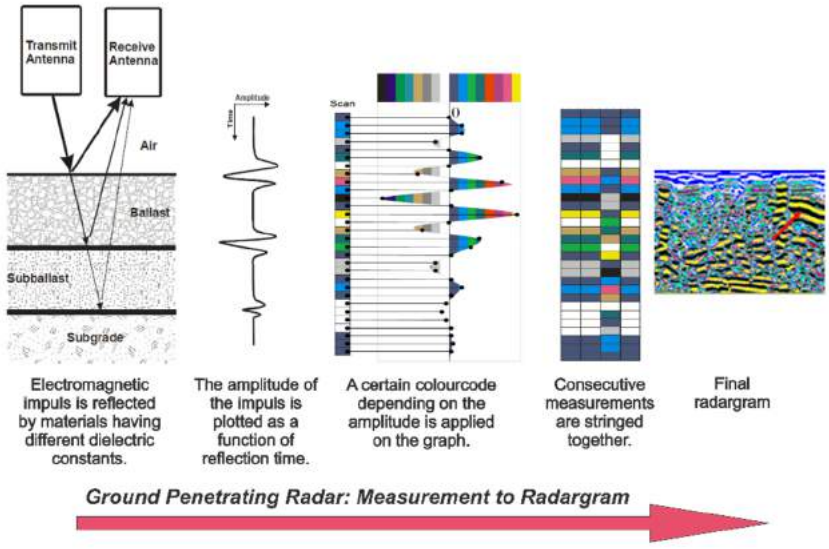

Figure 22 Creation of a radargram using GPR [Roberts & Rudy 2006; Sussman et al. 2003; Niessen 2005; De Bold 2011]

However, the present physical variables must be calculated to discern the material properties and depth of adjacent layers. The formula for the propagation of a dielectric medium [Daniels et al. 1988] can be described as follows:

$$v = \frac{c}{\sqrt{\varepsilon_r}}$$

Formula 1: Propagation of a dielectric medium

Where:

v … Propagation speed of the medium [m/s]

*c … Speed of light (3*108 m/s)*

ε_r … Dielectric constant of the medium

Since both the distance and time, and thus the speed of the reflected electromagnetic pulse are known, the only unknown in this formula is the dielectric constant. The dielectric constant determined in this manner can now be compared with the materials relevant in the railway sector (Table 2). This method thus allows for definition of the nature of the soil layers present.

	Material	ε_r	V [m/s]	
	Air	1.0	3.00*108	
	Water	81.0	0.33*108	
	Dry, pure ballast	3.0	1.73*108	
	Moist, pure ballast	3.5	1.60*108	
	Saturated, pure ballast	26.9	0.48*108	
	Dry, impure ballast	4.3	1.45*108	
	Moist, impure ballast	7.8	1.07*108	
	Saturated, unclean ballast	38.5	0.58*108	

Table 2 Dielectric constants for materials relevant in the railway sector [Clark et al. 2001]

Additionally to condition, also the thickness of the intermediate layer is also of interest. According to [Gallagher et al. 2000], this is defined by the following function:

$$t_r = \frac{2 * d}{v} = \frac{2 * d * \sqrt{\varepsilon_r}}{c}$$

Where:

t_r … Time difference between pulse emission and reception [s]

d … Distance between two layer boundaries (= layer thickness) [m]

v … Propagation speed of the medium [m/s]

*c … Speed of light (3*108 m/s)*

ε_r … Dielectric constant of the medium

The thickness of the individual layers can thus be calculated as the only unknown of the above formula.

3.2.2 Condition evaluation by GPR

One vital aspect for any form of condition analysis, apart from the true and fair assessment of the condition, is the simplicity of the analysis. The presentation of the final outcome must be concise and allow a wide range of users to apply and understand the methodology. This expectation is not quite met by the preliminary final product of the GPR, the radargram (Figure 22). For this reason, [Olhoeft 2000], [Sussman et al. 2003], [Eriksen et al. 2006] and [De Bold 2011], among others, developed specific indicators to summarise the findings of GPR runs. The amplitude-time charts (Figure 22) are used as a basis for determining the humidity, contamination, and clay fouling for the track system. The evenness of individual layers in the longitudinal direction is indicated by the roughness of the respective line in the radargram.

A comprehensive visualisation by Ground Control Geophysics & Consulting GmbH, currently used by the Austrian Federal Railways, is shown in Figure 23. In a longitudinal section of the track, the thickness of the ballast bed is shown by polluted and unpolluted sections, as well as the intermediate layer underneath. The colour-coded rating bands underneath relate to the information regarding the above-mentioned indicators, which are generated from the raw data to facilitate an improved understanding of the results. In addition, due to the profile measurements at the edges of track, the transverse inclination of the formation layer can also be evaluated. The various GPR providers use different output protocols due to the specific presentation software; however, the generated information is usually very similar.

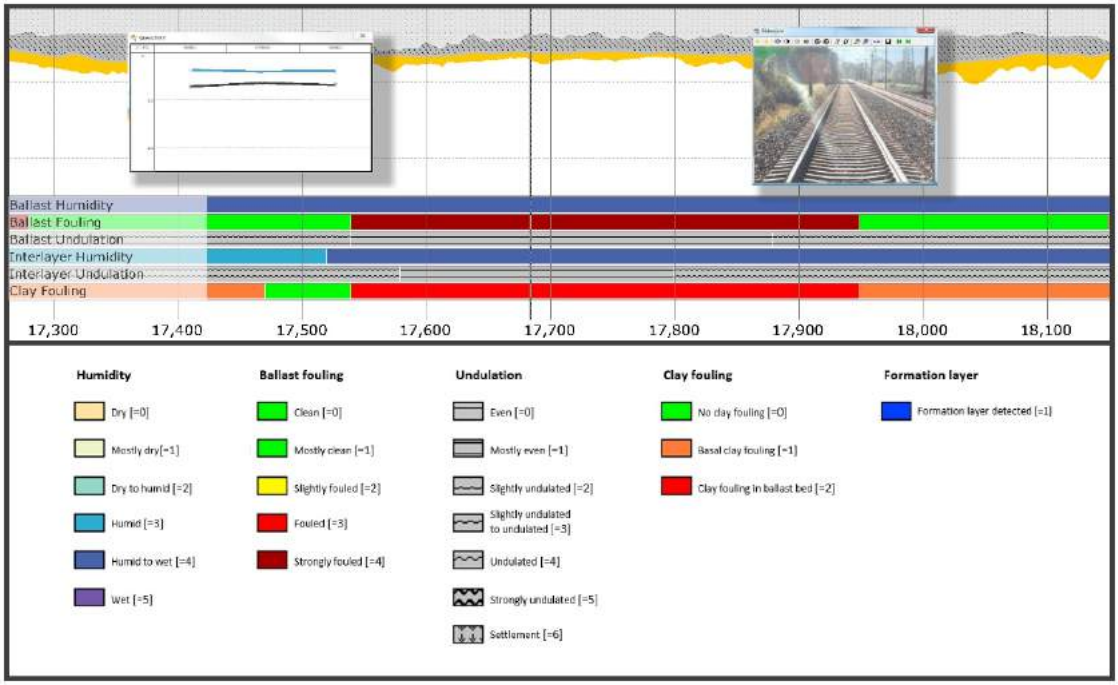

Figure 23 Representation of an ÖBB GPR analysis

3.2.3 Detailed analysis of GPR evaluation

In Austria, some 1,500 kilometres of track underwent GPR evaluations in the years 2012 to 2015. As a first step, the evaluations were prepared for linking with the TUG database at the Institute of Railway Engineering and Transport Economy. This enables for comprehensive analysis of the evaluations from GPR runs so as to examine them for their relevance to the railway sector; these analyses will be discussed in detail in the following chapter. In a further step, the link with the TUG database permits correlation of the GPR evaluation with the track geometry data, and the resulting fractal analysis of the vertical track geometry (Chapter 5).

3.2.3.1 Analysis of evaluated parameters

The distribution of the parameters for description of the ballast condition is shown in Figure 24. Regarding the pollution of the ballast, the rating *clean* is evidently awarded rarely; *mostly clean* describes most of the network. Also, when it comes to humidity, the highest rating of *dry* is only present in very few cases. Naturally, this may indicate that the track system is not in optimal condition, or that the top ratings in the evaluation of the GPR provider are very difficult to achieve. A basal or even clay fouling within the ballast bed is only apparent sporadically.

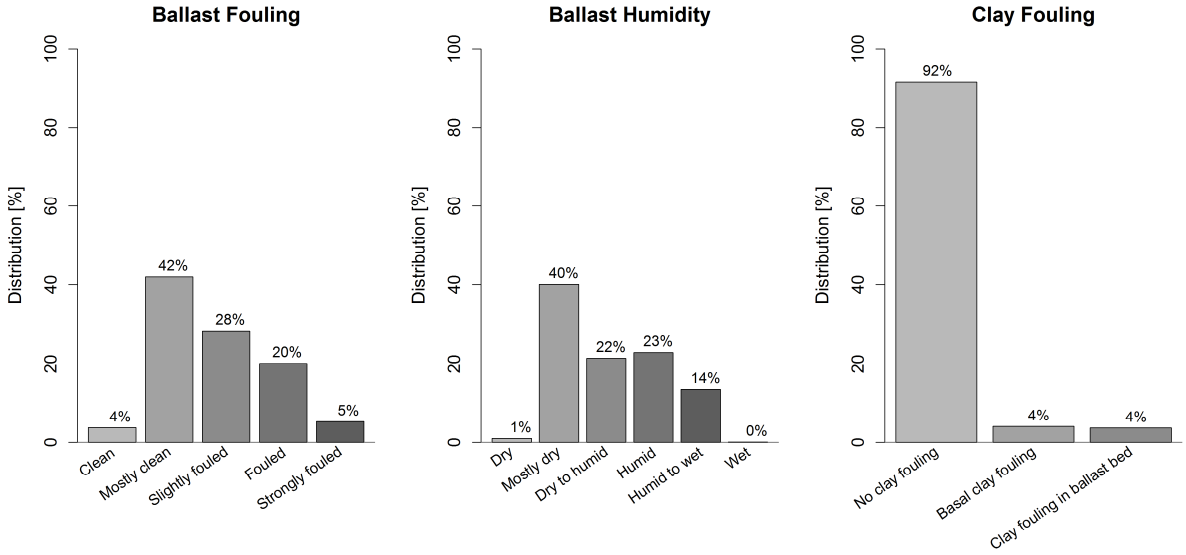

Figure 24 Distribution of GPR ballast parameters

The undulation of the ballast bed is of little cause for concern on the whole, since the ratings between *undulated to strongly undulated* and *settlement* (Figure 25) are only present in very few cases. Again, this shows that the optimal evaluation criterion is *de facto* not reached. Regarding the undulation of the intermediate layer, the criteria of *undulated to strongly undulated* are significantly more prevalent with ballast bed undulation. This is quite plausible, since this concerns the transition of the intermediate layer to the surrounding soil, which is typically only treated superficially.

Regarding the humidity, the rating *dry* is extremely rare. Moreover, the distribution of humidity indicates that there is more humidity in the intermediate layer compared to the track ballast. This may be attributed to the great variation in particle size distribution of the two layers, and is therefore regarded as plausible. The validation process (see 4.2.1.1) entails the detailed analysis of whether and how rainfall before and during the measurement influences these measurements.

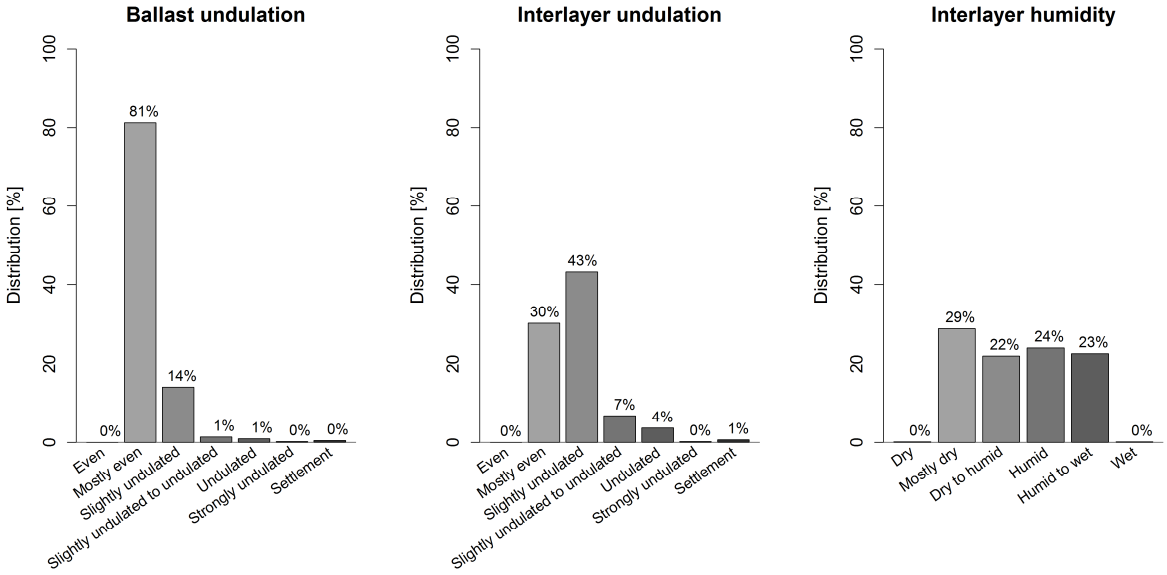

Figure 25 Distribution of GPR substructure/intermediate layer

The distribution of the detected formation layers (Figure 26) shows this effect for some 13% of cases. The nature of the formation layer is generally distinguished for Ground Penetrating Radar (GPR) runs. In the 160 km of sections with a detected formation layer, 120 km were specified as formation layer (PSS), and 40km as formation layer layer (TS).

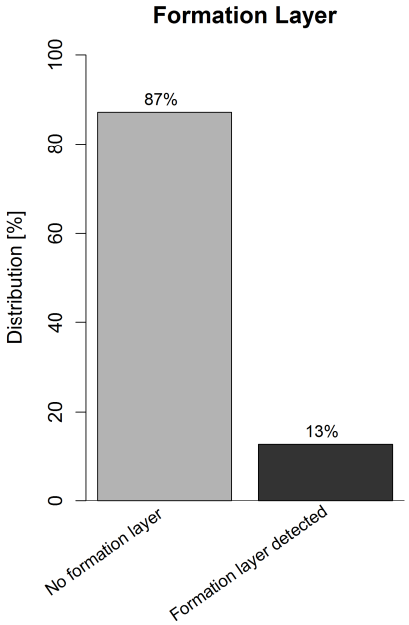

Figure 26 Distribution of GPR regarding detection of formation layer

Throughout the main network of the Austrian Federal Railways (ÖBB), 547 km of track substructure were renewed before 2007 [Auer et al. 2007]. These values, combined with the data regarding historic use of machinery and renewal from the TUG database (as of

2015), indicate that approximately 20% of track kilometres were subject to substructure renewal within the main network of Austrian Federal Railways (ÖBB). Ground Penetrating Radar was conducted on representative track sections with a length of 1,500 km; hence it can be assumed that this rate is also reflected. However, since GPR detected a formation layer for only 13% of the evaluated sections, the parameter formation layer will be analysed in more detail.

3.2.3.2 GPR formation layer recognition

Consultation with the provider of the GPR evaluation has revealed that a base court is reported as detected in the scope of a GPR run, if the following criteria are met:

- No longitudinal undulation
- Homogeneous layer of a specific thickness
- Clear separation layer between ballast bed and intermediate layer recognisable

These three requirements were selected and combined so as not to indicate presence of a formation layer in cases of doubt. Thus is to prevent confusion of solid and viable substructure with a built-in formation layer, while accepting that some areas with renewed substructure are not recognised as such.

As a result, elements such as bituminous formation layers are not always recognised, since aspects such as the thickness of the homogeneous layer (~ 30 cm) compared to a conventional formation layer are not present. Moreover, mixing of the formation layer with the ballast may recommence after several years in sections with particular difficult subsoil conditions. These sections have thus ceased to meet the above criteria, and are consequently no longer recognised as equipped with a formation layer.

The distribution of the time of formation rehabilitation for areas where a present formation layer was recognised or not is shown in Figure 27. This demonstrates that the formation layers correctly recognised by GPR were installed more recently. This confirms the assumption that formation layers are no longer recognised as soon as they lose their perfect initial quality, and thus cease to be clearly distinguishable from very good ground without substructure enhancement.

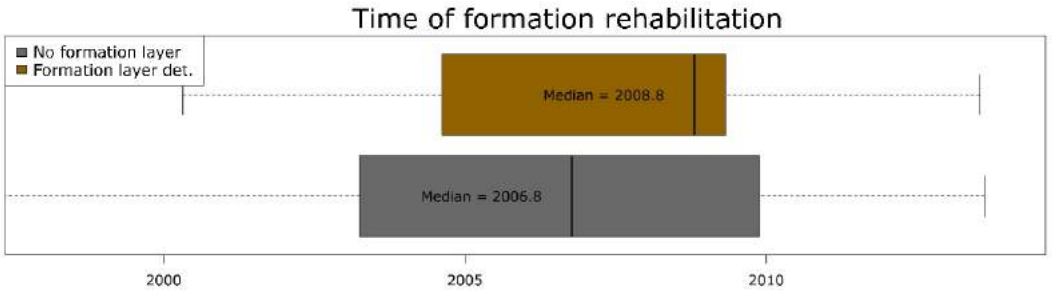

Figure 27 Timing of formation rehab. of recognised/unrecognised formation layers

Assuming that the GPR analyses fail to recognise a formation layer when it no longer fulfils its function perfectly, the track system would also be expected to be in worse condition in these sections. Accordingly, all sections that have undergone substructure enhancement since 2000 are examined in Figure 28. The aim was to find out whether areas where the formation layer was not recognised are actually in worse condition than the sections designated as having remediated substructure in the TUG database.

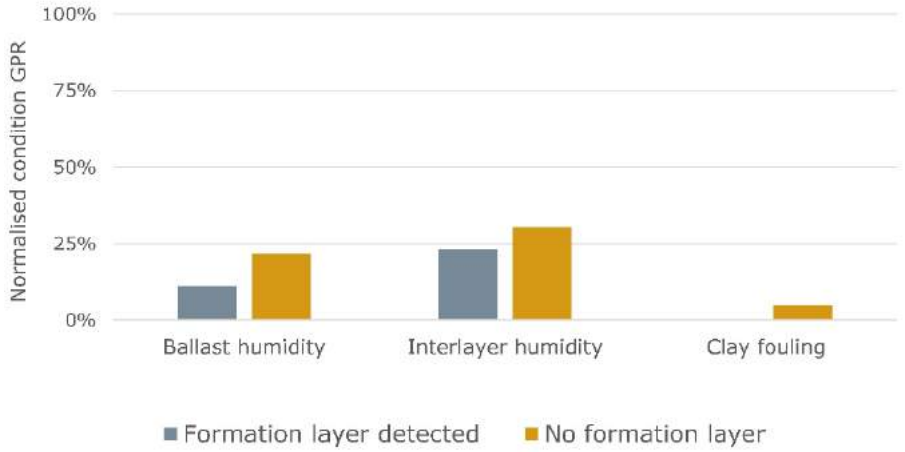

Figure 28 Condition of track system with remediated substructure for apparent/ unapparent formation layers

This demonstrates that the regions that are not recognised as having undergone substructure enhancement are clearly in worse condition evaluated by GPR. This is mainly due to the humidity in the intermediate layer, as well as the ballast bed. Furthermore, it also shows that few sections with clay fouling are only recognised where GPR indicates that no substructure improvement was executed.

Consequently, this indicates that adequately functioning formation layers are indeed recognised as such. However, sections where formation layers can no longer optimally meet its function are assessed by GPR as not having undergone substructure enhancement. This does not imply that the substructure condition is poor in these areas, but that the specific attributes qualifying for a formation layer are no longer present; this fact must be kept in mind when conducting condition analysis based on GPR results.

3.3 Other methods for determining the railway infrastructure condition

Apart from track geometry vehicle and GPR, a wide range of condition evaluation methods are used within railway infrastructure asset management: besides regular track inspections by professional staff, comprehensive geotechnical investigations are conducted, particularly in the context of reinvestment projects. The primary goal of such measures lies in detecting sections requiring subsoil enhancement. The investigations primarily entail three methods: (1) In-situ excavations to permit visual inspection of the structure of the soil layers; (2) examination of the particle size distribution of the ballast to assess the degree of contamination, and (3) plate-loading tests with a light drop-weight tester to determine the loading capacity of the surrounding soil [Auer et al. 2007].

Soil-mechanical cone penetration and the subsidence test vehicle are two further special detection methods in the scope of the validation process discussed below.

3.3.1 Soil-mechanical cone penetration test

Cone penetration tests (CPT) are used as an exploratory procedure in the context of track site investigation. The technique involves introducing a probe with conical tip (measuring cone) into the ground at constant speed. The bearing capacity of soil is determined based on the measured values of peak pressure and skin friction. Moreover, this method also allows for determining pore water pressure [Lunne et al. 1997].

As part of a pilot project in 2013 and 2014, rail-bound soil-mechanical CPTs were performed in order to investigate its feasibility of evaluating the loading capacity of the substructure and the nature of the surrounding soil. Excavators and a pressure sensor for the necessary ballast extraction are transported by special freight wagons. In a first step, a cladding tube is vibrated into the ballast bed, and the content is removed by rotary drilling. This permits introduction of the measuring cone into the surrounding soil, as well as examination of the extracted ballast samples.

Figure 29 Track-bound CPT (left: cladding tube driven in by vibration, centre: ballast extraction, right: pressure sensor)

The sampling takes around 20 min per examination point using the currently available assortment of rail-bound CPT technology. This methodology would therefore be suitable for evaluating specific track sections rather than network-wide application.

3.3.2 Subsidence test vehicle

In a conventional track geometry vehicle, all measuring equipment is situated directly on the vehicle sub-frame; consequently, the measurements refer to the track condition under train load. This is also appropriate, since all safety limits are referred to this load situation. However, one interesting parameter that is not measurable with an ordinary measuring car is the relative subsidence. This parameter mainly assesses the track stiffness. The necessary measuring equipment includes a vehicle with a load of 20 tonnes on the rear axle and two small measuring vehicles within a steel framework (Figure 30). This enables measuring of the relative subsidence between loaded and unloaded condition by using geometrical relationships [Luomala et al. 2014].

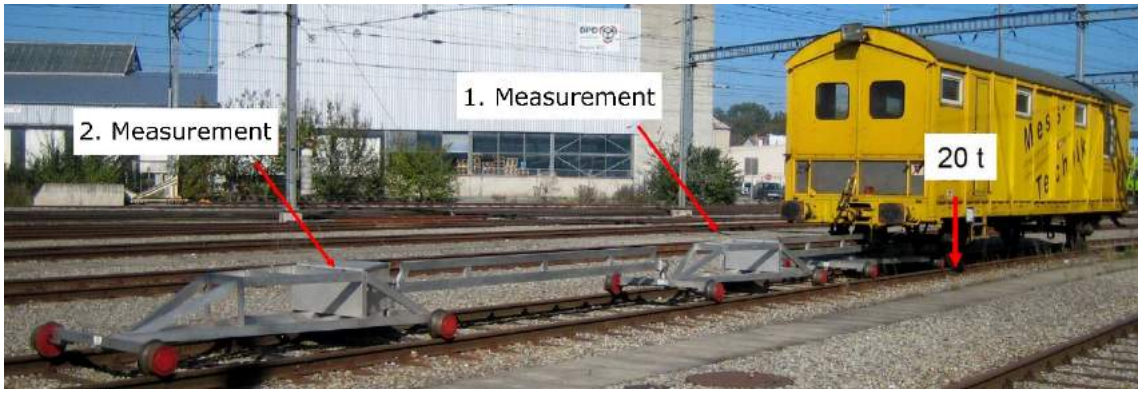

Figure 30 SBB subsidence test vehicle [according to Soldati 2013]

Typical subsidence values range from approximately 0.6 mm (ballast track with concrete sleeper) to around 2.0 mm (ballast track with concrete sleepers with USP) [Schilder 2013]. These values are also reflected in an exemplary representation of subsidence measurements for a five-kilometre section (Figure 31) performed by the Swiss Federal Railways (SBB) measuring team.

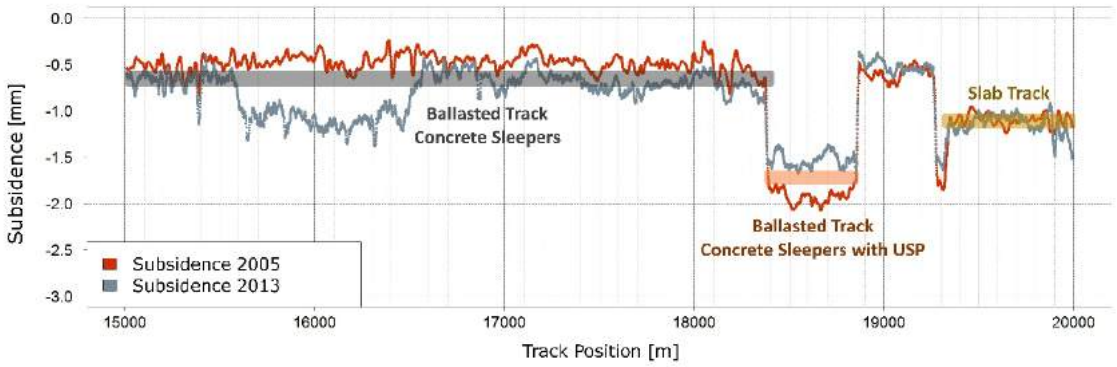

Figure 31 Representation of subsidence measurements

The variation in subsidence as a factor of the superstructure type is also reflected in the evaluation of the overall dataset (Figure 32), which covers around 55 km of track. Again, the concrete track without pads shows the least subsidence (median of around 0.7 mm), while track with under sleeper pads (USP) has the highest subsidence with a median of about 1.7 mm. The ranges for a slab track, which is used for tunnel sections, shows values between these two.

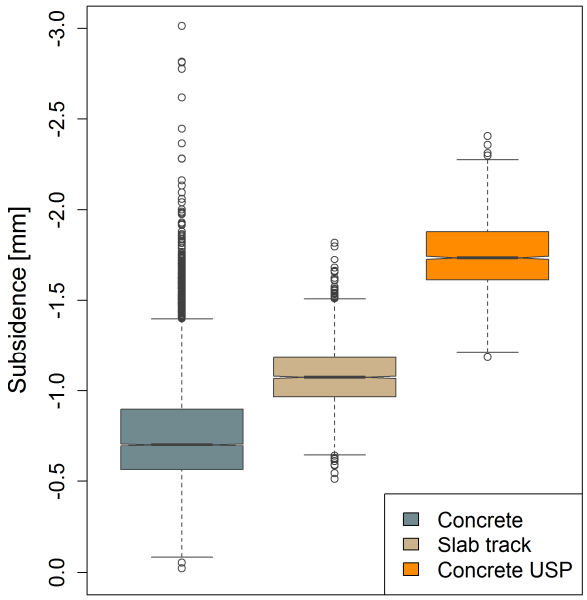

Figure 32 Subsidence for different superstructure types

4

Validation Process of the imported Analysis Methods

Within the present work, the various approaches of condition evaluation are based on a variety of different measurement methodologies, as explained in Chapter 3. In addition to geometry measurements using accelerometers or chord-based measuring (track geometry vehicle), geophysical measurement systems (GPR), geometric measurements (subsidence test vehicle), and a penetration of substructure (cone penetration test) are elaborated. Accordingly, the following question arises:

- Are the individual methods of condition evaluation capable of representing the real in-situ condition of track?

This question will be answered within the validation process conducted herein. For this purpose, network-wide analysis (input data for >100 km of tracks) and section-specific investigations, as well as comparisons with other measurement systems (input data for <100 km of tracks) are to be carried out. Conventional vertical track geometry analysis (see 3.1.1.3) plays a minor role, since its behaviour has already been subject of several research projects and publications [Hummitzsch 2009; Holzfeind 2009; Hansmann 2015; Esveld 2001; Auer 2004; Audley & Andrews 2013].

4.1 Network-wide validation process and trend analysis

Network-wide studies mostly involve stochastic analysis with the aim of explaining the influence of individual parameters and boundary conditions on the network-wide condition behaviour. Relevant methods are time series analyses and comparing evaluations of different detection methods before and after enhancement measures. This should yield information on whether the examined parameters correspond to the expected behaviour, and are thus capable of describing the behaviour.

4.1.1 The influence of different sleeper types

Different types of superstructure affect the infrastructure behaviour, and particularly wear in ballast and substructure. The network of the Austrian Federal Railways (ÖBB) is mainly equipped with a superstructure consisting of concrete sleepers (Figure 6), which has been the dominant technology since the 1970s.

However, within the past 15 years, concrete sleepers with under sleeper pads (USP) have caused a massive upheaval (see 2.3). The elastic properties of sleeper pads allow for a more continuous force transmission into the ballast bed. This is due to the enlarged contact surface and a significant reduction in pressures on the surrounding ballast layer [Freudenstein et al. 2011; Berghold 2016].

This change of (re)investment strategy regarding superstructure must be considered when examining the condition performance of various sleeper types in terms of fractal analysis and standard deviation for the modified gauge (SigModS).

Illustrating the parameters of fractal analysis for the different wavelength ranges (Figure 33) demonstrates the aforementioned good quality behaviour of concrete sleepers with USP for all sections. In the short wavelength range, wooden and concrete sleepers display nearly identical behaviour. This is due to the fact that the comparable age structure (Figure 8) correspondingly results in comparable wear in this wavelength range. While the increased values for concrete sleepers indicate inadequate interaction between sleeper and ballast and worn intermediate layers, wooden sleepers are mainly affected by the pressing in of the ribbed base plate into the sleeper body.

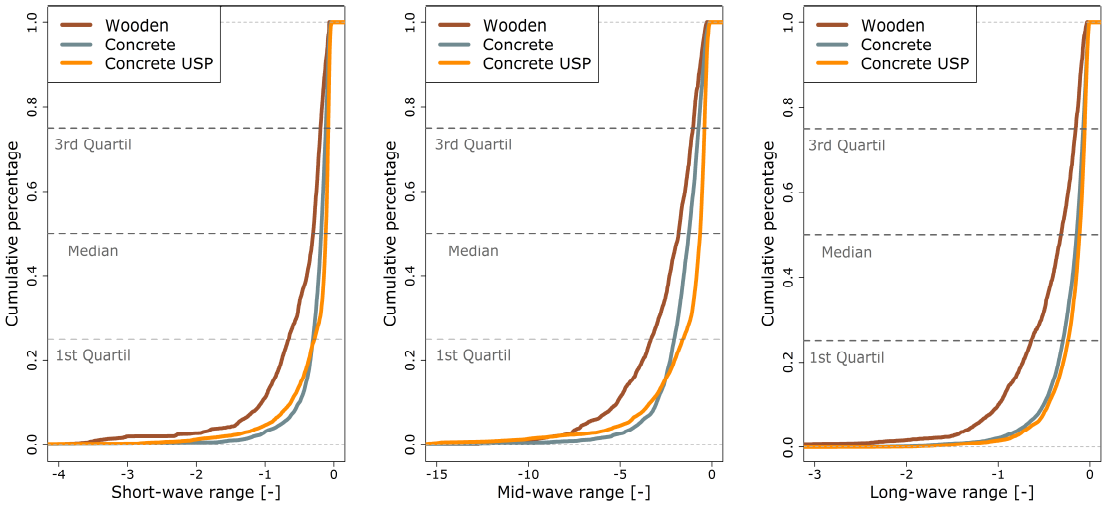

Figure 33 Sleeper-specific expression of fractal analysis

The medium-wave fractal range (Figure 33), however, clearly indicates that concrete sleepers (without USP) are in worst condition. This can be explained by the fact that concrete sleepers produce high stresses on the ballast bed due to their low elasticity, especially at the end of their service life when hanging sleepers (gaps between sleepers and ballast) cannot be avoided any longer. For this reason, there is a considerably greater ballast wear than with other sleeper types [Berghold 2016]. The long-wave fractal region, which represents the condition of the substructure, indicates the worst condition for wooden sleeper tracks, followed by concrete sleeper tracks. Due to their high average age and weight, the latter are naturally associated with suboptimal substructure condition. However, the fact that wooden sleepers are in worse condition despite their lower weight and increased elasticity is something of a surprise, even if their average age has a higher value (Figure 8). However, this may be explained by two boundary conditions: (1) Other than for their prescribed use (branch lines and tunnel areas with ballasted superstructure), wooden sleepers are currently used particularly for track sections with high variations in load capacity behaviour and/or low ballast bed thickness in the ÖBB track network - i.e. commonly on mountain sections; (2) In addition, around 550 km of subsoil were improved in combination with concrete sleeper installation between the years 1993 and 2007 alone [Auer et al. 2007]. These two circumstances necessarily mean that wooden sleepers are commonly installed in sections with poor structural condition, while concrete sleepers are typically combined with a formation layer, if required. This explains the slightly higher values in the long-wave fractal range for wooden sleepers.

Consideration of the impact of different sleeper types on the modified standard deviation for the gauge (SigModS) clearly shows a divergence between concrete and wooden sleepers (Figure 34). Due to the more rigid system, the former produce less jittering of the track

gauge signal. In this context, the behaviour of sleepers with USP is better than that of those without pads. The parameter discussed here primarily refers to the interaction between sleepers, rail pads and fastenings. In recent years, softer elements were installed in Austria, particularly when it comes to the padding layers, to make the overall system more flexible. However, this relates to concrete sleepers both with and without pads; the difference in cumulative frequency is thus also particularly explained by the difference in age distribution (Figure 8).

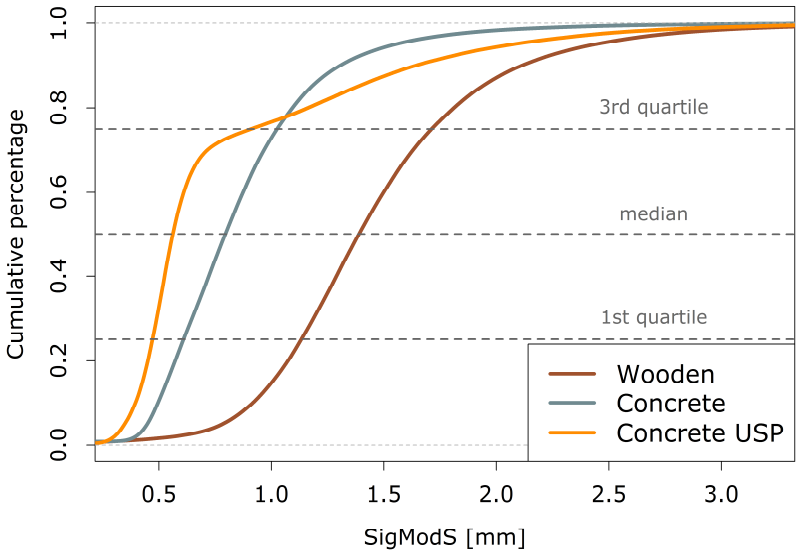

Figure 34 Sleeper-specific expression of SigModS

Wooden sleepers appear to be in significantly worse condition than concrete sleepers according to SigModS (Figure 34). This fact may be easily explained by the difference in component structure. While the padding is solely responsible for ensuring elastic behaviour between concrete sleepers and rails, wood is not as durable as concrete.

As a conclusion, it may be stated that the behaviour of different sleeper types is demonstrable both under fractal analysis and standard deviation of the modified gauge (SigModS) and follows logical patterns. Hence, this indicates that these types of track data analyses are able to evaluate the components condition.

4.1.2 Global behaviour over track service life

In order to answer the question whether the presented methods are capable of describing actual infrastructure state, it is crucial to analyse their behaviour over time. However, this analysis should not only consider track age, but also the loads on the various track sections. Accordingly, the temporal behaviour is not evaluated as a period in years, but rather as cumulative load (see 2.2). This is allocated to each cross-section in the database (see 2.2), enabling a trend analysis over the entire service life of the track, even though the measurement database merely contains quality signals for the past 15 years. It should be kept in mind that this does not yield a continuous temporal analysis of one and the same cross-section; rather, younger sections are represented by lower cumulative load values and older sections by higher values.

4.1.2.1 Fractal analysis

Fractal analysis enables for distinguishing specific wavelength-ranges within irregularities of track geometry (see 3.1.2). In this context, the theory that the short wavelength dimension could provide an insight into the sleeper condition, and thus the interaction between sleeper and ballast bed, has been formulated. The medium- or long-wave dimension ought to be capable of quantifying the ballast and substructure condition, respectively. The latter, insofar as it has been evaluated adequately, is expected to be subject to relatively minor deterioration over the service life. On the one hand, this may be explained by the fact that wear of superstructure components should not affect the substructure quality under favourable geotechnical conditions. On the other hand, insufficient loading capacity is compensated by sustainable substructure enhancement (i.e. for more than one set of tracks), while the overlying components are more exposed to direct wear, which limits their service life. Accordingly, a significant deterioration in the long wavelength range is more likely in sections with poor subsoil conditions, which have (yet) to be remediated, or where enhancement is difficult. The expected effects are shown in Figure 35: The short and medium wavelength dimensions are subject to significant deterioration for the cumulative load. This is visually represented by the sequence of box plots, each of which represents a value range of 25 million tonnes of cumulative load. The long wavelength dimension, however, shows an increase at the beginning of the cumulative load, which then remains almost constant over time.

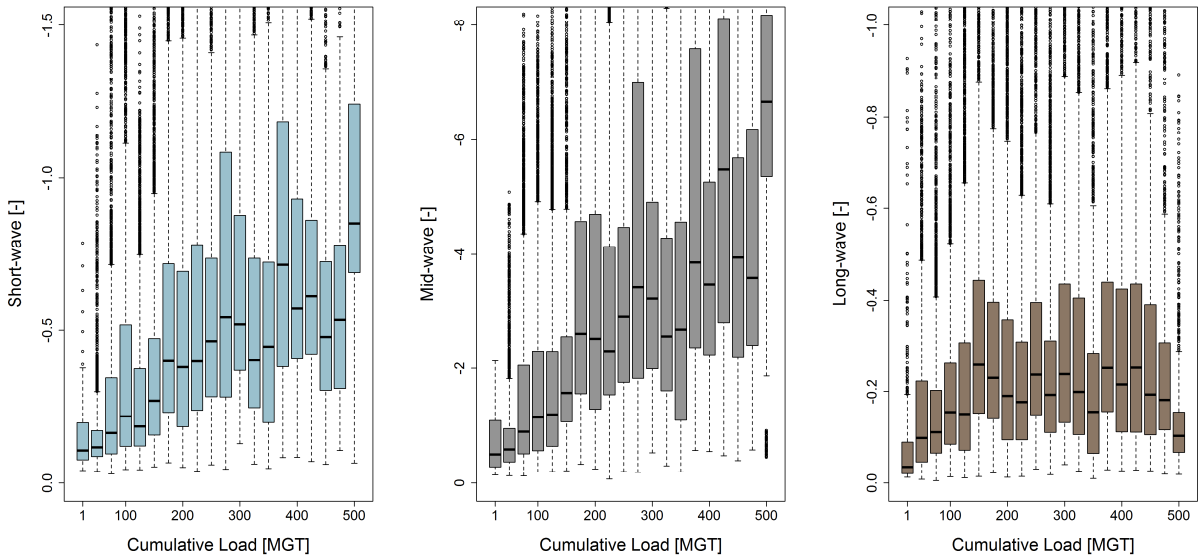

Figure 35 Fractal analysis of cumulative loads

Consideration of the long wavelength dimension in the context of sleeper-specific analysis (Figure 36), however, shows strongly diverging behaviour for different superstructure types, which are represented by the various smoothing curves. These so-called splines arise from piecewise polynomial functions with a smoothing factor of 0.8. In the background, box plots without a distinction by superstructure types are shown to facilitate comparison to Figure 35.

Concrete sleepers, with a dominant share of around two-thirds of the network, show the aforementioned constant course with regard to the long wavelength dimension. The wooden sleeper track, by contrast, shows significant deterioration similar to the short and medium-wave dimension. Again, this may be due to the fact that wooden sleepers are now primarily installed on mountainous lines, sections with extremely heterogeneous loading capacity behaviour and low ballast bed thickness. Accordingly, the fractal value for the long-wave dimension already starts at a relatively high level, and continuously deteriorates with increasing irregularities in the longitudinal level of track geometry. The newest technology, sleepers with Under Sleeper Pads (USP), clearly shows the optimal condition in terms of the long-wave fractal value, as expected. However, the analyses of this superstructure design are naturally only available for the first half of the expected service life at the present time, since the network-wide installation only commenced in 2005.

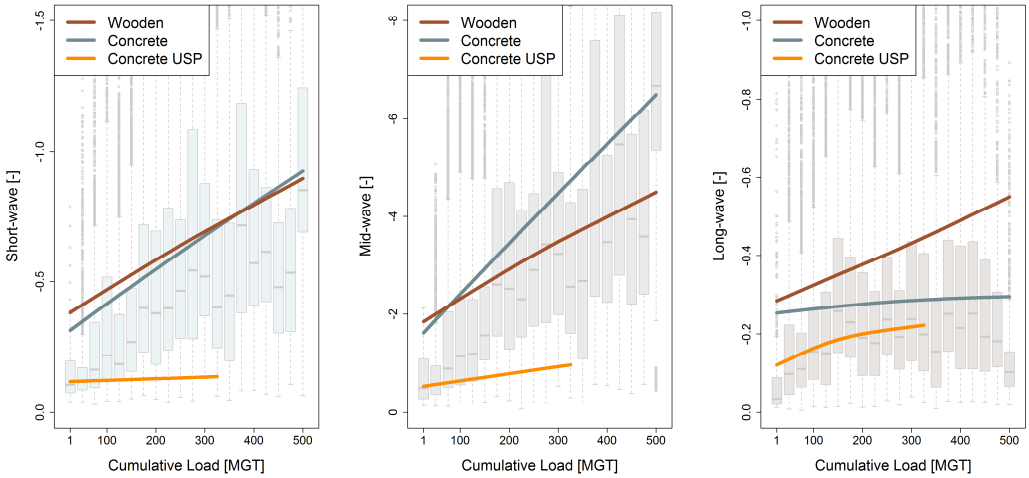

Figure 36 Fractal analysis of cumulative load by sleeper type

The excellent condition of sections with concrete sleepers equipped with USP is apparent both in the short and medium wavelength range (Figure 36). This is hardly surprising, since the elasticity introduced to the system is mitigated by the entire ballast bed. Accordingly, the medium-waved fractal dimension not only shows improved initial quality, but also a significantly reduced rate of deterioration compared to the other superstructure types. This mainly reflects the relatively high stress to the ballast bed from conventional concrete sleepers, which is in the worst condition according to the medium-wave fractal value. This is further amplified by the aforementioned fact that wooden sleepers are typically deployed for challenging and sometimes difficult boundary conditions. Nevertheless, the elasticity and associated increase in load transfer area of the wooden sleepers result in lower wear of the ballast bed and thus less ballast contamination.

The use of elastic under sleeper pads particularly results in significant reduction of contact stress between sleeper and top ballast layer [Freudenstein et al. 2011], which explains the good short-waved fractal values. This situation is certainly due to the fact that this superstructure system is used for Austria's most important sections. Thus, it can be assumed that the relevant components are sophisticated and specifically matched, such as rail fasteners, rail pads, and the like. Since the short-waved fractal dimension would be expected to describe this particular effective range as explained above, the detected condition is most likely not solely caused by under sleeper pads.

The fact that wooden sleepers are in a similar condition to conventional concrete sleepers may be explained by the effect that wooden sleepers tend to provide deteriorating traction with the extension of mounting holes and cracks in the sleeper. The pressing-in of base plates into the surrounding sleeper material also contributes to this effect [Schultheiss & Schulz 1985].

The quality signals for the short and medium wavelength fractal dimensions show a higher rate of deterioration over the service life of track compared to the long wavelength dimension. This confirms the assumption that wear is more significant for the components sleeper and ballast than is the case with substructure. In respect of the assessed components, superstructures with elastically padded sleepers (equipped with USP) are in the best condition. Conventional concrete sleepers, however, particularly show relatively poor condition for the medium wavelength fractal dimension, which may be attributed to the sub-optimal interaction between ballast and sleeper.

4.1.2.2 SigModS - standard deviation of modified gauge

The condition evaluation of sleepers or rather the interaction between rail and sleeper, takes place by calculation of the moving standard deviation of a low-pass filtered gauge signal (see 3.1.3) called SigModS. As is the case with fractal analysis, the temporal condition is to be assessed in consideration of cumulative load (see 2.2) by application of a simple linear regression of median values, each of which refers to 25 million tonnes of cumulative load. This shows the continuous deterioration of the signal with increasing load (Figure 37, left).

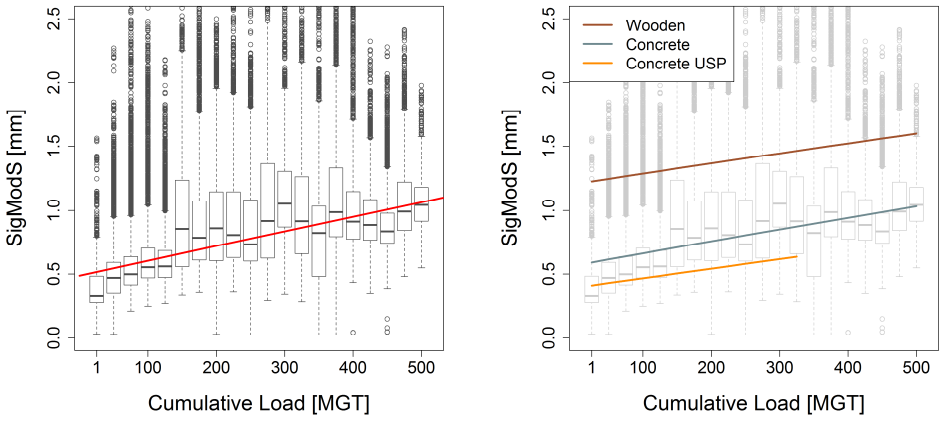

Figure 37 SigModS of cumulative load by sleeper type

Illustrating the behaviour of the specific superstructure types (Figure 37, right) clearly reveals the highest values for tracks with wooden sleepers. The lower signal noise thus demonstrated for concrete sleepers may be justified by the better resistance of the material to the introduced loads. This ensures adequate adhesion between sleeper screws and the sleeper itself, and prevention of sustainable damage to the track components, provided that the rail pad is replaced when necessary. The concrete sleepers with USP show similar behaviour patterns compared to conventional concrete sleepers, since the influence of the under sleeper pad assumes a minor role in the interaction between rails, rail fastening and sleeper.

4.1.3 Installation and renewal quality

Properly performed enhancement and renewal measures result in an improvement of initial quality in any asset. Naturally, this also applies to track components. In Austria, track renewal refers almost exclusively to the renewal of all components from the rails to the ballast bed. In addition, subsoil enhancement (USan) is carried out if loading capacity of the subsoil cannot be warranted.

Accordingly, to serve as useful tools, the measurement and quality signals for condition evaluation must be capable of recognising this qualitative difference. The following evaluations are based on the outcomes of GPR runs and fractal analysis, since a corresponding study of the standard deviation of modified gauge has already been carried out successfully [Hansmann 2015].

4.1.3.1 Fractal analysis of vertical track geometry

The assessment of the impact of renewal measures does not just relate to the last value before or the first value after renewal measures, since this methodology does not warrant the required robustness in respect of measurement outliers. Accordingly, the average of all measurements for a year before and a year after the renewal measure is used for comparison.

The results indicate that the fractal values of short and medium wavelength ranges show the expected significant improvement from the renewal measure (Figure 38). The improvement does not just affect the median value, but also and especially the deviation of the values, which shows that renewed sections display a homogeneous increase in quality. The improvement is almost identical for the two wavelength ranges. This reflects the complete replacement of the components described by these quality signals.

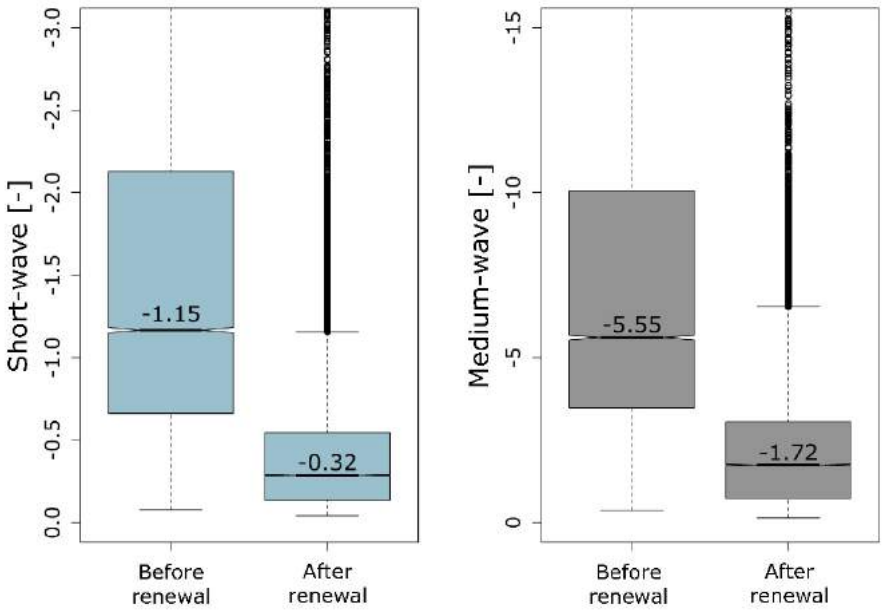

Figure 38 Short and medium wavelength fractal before and after track renewal

The long-wave fractal region and substructure quality ought to be analysed in more detail. In many cases, substructure is not explicitly treated, even though the contaminated transition layer between ballast and substructure is removed as part of ballast bed cleaning, and an adequate substructure is thus (re)produced. In addition to the loading capacity of the subsoil, the long-waved fractal dimension is also primarily affected by the condition, or rather, degree of contamination, of the transition layer. Track renewal measures should thus always result in an improvement for this quality signal. However, it is assumed that the quality improvement is greater if subsoil enhancement (USan) is performed as part of track renewal. Accordingly, the analysis of the installation or renewal quality is not limited to the general track renewal in this particular case of the long wavelength dimension. Rather, the installation/renewal qualities of track renewal distinguish between measures with or without subsoil enhancement. The renewal quality appears to be in significantly worse condition if the underlying subsoil was also remediated in the scope of track renewal (Figure 39). This confirms both the adequate operation of this analysis method and the decision of the asset manager to carry out subsoil enhancement in these areas.

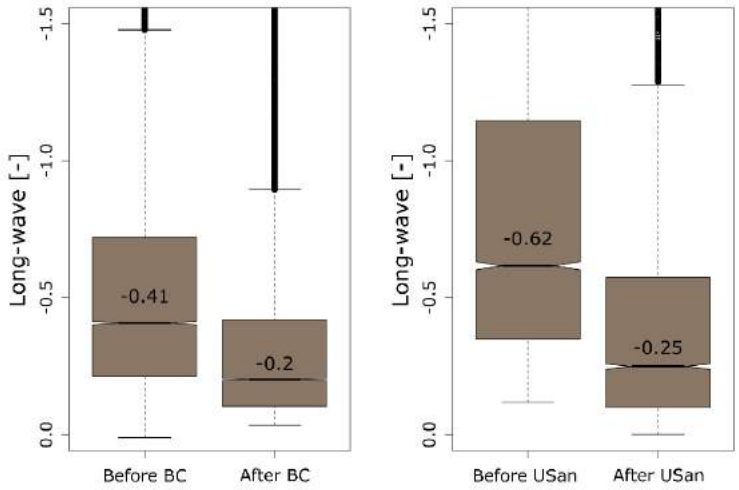

Figure 39 Long wavelength fractal before and after track renewal with substructure enhancement (USan) or ballast cleaning (BC) only

Another, albeit less significant, difference between the two methods of renewal is also manifested in the apparent initial quality after the measure (Figure 39). Ballast bed cleaning does not just yield a slightly better initial quality, but also less scatter. This is partly due to the fact that sections that do not require substructure enhancement are built on natural soil with the required loading capacity. These naturally occurring soil types, which are advantageous to railway transport, typically display excellent deformation moduli. On the other hand, it has been established that the loading capacity of the substructure improves by a factor of up to 2.0 within the 2000 days after formation layer installation, due to settling effects [Auer et al. 2007]. Accordingly, substructure enhancement delivers a sustained improvement in loading capacity, and the full effect on track geometry typically becomes apparent in due course [Vidovic 2016].

Nevertheless, an increased relative improvement of ballast bed cleaning (improvement factor of 2.0), as well as substructure enhancement (factor 2.5) is carried out in the scope of track renewal.

4.1.3.2 GPR

The outcomes of GPR analysis investigating renewed track sections are discussed below. Since this analysis methodology (see 3.2) entails parameters describing both ballast and substructure, this case also necessitates consideration of the execution type (with or without substructure enhancement). Previous substructure enhancement measures were mainly carried out before the bulk of GPR runs in the years 2012 to 2015. However, there are also cross-sections that were subject to substructure enhancement after GPR analysis. This permits an analysis of whether the track sections requiring improvement are in worse condition than the sections that were previously renewed according to GPR. However, in

contrast to fractal analysis, the installation and renewal quality of the same cross-section cannot be assessed. This is due to the fact that only a short stretch (50 km) was subject to two GPR runs; this stretch will be treated in more detail (see 4.2.1). Cross-sections used for determining installation or renewal quality in the following analysis have been subjected to a GPR run within one year before or after the renewal measure.

Insofar as substructure enhancement was omitted during track renewals, the condition of the track before a reinvestment should be better than for those deemed to require enhancement. Figure 40 confirms this assumption as both the intermediate layer and ballast bed contain significantly less humidity, if ballast bed cleaning was considered sufficient in the scope of project planning.

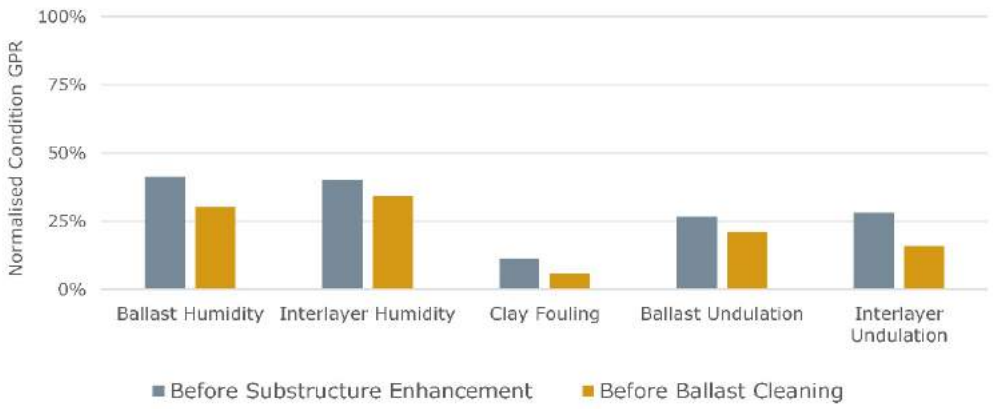

Figure 40 GPR before renewal: substructure remediated vs. ballast cleaned

A similar picture emerges in respect of undulation and clay fouling. If the geotechnical experts recommended substructure enhancement, the GPR indicates a higher clay fouling and undulation of ballast bed and intermediate layer for these sections.

An overview of the humidity parameters shows slightly different behaviour patterns before after and subsoil enhancement (Figure 41). The humidity of the intermediate layer, but, above all, the humidity of the track ballast shows the positive impact of substructure enhancement (USan) or rather track renewal on the humidity content of the track body. This may be considered as unequivocal evidence that the GPR provides an accurate description of the track body. However, the reduction in humidity content is much higher when it comes to ballast than with the intermediate layer. This is certainly largely due to the fact that the ballast is entirely replaced in the scope of renewal measures with substructure enhancement, while the intermediate layer is remediated or rather provided with recovered materials (recycled ballast). Furthermore, the formation layer is already installed with a specific humidity content at an optimal 7.4% [Schilder & Piereder 2000].

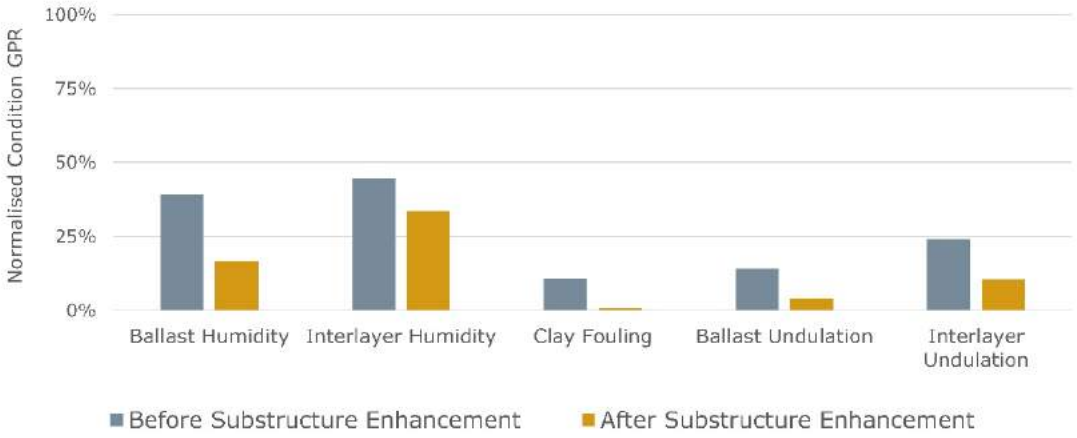

Figure 41 Condition according to GPR before and after track renewal with substructure enhancement

The *clay fouling* parameter is of essential importance to the substructure. This shows that the analyses of the GPR, and the implementation of the subsoil enhancement, can be considered effective. While *basal* or high *clay fouling* were detected before AHM deployments (substructure enhancement machine used in Austria), the measure has removed the clay almost entirely.

4.1.4 The effects of water on the track body

One of the essential advantages of infrastructure evaluation using GPR (see 3.2) is the fact that this methodology is capable of detecting water molecules in the individual layers. This permits conclusions about the drainage condition of the infrastructure, since If the ballast bed or an intermediate layer is detected as moist on basis of Ground Penetrating Radar (GPR) this points to an inadequate drainage condition. In this case, the parameter *Ballast Humidity* is linked with *Interlayer Humidity* for evaluating drainage condition. Subsequently, cross-sections in the lower quartile, i.e. the "wettest" 25%, are classified as been equipped with a poor drainage. The classification good drainage is thus attributed to the top quartile, i.e. the "driest" 25%.

An analysis of the drainage condition using the ground penetrating radar in comparison to fractal analysis (see 3.1.2) shows the advantage of the special method of fractal analysis in contrast to conventional forms of track geometry analysis. Figure 42 demonstrates that poorly drained areas display a moderate increase in the medium-wave fractal range (15%), while the long-wave range is significantly higher (around 40%). In this context, the points within the scatterplot each represent a cross-section, which is described by a fractal value in the medium-wave and long-wave dimension. Due to the effects of gravity, an increased water volume in the track body migrates downward, i.e. to the intermediate layer or the

subsoil. Accordingly, it must be presumed from a technical perspective that an increased water volume has a negative effect on the loading capacity of the substructure. The above-average rise in the long-wave fractal range thus confirms that it serves as a realistic indicator of the substructure condition, which is negatively affected by the water ingress among other factors. The evaluated sections with concrete sleepers have an almost identical age structure (Figure 42, right) in both cases (both good and poor drainage), which means the section with this track system is a good example; a distortion of outcomes due to different age distributions can be excluded.

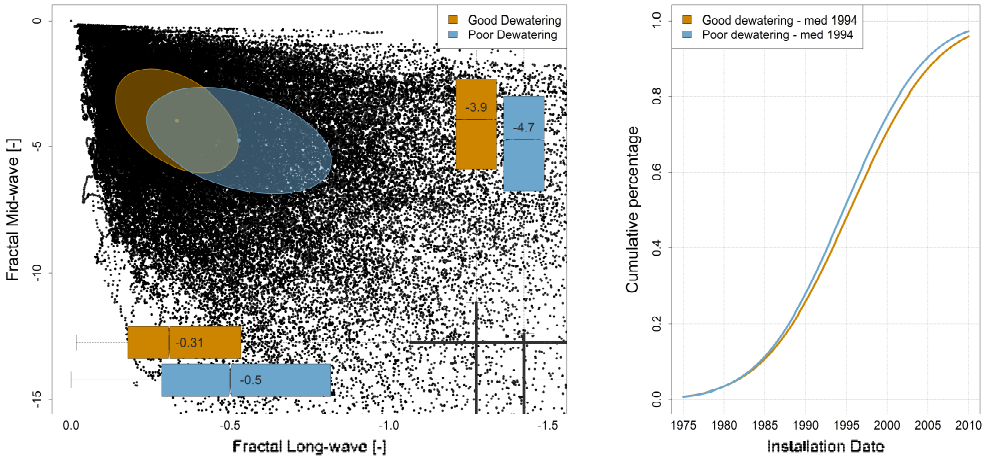

Figure 42 Influence on drainage in the scope of fractal analysis, concrete sleepers

In the following, the different quality conditions of the drainage behaviour will also be compared with the results of conventional track geometry analysis. Naturally, the age distribution of concrete sleepers inherently remains the same, since the same population is used for the analysis. The results show that the standard deviation of both the longitudinal level and the deterioration rate respond to the condition of the drainage system (Figure 43). In contrast to fractal analysis, the correlation is not significantly stronger for either of the two parameters.

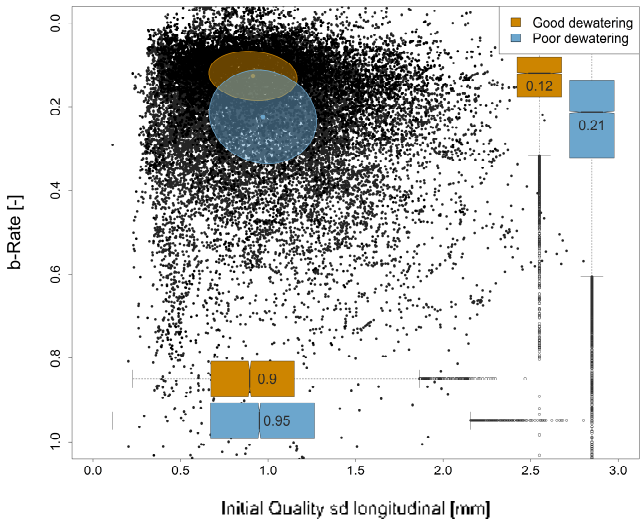

Figure 43 Influence on drainage on track geometry, concrete sleepers

Accordingly, this shows the impact of impaired drainage capacity of the track body on its condition. On the other hand, this example demonstrates what additional information may be derived from fractal analysis of the vertical track geometry. While conventional track geometry analysis only provides a limited representation of the negative effects on the substructure, fractal analysis shows that the loss of loading capacity becomes quantifiable by the long wavelength dimension of this analysis method.

4.2 Section-specific validations of the individual measurement methods

In the scope of section-specific analyses, parameters and detection methods are analysed that are primarily feasible for sections of less than 100 km, especially due to the speed and duration of the respective evaluation method. Furthermore, fractal analysis, GPR and standard deviation of modified gauge (SigModS) are compared with these evaluation methods. It has already been demonstrated that the outlined methods of analyses show plausible results in network-wide comparison. The following evaluations are intended to verify whether these methods are also capable of describing the section-specific condition of the infrastructure.

4.2.1 Time series of GPR evaluation

In 2015, 55 km of track were subject to GPR inspection, which had already been evaluated in 2012. This permits time series analyses of the condition evaluation conducted by GPR. A track section with significant quality differences was selected to cover trends of different quality levels. Moreover, the chosen track range also includes sections that were renewed between 2012 and 2015. Thus, the effect of track renewal on GPR evaluations can also be analysed.

4.2.1.1 Evaluation criterion humidity

The expected change over time for the entire, repeatedly evaluated, track section would be expected to show continuous deterioration of the parameters. Even though maintenance activities and track renewal measures were implemented for specific sections, this should not affect the overall trend for the entire section.

An analysis of the development regarding the humidity parameters for 2012 until 2015 shows the expected deterioration in the condition (Figure 44). Firstly, the parameter *ballast humidity* (Figure 44, left) displays a continuous increase in humidity according to GPR, since the maximum value of the density curve has merely shifted horizontally. The mean changes from 2.3 (dry to moist, see Figure 23) to 3.0 (wet). This can mainly be explained by the fact that the fraction of fine particles in the ballast bed increases continuously. The higher that fine-grained fraction, the more water molecules can penetrate the ballast bed, which ultimately raises the humidity content. Also, the intermediate layer shows an increase in humidity content (Figure 44, right), which is more strongly expressed than in the ballast bed over the investigation period. The intermediate layer is already classed as moist to wet for the reference track section (Figure 23). A proportionally higher humidity gain than in the ballast bed would seem reasonable, since the intermediate layer is excessively stressed when the track ballast can no longer perform its drainage function adequately.

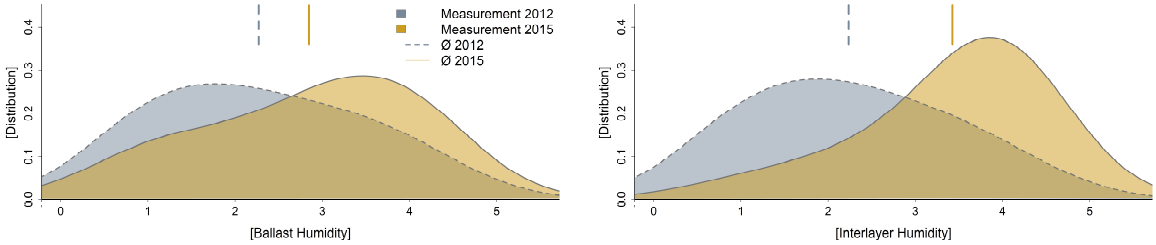

Figure 44 Time series GPR humidity content

Nevertheless, the development of humidity in the intermediate layer is surprisingly intense. For this reason, the precipitation volumes of two nearby weather stations were analysed for the relevant measurement week (Figure 45). The data shows that no excessive rainfall was recorded in the days before, however, moderate to severe precipitation was reported by nearby weather stations on the day of measurement [Koppe & Stozek 1999].

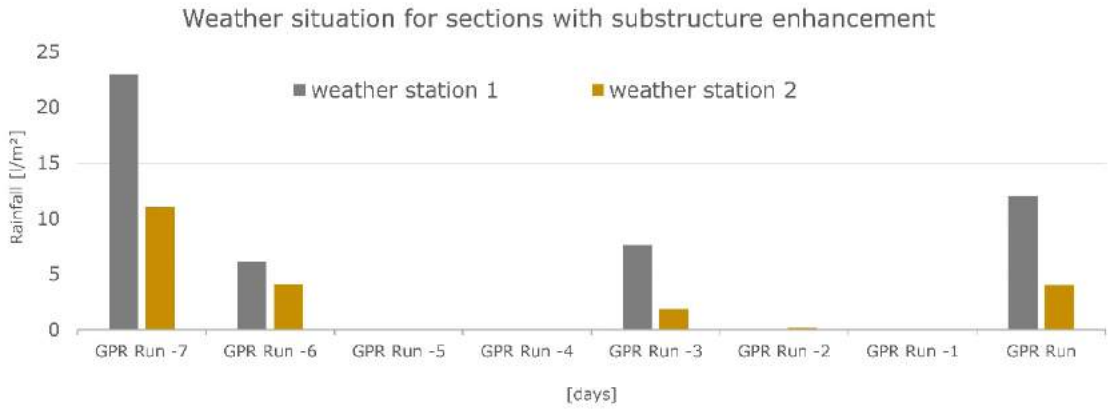

Figure 45 Weather query GPR 2015 [http://at.wetter.com/]

The track images recorded during the GPR run (Figure 46) also indicate that it had rained recently, and the route (see especially concrete sleepers on the right) was drying at the time. Accordingly, it can be assumed that the moderate increase in the ballast bed corresponds to the real condition, since this had already drained the water downwards. However, the intermediate layer seems to be affected by the precipitation.

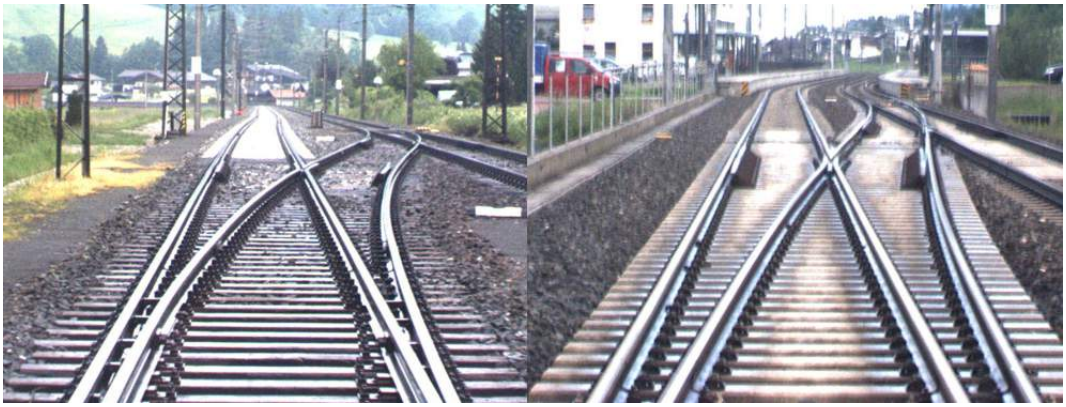

Figure 46 Track images for detecting precipitation, GPRO run 2015

Thus, it must be presumed that precipitation immediately before the measurement (less than 60 min) tends to affect the humidity measurement for the intermediate layer. Or to put it in other words: The GPR measures the actual condition at that time but due to the precipitation this condition does not represent a comparable measurement in regards to time series analyses. For the 55 km of GPR runs, it must accordingly be taken into consideration that this parameter is elevated due to this fact. For the purposes of excluding such effects over the entire GPR-measured network, a review of the influence of weather conditions for all track sections investigated by a single GPR run (approximately 1,400 track km) will be conducted at this point.

Digression: Network-wide analysis of weather influence on GPR measurements

For the in-depth analysis, weather data for the respective periods along all relevant track sections were requested from the "Zentralanstalt für Meteorologie und Geodynamik" (ZAMG). The humidity content and precipitation volume data were prepared starting as early as seven days prior to the run. Humidity does not appear to have biased the network-wide GPR measurements (Figure 47). The recognisable anomalies are attributable to varying characteristics of the track sections. For instance, route 8 shows the highest humidity content in ballast and track substructure according to GPR values. This is because this track is mainly a mountainous route, resulting in a difficult drainage situation. Route 14, in turn, is largely equipped with a bituminous formation layer, which typically has exceptionally good drainage characteristics. The positive GPR values reflect this circumstance accurately.

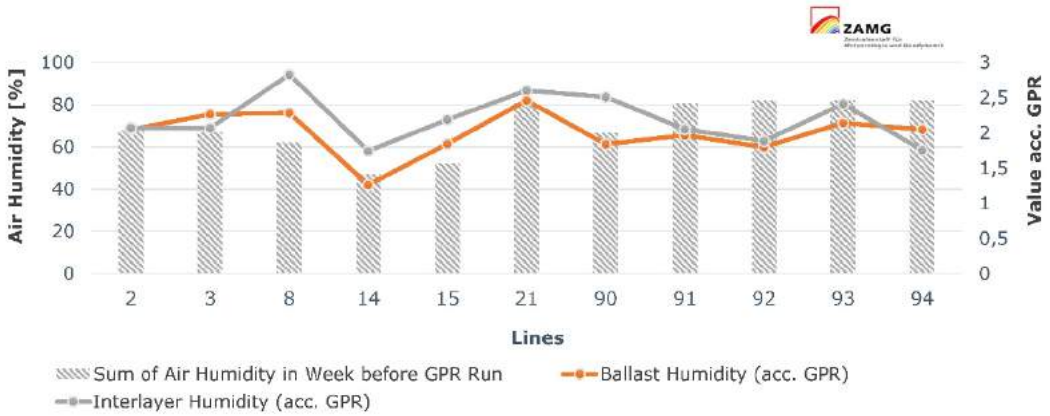

Figure 47 Comparison of humidity and GPR measurements

The measured precipitation volumes were generally low (Figure 48), considering the fact that a heavy rain event is defined as more than 4 l/m² per hour [Koppe & Stozek 1999]. This evaluation revealed that route 8 was exposed to the greatest rainfall with a sum of 1.58 l/m² in the seven days leading up to the GPR run. The most recent rainfall event of relevance to the GPR measurements took place on route 15 around twelve hours prior to the measurement run. The fact that the GPR values are subject to a significant fluctuation, which is seemingly not correlated with precipitation in all route sections, thus indicates that the prevailing weather conditions had no significant effect these on measurements.

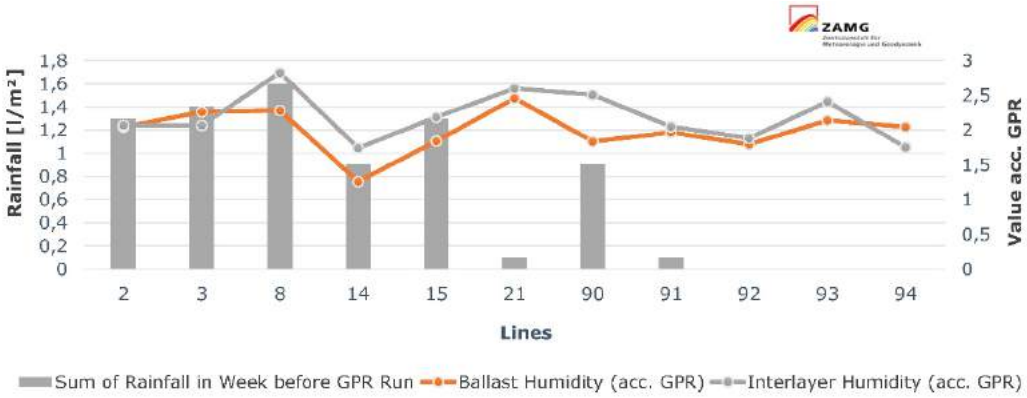

Figure 48 Comparison of rainfall in measurement week and GPR values

Furthermore, the routes 21 and 91, and 92, 93 and 94 are all in the same region and were therefore evaluated on the same day, and thus under identical weather conditions. The results of GPR measurement show that there are significant differences, particularly between routes 21 and 91, and 92 and 93. This, in turn, indicates that the GPR evaluation in terms of humidity of the track substructure and ballast is not dependent on weather conditions, but on the actual condition of the specific track sections.

The findings of the aforementioned time-series analysis (Figure 44) and the previous network-wide analysis indicate the following in respect of the influence of weather conditions: Rain events during or shortly prior to the GPR run appear to have a minor effect on the humidity measurement in the substructure; these sections were thus not taken into account for the following, network-wide correlation analyses. The humidity content of the ballast bed seemingly remains unaffected. Rain events more than twelve hours before measurement appear to have no influence on GPR evaluation.

4.2.1.2 The evaluation criteria of contamination, clay fouling and undulation

Results in respect of the contamination of the track ballast or clay fouling of the intermediate layser are divergent. The parameter *ballast fouling* is subject to significant deterioration during the three-year investigation period (Figure 49, left). This supports the previously proposed theory that the humidity content of track ballast increases due to increased fine particle content, among other factors. The parameter of *clay fouling*, on the other hand, shows an almost identical distribution in 2015 compared to three years earlier (Figure 49, right). The average values indicate that the deterioration was only marginal. This may be because a clay layer in the track body is mainly affected by the soil-mechanical properties of the affected track layers. The wear caused by the loads introduced plays a relatively minor role in this context. This applies if the section shows a good general substructure behaviour. Any influence of the aforementioned precipitation the night before (Figure 45) can be ruled out for these parameters.

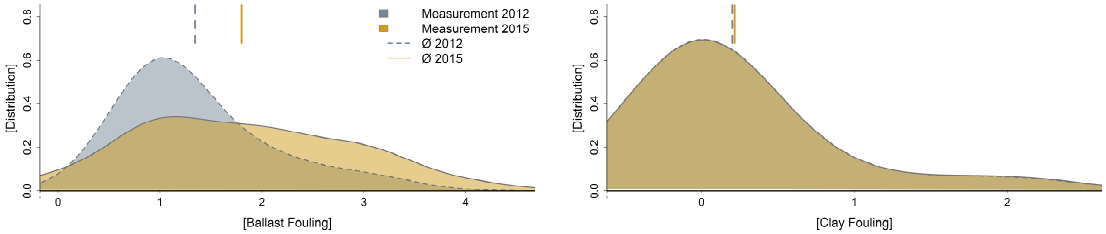

Figure 49 Time series GPR contamination

The soil-mechanical structure along a railway track is subject to a certain degree of inhomogeneity. This is mainly due to the natural composition of soil, as well as different route elements, such as embankments and trenches. This is also caused by the fact that some sections were subject to terrain improvement or subsoil enhancement. The changes in soil-mechanical properties result in a variation in loading capacity, which subsequently leads to inhomogeneous subsidence in the intermediate layer. As part of the infrastructure condition evaluation by GPR, the inhomogeneous subsidence is referred to as undulation. The undulation of the ballast bed would be expected to be minimal after track renewal measures, in particular, if executed with substructure enhancement. Over time, however, the value increases, unless comprehensive maintenance measures were carried out. This very increase is shown in Figure 50 as a deterioration in the parameters of *ballast bed* and *intermediate layer undulation*. Here, the undulation of the intermediate layer is subject to greater deterioration, which may be due to the higher increase in humidity content in this area (Figure 44).

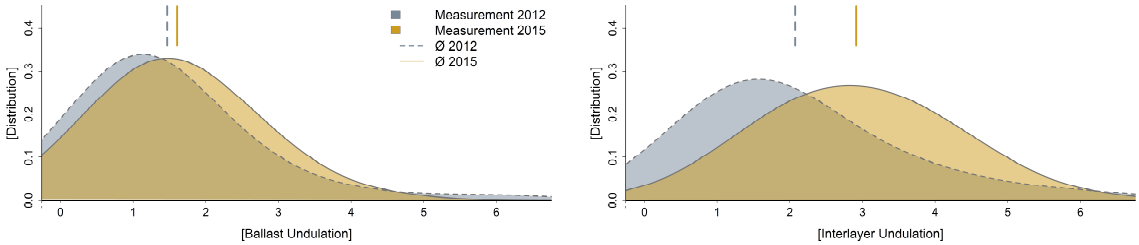

Figure 50 Time series GPR undulation

Again, an effect of the previously discussed precipitation on the degradation behaviour of the parameters relating to undulation may be precluded in this case.

4.2.2 Effects of maintenance measures

In addition to the previously investigated installation or renewal quality for the respective methods of analysis (see 4.1.3), the effects of maintenance activities on quality are naturally also of importance. This places conflicting expectations on the tools of analysis. The standard deviation of the modified gauge (SigModS) describes the noise of the gauge signal, and thus primarily the adhesion or rather the load transfer between rails, rail fastening and sleeper. If the sleeper material has therefore not yet been seriously damaged, maintenance measures must necessarily result in an improvement of the quality signal. However, fractal analysis primarily describes the ballast condition or the substructure quality. Since conventional tamping operations correct the track geometry without affecting the condition of the latter two components, this type of maintenance measure should only affect the fractal analysis to a minor extent. Since no sufficient time series are available for GPR evaluations, this method cannot be carried out for this evaluation methodology.

In this context, the impact of maintenance measures on the standard deviation of the modified gauge (SigModS) is examined for sections of a mountainous route with narrow curves. The infrastructure operator supplied detailed maintenance records for these sections. The areas with the smallest radii are naturally equipped with wooden sleepers (Table 3). The maintenance task consisted of replacement of fastenings. The concrete sleepers in areas with slightly larger radii were subjected to comprehensive padding replacement.

Sleeper type	Length	Median radius	Maintenance activities; date
Wood	675 m	189 m	Replacement baseplate, screw hook and spring washer; autumn 2012
Concrete	2250 m	575 m	Replacement of padding; autumn 2012

Table 3 List of maintenance activities for sleepers in curve sections

The analysis (Figure 51, right) – as expected – shows very high values for wooden sleepers in tight curves. In addition to material properties of the wooden sleepers, this is also due to their installation with rail joints in tight curves. Both the overall quality level of the wooden sleepers, as well as their deterioration, are thus quite significant. However, the measure executed in 2012 was correspondingly rather effective. The analyses of areas equipped with concrete sleepers show a much better quality level. This is of course due to the material properties of the concrete sleepers, but also because the radii in this area are not that narrow. The quality before the exchange of rail pads for concrete sleepers (Figure 51, left) of around 1.2 mm SigModS correspond to limits that were previously proposed [Hansmann 2015] to prevent lasting damage to the sleeper material.

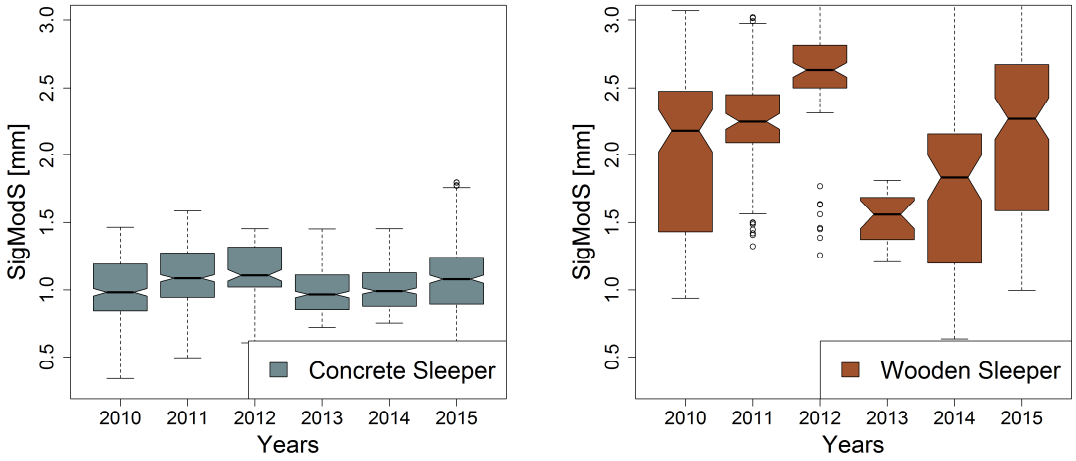

Figure 51 Influence of padding replacement on concrete and wooden sleepers

Therefore, it can be stated that the maintenance measures were recognised in the scope of time-series analysis of the quality signal SigModS. As mentioned above, the expectations for the time series for fractal analysis are entirely different. If fractal analysis is indeed capable of describing the condition of the ballast bed and substructure, it should only be affected to a minor extent by maintenance measures, such as the tamping operations in the present case. This assumption was tested using regression algorithms for the fractal analysis (see 3.1.2) and the standard deviation of longitudinal level (sigmaH) (see 3.1.1). The latter is used as an indicator for required tamping operations, and is accordingly strongly affected by them. This is also reflected in the example cross-section (Figure 52, right), which was subject to two tamping operations after track installation in autumn 2009. These maintenance activities and the achieved improvement are clearly visible in the quality signal. In contrast, both the medium- and long-wave fractal area (Figure 52, left) show a relatively constant progression over time, which is not related to the volume of maintenance activities. This seems to confirm that fractal analysis is not affected much by short-term improvements to track geometry in form of tamping operations, and is thus capable of describing the substantial condition of track.

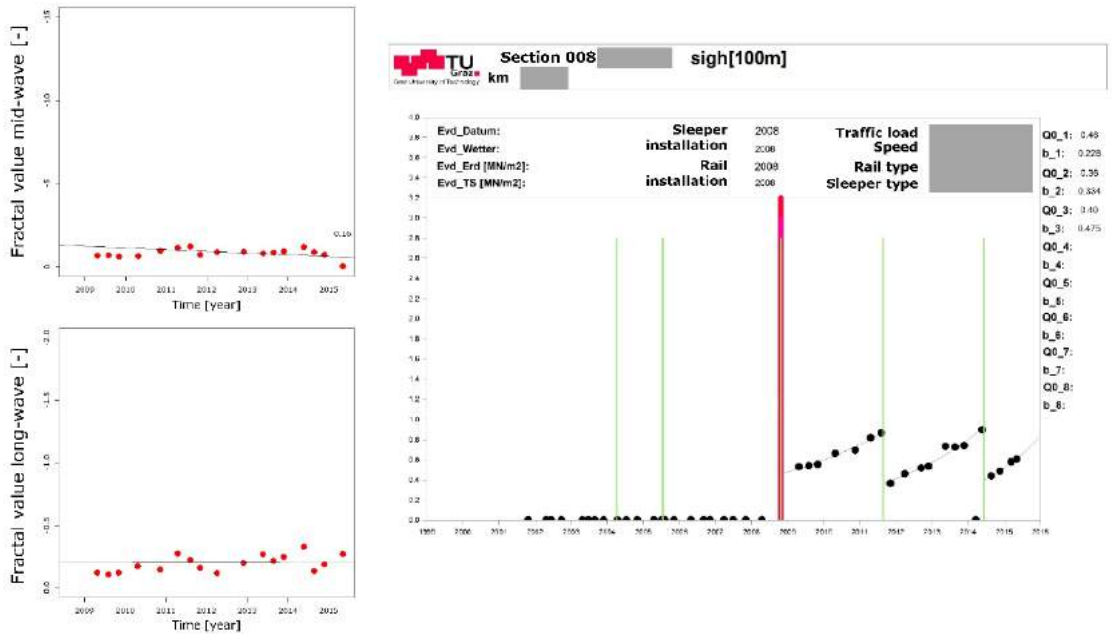

Figure 52 Comparison of the regression algorithm for fractal analysis and sigmaH

However, since this statement cannot be based on a single track cross-section, 20 km of an Austrian main route were analysed for this aspect. The study investigated how many improvements through maintenance measures (number of regressions) were detected on the basis of sigmaH or fractal analysis for medium and long wavelengths. The algorithm determined around 5,500 regressions in 4,000 examined cross-sections in the scope of fractal analysis (Figure 53, left). The medium-wave range responded slightly more sensitively to tamping operations than the long-wave fractal dimension. However, the algorithm-based number of regressions in the scope of sigmaH evaluation came to more than 14,000. Accordingly, conventional track geometry analysis recognises the effects of 2.5 machine deployments per cross-section since 2005 (Figure 53, right). Fractal analysis, on the other hand, only indicated machine deployments on half of the cross-sections. However, this may be partially due to the effect from ballast supplementation in the scope of tamping operations. This method is used particularly if the track geometry of a section is very poor, since the addition of new ballast is the only way to achieve sustainable elevation, and thus to improve track geometry quality. Accordingly, this measure is also apparent in the quality signal from fractal analysis.

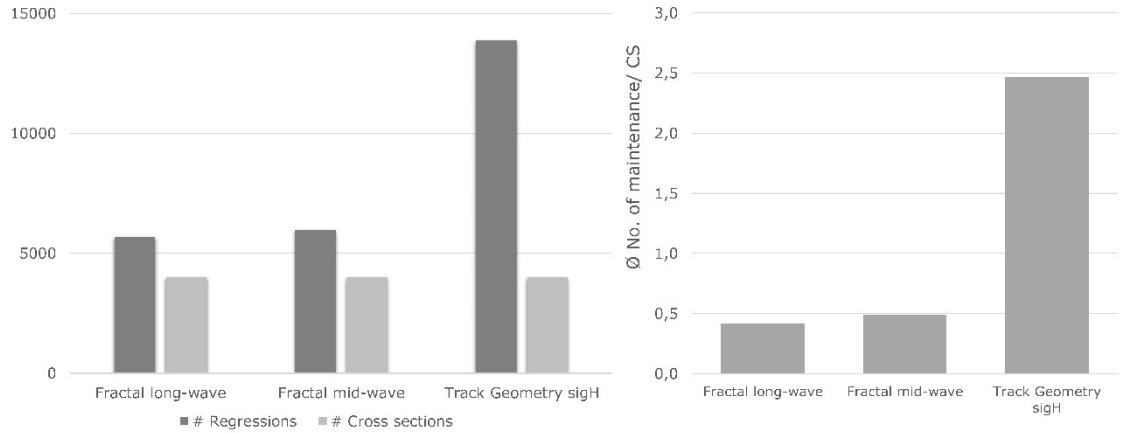

Figure 53 Effects of maintenance activities on fractal analysis

The above-formulated assumption that fractal analysis describes the substantial condition of ballast bed and substructure can thus be confirmed.

4.2.3 Evaluations of GPR and fractal analysis versus CPT

As part of a pilot project, three sections were sampled using soil-mechanical cone penetration test (see 3.3.1). Thereof, the two sections A and B will be considered in more detail as part of this study. These two sections are distinguished by the availability of reference values with GPR evaluation and/or fractal analysis. In addition to the evaluation of the soil-mechanical findings, the latter were also correlated against the results of the measurement data in the TUG database.

Due to the prior ballast extraction, the medium-wave range of fractal analysis is naturally not suitable for this comparison; accordingly, only the long-wave range, which describes the substructure or rather subsoil of the section, was examined. A qualitative representation of results for cone penetration tests evaluated by the Institute of Soil Mechanics and Foundation Engineering (TU Graz) is shown at the top of Figure 54. This method covers sections 1, 2 and 4, since the TUG database does not contain track geometry data for section 2 meaning that fractal analyses cannot be calculated for this section. Section 3, as highlighted in green, still appears to have proportionally good cone resistance values at a depth of one to two metres below the rail level, and thus has a good loading capacity. This also applies to a depth greater than two metres to a lesser degree. Section 1, however, shows lower resistance values in the upper area, but also virtually no cone resistance beyond a depth of two metres; this section is thus definitely in worse shape. However, by far the worst condition as indicated by soil-mechanical cone penetration testing appears to be section 4. Here, only very low cone resistance was measured right from the outset, which fell to nearly zero MPa at a depth of around 1.5 m.

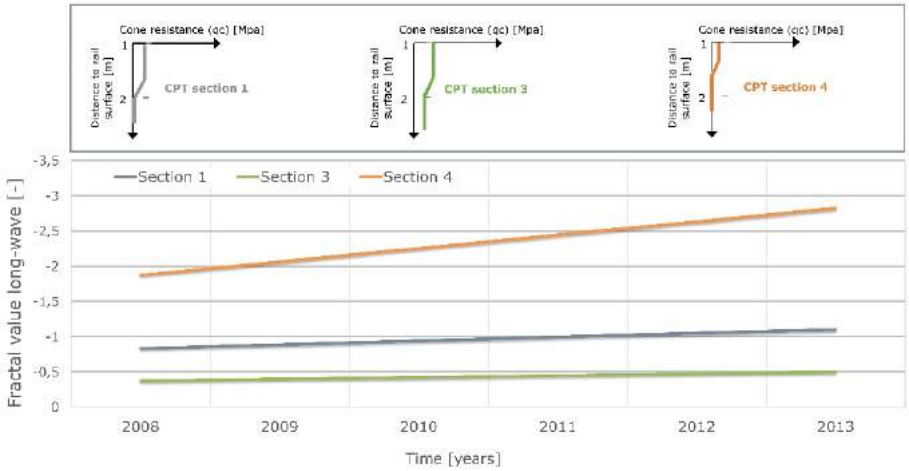

Figure 54 CPT section A: Comparison to fractal analysis

Comparing the discussed outcomes of the soil-mechanical cone penetration test with those of long-wave fractal analysis reveals an excellent correlation for the examined areas. Section 3, with the highest loading capacity, displays the best fractal analysis values at this time, as well as the lowest deterioration rate within the last five years. Section 1, which was evaluated as average by soil-mechanical pressure testing, showed significantly worse fractal analysis results. By far the worst section in regards to fractal analysis is section 4, which also supports the results of the soil-mechanical cone penetration test.

In the same route section, a comparison with GPR evaluation data is also available for sections 1 and 2. The results of the two test methods coincide in their basic statements; both identify section 1 as significantly poorer (Figure 55). The loading capacity was rated as inadequate by soil-mechanical cone penetration testing; this was confirmed by the presence of strong undulation of the ballast bed and intermediate layer in the GPR. The humidity content of the track ballast and intermediate layer plays a subordinate role in this context. The low contamination of the ballast in section 2 is probably due to rising fine particles. However, this cannot be analysed further at this point, since, as mentioned above, the pressure probe is inserted into the track substructure, and the ballast is removed beforehand.

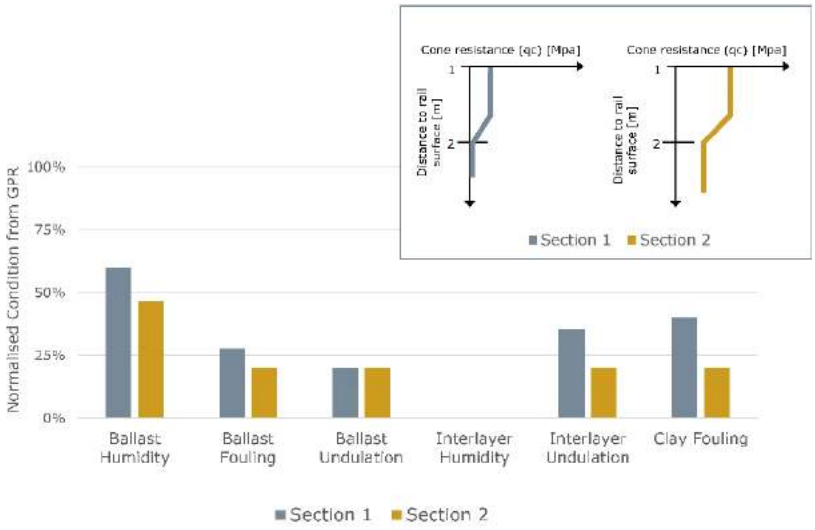

Figure 55 CPT section A: Comparison to GPR

As part of the pilot project, detailed soil-mechanical testing was also carried out for a further section, B. This was not just subject to soil-mechanical cone penetration testing, but also an in-depth analysis of the previously removed ballast and the humidity content.

The evaluations of the ballast samples (Figure 56) clearly show that the contamination of the ballast bed (top 30 cm) increases in direction of mileage. The underlying layer (layer no. 4), on the contrary, shows no significant change in particle size distribution. This coincides with the results of the GPR (Figure 58), which shows a major increase in ballast contamination from km 6.400 onwards, while no clay fouling is detected over the entire section.

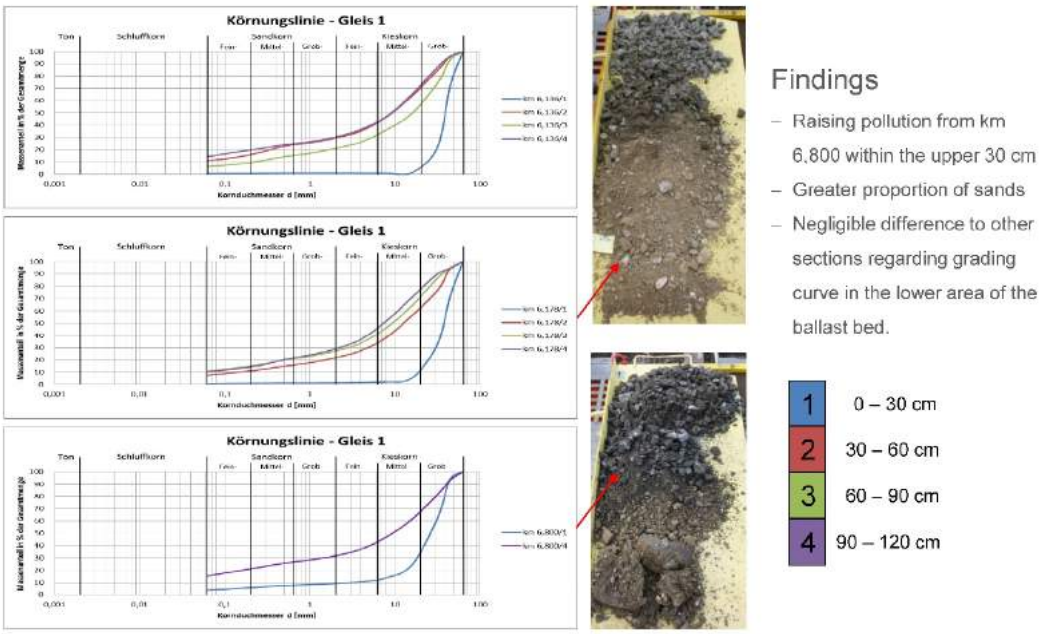

Figure 56 CPT section B: Ballast sampling

The increasing humidity content (Figure 57) as detected by the soil-mechanical investigations is also partially reflected in the GPR data (Figure 58), since the humidity content of the intermediate layer increases. However, by contrast with the CPT investigations, it decreases slightly later on, the relationship is thus referred to as partial.

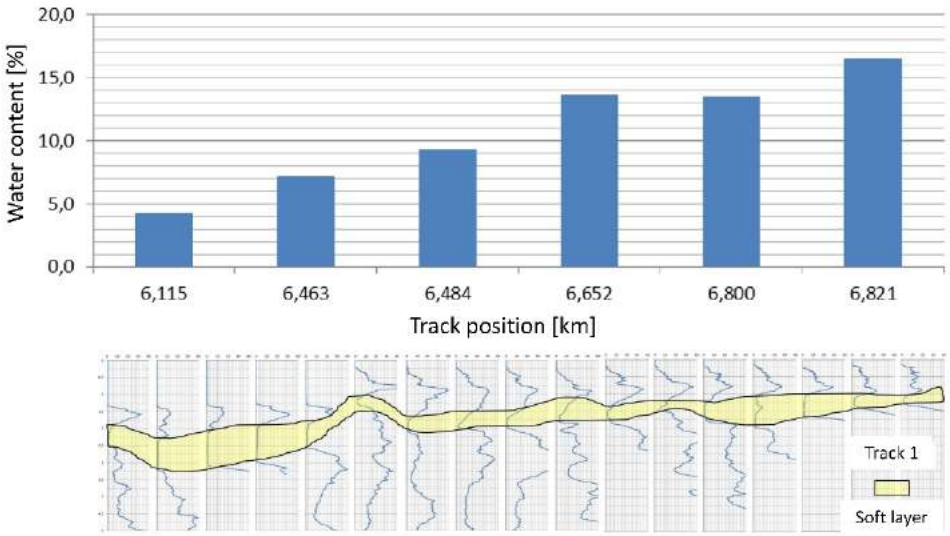

Figure 57 CPT section B: humidity content and analysis of soil layers

An analysis of the deeper soil layers within the soil-mechanical cone penetration test shows migration of a soft layer (Figure 57) towards the surface. This phenomenon is also readily apparent from the GPR illustrations. From around km 6.400, both an undulated ballast bed and intermediate layer are detected (Figure 58), suggesting a decrease in load bearing capacity. In the prior sections, these layers are detected as level; this also corresponds to the CPT findings, which detect the soft layer much lower down in the ground. The negative impact on the substructure is also correspondingly lower.

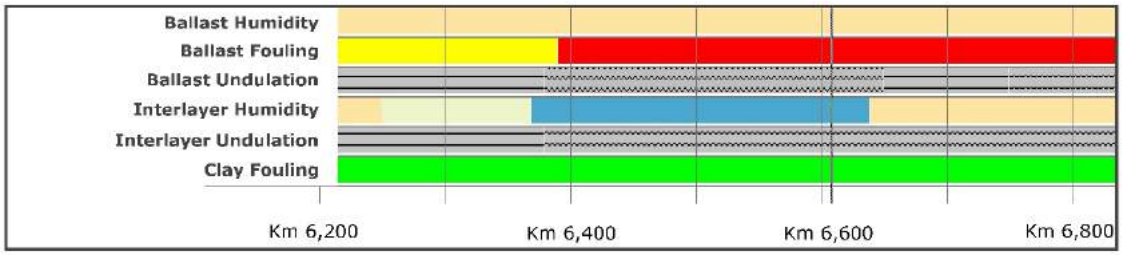

Figure 58 CPT section B: Results of GPR evaluation

The findings from GPR runs are thus confirmed by selectively executed soil-mechanical testing for this route section. The GPR may serve as a qualitative indicator of the condition of the evaluated components, which permits for prediction, as well as condition evaluation. The validation process performed in the scope of the present work confirms that such use of the GPR appears plausible. However, this method of analysis cannot achieve the level of detail and accuracy of a soil-mechanical examination.

4.2.4 Fractal analysis and visual *in-situ* behaviour

The easiest and probably most comprehensive, albeit also the most expensive and subjective way to cover all boundary conditions of railway infrastructure continues to be visual track inspection. Visual condition evaluation continues to form an integral part of the inspection and maintenance strategies of railway infrastructure managers. During the validation process of the fractal analyses, several track inspections were carried out under professional supervision. In addition to previously studied cases of the useful application of the medium-wave fractal range to describe ballast condition [Hansmann 2015], the long-wave range will be analysed here in depth. For this purpose, two track sections are outlined in more detail by way of example.

Case I (Figure 59) presents fractal analysis results from 2005 to 2013, illustrated in the longitudinal direction, in comparison to locally detected behaviour. In addition, GPR runs are available for this section. The fractal analysis shows damage in the medium and long-wave range, as well as an overlap thereof. The visual track inspection revealed massive ballast abrasion ("white spots") on the uppermost layer of the ballast bed. Moreover, removal of this top layer shows that the ballast bed is also contaminated by fine particles rising from the substructure. Consequently, the load bearing capacity, as well as the separation and filtration effect of the surrounding soil, is presumably inadequate. Secondly, the ballast bed is no longer capable of conducting its main task, water drainage, which would explain the visibly high humidity content of the ballast. One possible cause of the apparent condition may be due to an entirely blocked drainage system, thus preventing adequate dissipation of surface water via the track substructure. The resulting, reduced capacity leads to rising fine particles, and the consequent contamination of the ballast bed.

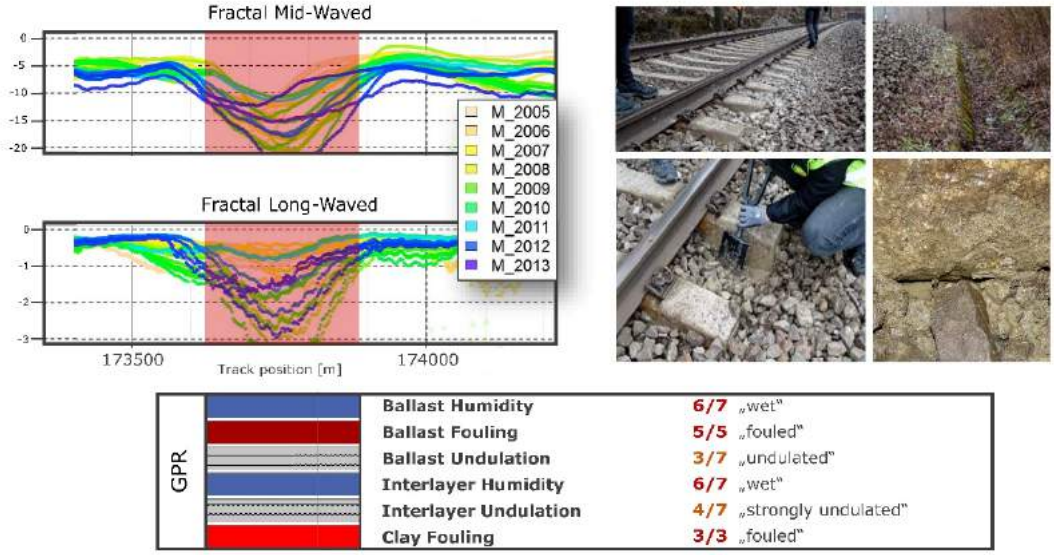

Figure 59 Validation of fractal analysis - track visual inspection case I

The condition of the track system, as recognised correctly by fractal analysis, was also confirmed by the GPR run (Figure 59, below). The humidity parameters of both the track ballast and the intermediate layer were evaluated as second-worst out of seven assessment grades (Figure 23). Moreover, the track ballast was calssified as heavily contaminated, and the presence of a clay fouling that had migrated from the surrounding soil into the ballast bed was recognised. The undulation of the ballast bed and intermediate layer in the longitudinal direction also suggests that the load bearing capacity of this section is heterogeneous.

Standard deviation of longitudinal level primarily describes the amplitudes of the signal, while the fractal analysis is primarily capable of detecting the wavelengths (see 3.1.2). Accordingly, it is also feasible to detect certain phenomena, based on the fractal analysis of vertical track geometry, which cannot be detected by conventional track geometry analysis like standard deviation of longitudinal level, or at least not in an early stage. This is illustrated within the second validation example (Figure 60). The case refers to a track section that was built in 2001 and equipped with conventional concrete sleepers. The substructure condition of two cross-sections (QS 1 and QS 2) separated by around 180 metres are compared. Conventional track geometry analysis (sigmaH) showed almost no difference between the two locations. The track geometry behaviour after installation can be described as very good, and was further significantly improved by tamping operations in 2006. This is also confirmed by the fact that the attention threshold (AS) was not nearly reached, and is also not expected to in the next few years due to the low deterioration rate.

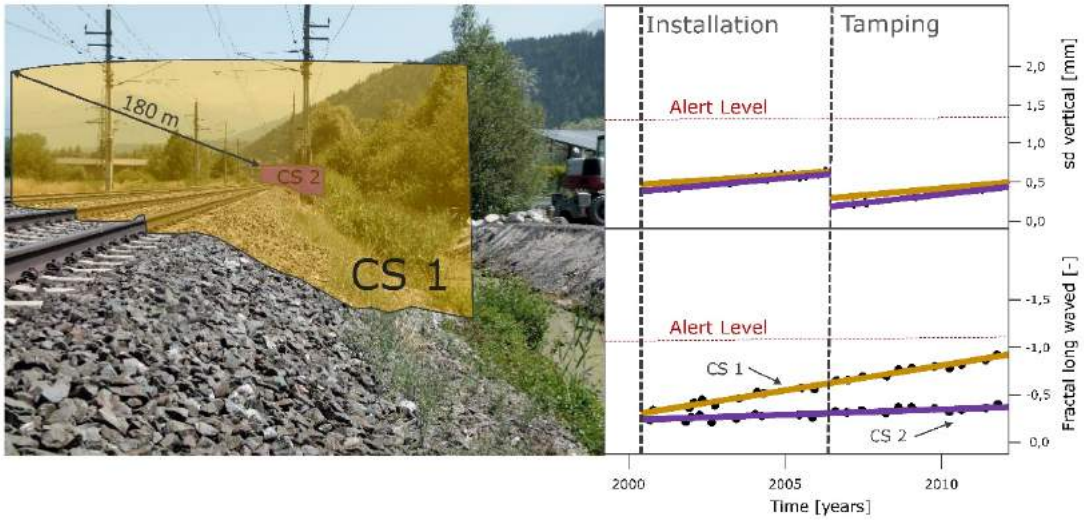

Figure 60 Validation of fractal analysis - track visual inspection case II

However, the situation is rather different when evaluating the two cross-sections by means of the long wavelength dimension of fractal analysis. First, this quality signal is apparently unaffected by the tamping operations in 2006. This again confirms the assumption thoroughly examined above (see 4.2.2), namely that fractal analysis is actually quite capable of describing the substantial behaviour of substructure, and is thus not affected significantly by short-term corrective track geometry measures. Moreover, and in contrast to the analysis according to sigmaH, a significant difference in quality between the two cross-sections is also apparent (Figure 60). Cross-section 2 corresponds to the excellent behaviour detected in the context of conventional track geometry analysis, with extremely low deterioration over time. Cross-section 1, however, shows significant deterioration in the condition, and threatens to reach the attention threshold [Hansmann 2015] of -1.1 [-] as determined from network-wide analysis in the near future.

The cause of this behaviour can be revealed trough track inspection. While no specific abnormalities were apparent in cross-section 2, the drainage ditch in cross-section 1 was filled with water. This accumulation of water is due to a non-functional water passage, coupled with a relatively high groundwater level, leading to the assumption that the accumulated water is also present in the substructure of the track, negatively influencing the load bearing capacity of the substructure. The height and resulting weight of the embankment causes inhomogeneous subsidence. This problem, however, can be detected in an early stage using fractal analysis. Accordingly, the described behaviour can be counteracted, thereby preventing more extensive maintenance requirements in the future.

4.2.5 Relative subsidence measurement in combination with fractal analysis of vertical track geometry

As part of the present evaluation, the question of whether there is a relationship between subsidence values (see 3.3.2) and fractal analysis should be addressed. The analysis involves a track section of approximately 50 km. The entire section was built in 2003, and the track substructure is installed in form of a bituminous formation layer. Since substructure problems are negligible as a result, the investigation focusses on an assessment of the open track sections (valid length, see 2.2) for the medium-wave fractal range. This is compared to the measured values of the relative subsidence by way of a scatter plot. As explained above (see 4.1.1), fractal analysis reacts differently to the various superstructure types. For this reason, the superstructure types concrete sleepers, concrete sleepers with USP and slab tracks are colour coded in Figure 61.

The relationship between relative subsidence and superstructure type is apparent at first glance. While the concrete sleepers exhibited a relative subsidence of around 0.7 mm, the track body for slab tracks and concrete sleepers subsided by an average of 1.2 mm and 1.7 mm respectively. The higher quality in terms of fractal analysis is also visible at higher subsidence levels, i.e. for slab track and concrete sleepers. Concrete sleepers without under sleeper pads do not just exhibit the highest medium-wave fractal values, but also the largest scattering thereof. This confirms the above-explained effect: The interaction or rather load transfer between concrete sleepers and ballast bed is improved by installation of an under sleeper pad between them.

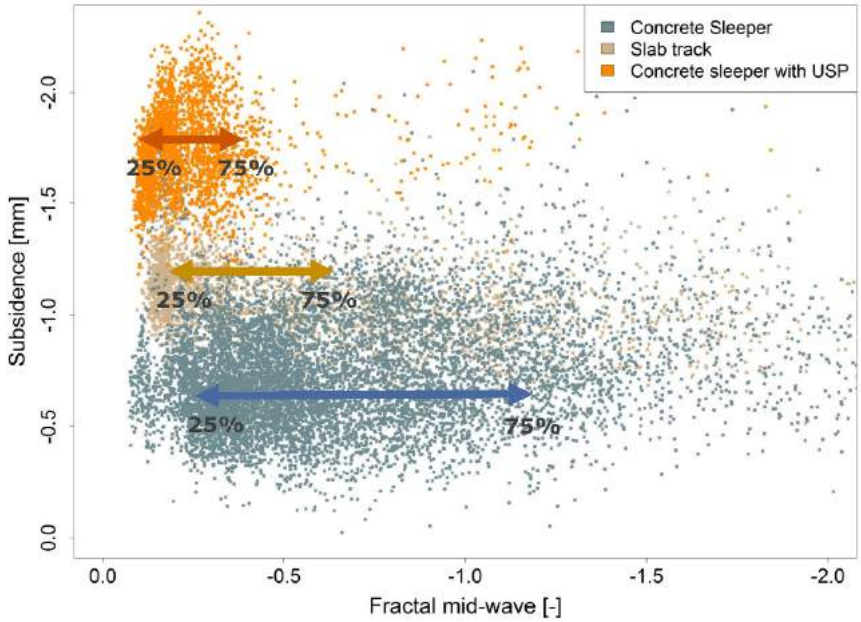

Figure 61 Correlation of results of subsidence measurements and fractal analysis of the medium-wave range

The scattering in the sections with slab track (Figure 61) is also striking, which implies that increased values are also present in this superstructure type. The elevated levels in the medium wave range may indicate that there are sections where the built-in base plates of the slab track are subject to unintended movements. Thus, there is certainly need for future research to establish whether fractal analysis is capable of describing the condition of slab track sections.

Apart from the subsidence of the various superstructure types, the subsidence of the transition zones is also of essential importance. This data indicates whether a continuous stiffness profile or reduction thereof was attained. The analysis (Figure 62) shows that this was the case for transition zones of concrete sleepers to concrete sleepers with under sleeper pads (USP), and especially from slab track to concrete sleepers with USP. However, the transition zone between concrete sleepers without USP and slab tracks does not show a continuous increase in stiffness (Figure 62, middle). This is because under sleeper pads were installed on a section of around 50 metres in these transition zones, which have greater subsidence than both the concrete sleeper without pads and the slab track. Accordingly, a leap in stiffness occurs in these special transition zones between the two linked superstructure types.

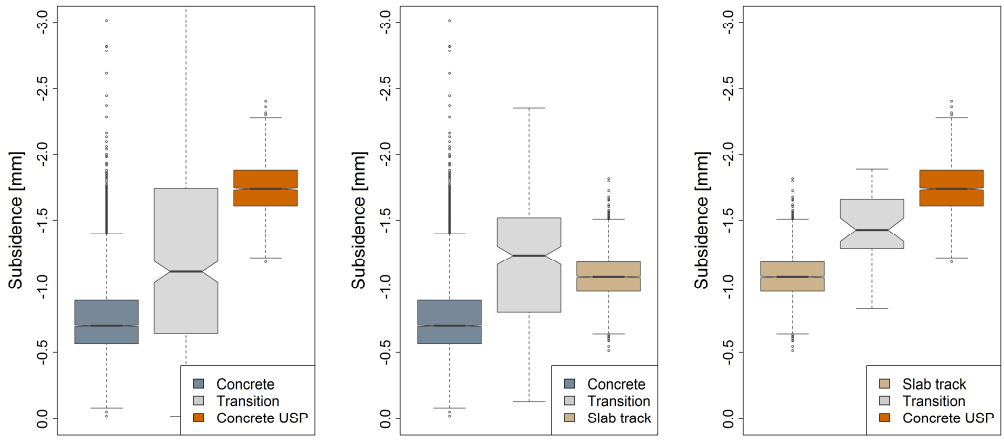

Figure 62 Subsidence in transition zones between two superstructure types

The evaluation of the transition zones in the scope of fractal analysis also showed remarkable results. Both the short and especially the medium wavelength range demonstrated the negative impact of transitions from concrete sleepers without pads to slab track. As discussed above, the transitional zones were equipped with under sleeper pads over a short 50 m section, which, however, resulted in an undesirable leap in stiffness (Figure 62). The fractal analysis (Figure 63) also clearly identifies these areas as problematic. The slab track provides an almost perfect signal in terms of the long wavelength dimension of fractal analysis; the characteristics of the transition areas to the slab track are thus particularly striking.

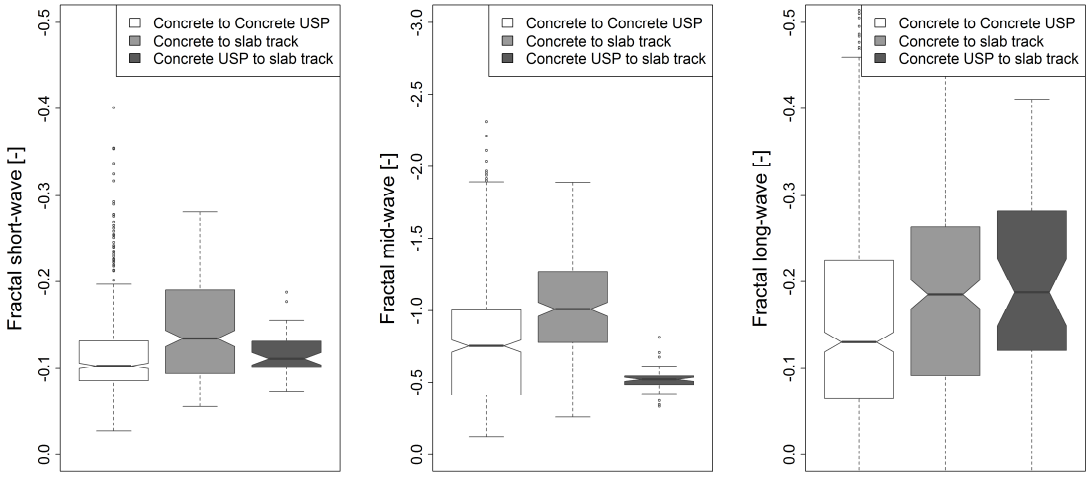

Figure 63 Fractal analysis of transition zones between two superstructure types

The transition zones from conventional concrete sleeper and slab track to sections with concrete sleepers including USP are also classified by fractal analysis as being in very good condition (Figure 63). This demonstrates the positive impact of technically flawless transition zones. Adverse leaps in stiffness, however, lead to problematic areas, and consequently increased maintenance efforts.

In summary, it appears that higher relative subsidence and the associated higher elasticity in the overall track system mean that the load transfer to the tracks is gentler. Naturally, the increased elasticity must be adjusted to the infrastructure components as built. Furthermore, it should also be considered that the increase in elasticity is only advantageous to the overall system up to a certain extent. Accordingly, relative subsidence of more than 3 mm thus suggests that the track is no longer in an optimal condition [Luomala et al. 2014]. The specific definition of intervention thresholds is of course dependent on the speed of travel and the introduced loads.

4.2.6 Analysis of load plate pressure tests

The results of the GPR evaluations were also validated by comparison with the dynamic deformation modulus (E_{vd} values). These are generally executed as a sufficient and reliable form of substructure evaluation in the scope of planning track renewal projects [ÖBB-Infrastruktur AG 2014]. The load bearing capacity of the underlying subsoil for any elevation position in the course of track prospecting can be determined relatively easily by way of geotechnical investigation using the light drop-weight tester [Auer et al. 2007]. A range of such geotechnical investigations were carried out on the track sections measured by GPR, which may be used for comparison with the GPR parameters. The relevant geotechnical explorations were conducted in the last third of the track service life for use in planning of a pending reinvestment in the medium-term. The GPR parameters of interest to the loading

capacity behaviour are the humidity of the intermediate layer, the undulation of the ballast bed, and any recognised clay fouling.

This comparison (Figure 64) clearly demonstrates the following: The higher the humidity content of the intermediate layer and substrate according to ground-penetrating radar, the lower the load bearing capacity as indicated by the deformation modulus. The undulation of the ballast bed is also rated as poorer for lower measured E_{vd} values. Regarding the clay fouling parameter, it should be noted that the absence of a fine particle layer in the track body does not automatically imply high load capacity for the track substructure, since other factors also play a significant role in this context. However, if a clay fouling is detected, the measured E_{vd} values are reduced if the clay fouling was detected already within the ballast bed.

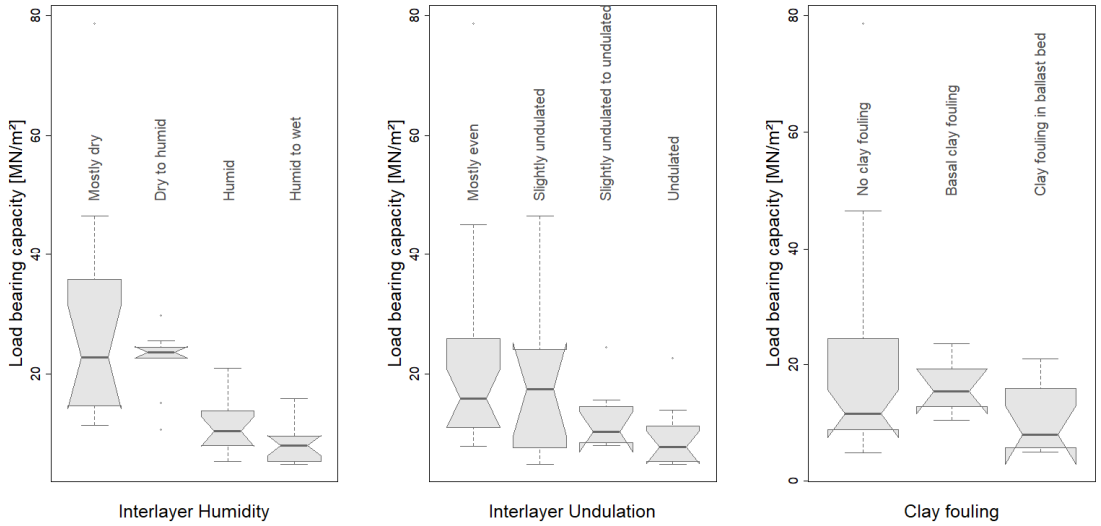

Figure 64 Results of base plate load testing compared to GPR evaluation

These documented load plate pressure tests naturally also represent an opportunity to validate the findings of fractal analysis. This is particularly suitable for the long-wavelength dimension of fractal analysis, since it evaluates the condition of substructure, and thus its load bearing capacity to some extent. Consequently, the findings demonstrate a strong correlation between the selectively measured loading capacity and the associated fractal analysis values (Figure 65). The smoothing curve with related confidence band especially shows that higher load bearing capacity means lower expression of the long-wave fractal range.

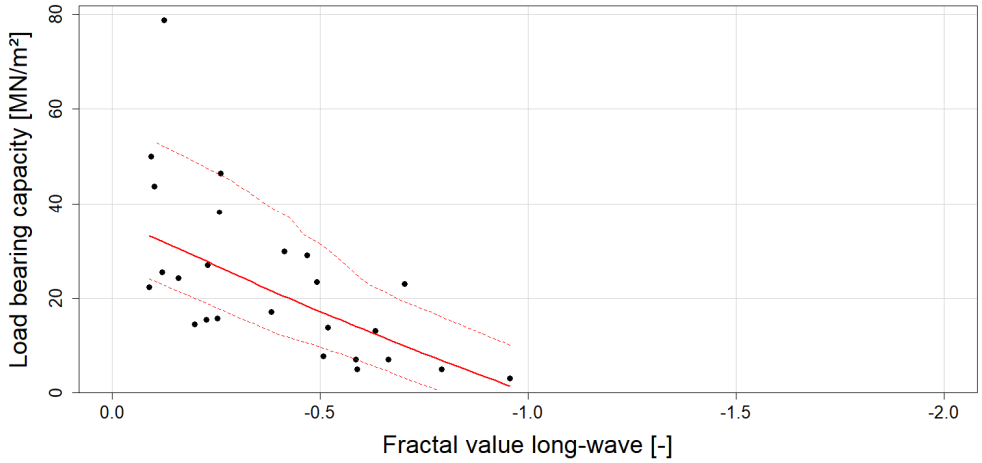

Figure 65 Base plate load testing compared to long-wave fractal analysis

Accordingly, the basic outcomes of fractal analysis and GPR runs were also confirmed by the determined loading capacity as determined by base plate load testing.

5 Stochastic Correlation Analyses

The methods for condition evaluation introduced in the present work (fractal analysis, GPR, SigModS) differ mostly in respect of their measurement methodologies. The analytical methods developed for track geometry measurements (fractal analysis, SigModS) are based on geometry measurements using accelerometers or chord measurement methods. GPR, however, is based on a geophysical measurement system that acts both as a transmitter and receiver of electromagnetic impulses. Accordingly, this raises the following question:

- Do these detection methods, with their specific characteristics, produce a consistent condition evaluation for the individual infrastructure components?

This question should be analysed using stochastic correlation analysis within the following chaper. The correlation analysis findings are eventually to serve as a basis for determining whether or how outcomes of the various measurement methods may be aggregated to generate a holistic condition evaluation.

5.1 Correlation coefficients and their significance

In the scope of this study, parameters of different scale levels are examined. While data coming from the track geometry vehicle (fractal analysis, SigModS, sigmaH) are based on the ratio (metric) scale, the evaluations of the GPR are at ordinal scale. The scale levels of measure result in different options for stochastic correlation analyses [Piazolo 2011] of two statistical variables x and y (Figure 66).

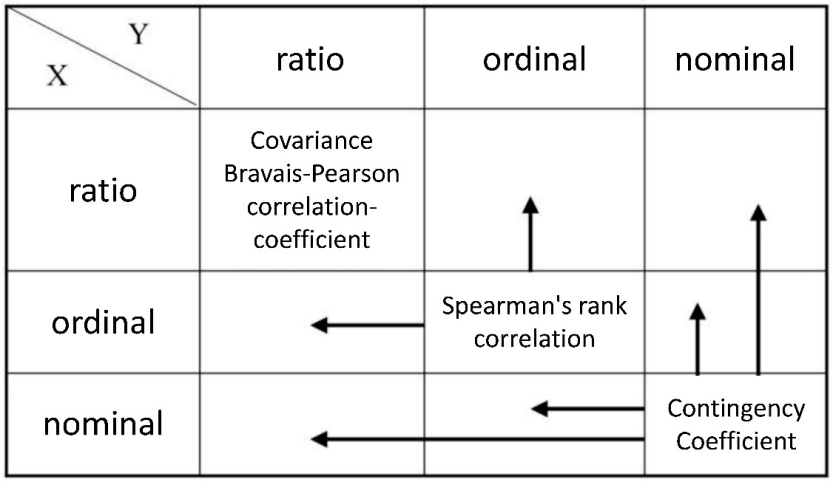

Figure 66 Correlation analyses depending on the scale level of measure [according to Piazolo 2011]

Accordingly, the correlation analysis in this work is based on Spearman's rank correlation, which is a common methodology for variables at both the metric and ordinal scale. Furthermore, this form of analysis has the advantage that it also detects non-linear relationships, and does not require the data to be normally distributed. The correlation analyses presented are executed with the valid length filter (see 2.2), since the description of generally applicable laws is the top priority in this work. Parameter-specific differentials within switch areas, bridges, and the like would distort the representation of these principles.

5.1.1 Spearman's rank correlation

Spearman's rank correlation [Fahrmeir et al. 2007], also known as the rank correlation coefficient, is employed for methods of analysis involving ordinal scaled data. A rank correlation coefficient is a non-parametric measure of correlation. This means that it determines how well an arbitrary monotonic function describes the relationship between two variables. Assumptions on the probability distribution of the variables are not made in this case. Spearman's correlation coefficient ρ_{SP} (also known as Spearman's rho) is formed by converting the data to ranks prior to calculation of the correlation coefficient as follows:

$$\rho_{SP} = \frac{\sum_i (rg(x_i) - \overline{rg}_x)\,(rg(y_i) - \overline{rg}_y)}{\sqrt{\sum_i (rg(x_i) - \overline{rg}_x)^2 \sum_i (rg(y_i) - \overline{rg}_y)^2}} = \frac{Cov\,(rg_x, rg_y)}{\sigma_{rg_x}\,\sigma_{rg_x}}$$

Formula 2 Spearman's rho correlation coefficient [Fahrmeir et al. 2007]

Where:

$rg(x_i)$ *is the rank of* x_i *(the same is true for* y_i*),*
$\overline{rg}_x$ *the means of the ranks of x (the same is true for y),*
σ_{rg_x} *the standard deviations of the ranks of x (the same is true for y) and* $Cov(rg_x, rg_y)$ *the covariance of rg(x) and rg(y).*

The values of Spearman's correlation coefficient ρ_{SP} are thus interpreted as follows:

Value range: $-1 \leq \rho_{SP} \leq 1$	
$\rho_{SP} > 0$	Concordant monotonic relationship, Trend: x large → y large; x small → y small
$\rho_{SP} < 0$	Inverse monotonic relationship, Trend: x large → y small; x small → y large
$\rho_{SP} \approx 0$	Non-monotonic relationship

The minimum value of a variable for a statistically significant correlation, however, is strongly dependent on the scaling of the input data, and especially the population of the data. Accordingly, the level of significance of Spearman's correlation will be examined further below.

5.1.2 Significance level of a correlation

The aforementioned explanations point to the fact that a certain correlation is present between the input parameters insofar as the correlation coefficient is not equal to zero. However, what value indicates significant correlation? The probability value (p-value, Figure 67), which estimates the probability of the occurrence of the null hypothesis, is applied for this purpose. As part of a correlation analysis, the null hypothesis describes the case of independence, or rather non-correlation [Fahrmeir et al. 2007]. The probability for occurrence of this null hypothesis is estimated at 2.2*10-16 (Figure 67), which means that the null hypothesis is to be discarded, and correlation is demonstrably present.

```
        Spearman's rank correlation rho

data:  Ballast_Fouling and Fraktal_Slope_2_l_Netzweit_Mittelwert_41_X2013
S = 6.509786e+12, p-value < 2.2e-16
alternative hypothesis: true rho is not equal to 0
sample estimates:
       rho
-0.2172485
```

Figure 67 Correlation analysis in R-Project

Generally, the level of significance of a correlation is highly affected by the number of observations. For observations of n > 30, the t-distribution (also known as the Student distribution) requires a value t above 2.3263 to confirm a significant correlation with a probability of at least 99% (Formula 3).

$$t = \left| \left(\frac{\rho_{SP}}{\sqrt{1-\rho_{SP}^2}} \times \sqrt{n-2} \right) \right| > 2{,}3263$$

Formula 3 Significance of t-distribution

Accordingly, the critical correlation factor ρ_{SP}, the minimum for a significant correlation between the input parameters, can be determined for various observation quantities n. The smaller the observation quantity, the higher the required ρ_{krit} for the presence of correlation. As part of the correlation analyses conducted for this project, more than 50,000 observations are available for all input parameters. The ρ_{krit} resulting from Formula 3 is thus ± 0.0104.

Critical ρ	Observations n	Probability of independence (null hypothesis)	$t_{0.99}(50{,}000)$
±0.0104	50,000	2.2*10-16	± 2.3263

Table 4 Determination of ρ_{krit} for significant correlation

It can therefore be stated that the analyses carried out so far have a statistically significant correlation once the Spearman correlation coefficient ρ_{SP} exceeds the value ± 0.0104.

5.2 GPR and the track geometry vehicle

In this section, possible correlations between the GPR and track geometry vehicle are examined with reference to the described methodology. The compared values are GPR parameters based on one-off measurements (see 3.2.3), and the temporally closest values from the track geometry measurements. The parameters of the track geometry vehicle include conventional track geometry analysis (sigmaH and its rate of deterioration), and the results of fractal analysis of vertical track geometry.

5.2.1 GPR vs. conventional track geometry analysis (sigmaH)

The correlation analysis of GPR and track geometry shows that the previously established value (Table 4) of ± 0.0104 is fulfilled by just about all parameters. These relationships thus meet the criterion of statistically significant correlation. The results of the correlation analysis between standard deviation of the longitudinal level (sigmaH) and its deterioration rate (b-rate) with the GPR parameters are as follows (Figure 68):

- The parameters *clay fouling*, *ballast humidity* and *interlayer humidity* affect both sigmaH and its deterioration rate to the same extent. An unambiguous matching of the damage types to either of the two track geometry parameters is thus not feasible.
- The ballast fouling is particularly reflected in the standard deviation of longitudinal level.
- The evaluations regarding the undulation (ballast and interlayer) show no consistent findings.
- The recognition of formation layers primarily results in a significant improvement in standard deviation of longitudinal level.

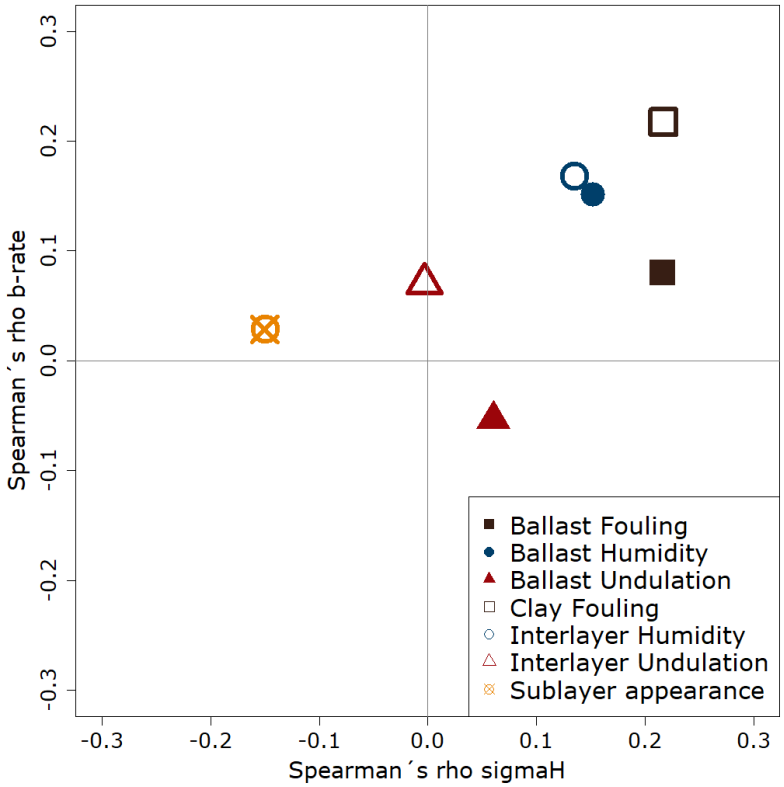

Figure 68 Correlation of GPR and track geometry behaviour, detail

The graphically illustrated results in Figure 69 are also listed in tabular form. This clearly shows that the minimum of ± 0.0104 required for Spearman's correlation coefficient is achieved in 13 out of 14 cases. Solely the relationship between the standard deviation of the longitudinal level and the undulation of the intermediate layer lack statistically significant correlation.

ρ_{SP}	Parameter	ρ_{SP}
0,215	Ballast Fouling	0,080
0,154	Ballast Humidity	0,151
0,061	Ballast Undulation	-0,053
0,216	Clay Fouling	0,217
0,137	Interlayer Humidity	0,168
0,002	Interlayer Undulation	0,070
-0,145	Sublayer appearance	0,029

Figure 69 Correlation of GPR and track geometry behaviour, overview

In summary, it can be stated that the holistic track geometry behaviour is strongly affected by the damage types evaluated by the GPR. However, allocation of the individual damage types to the track geometry parameters (sigmaH, deterioration rate) is only possible in exceptional cases (ballast contamination and detected formation layer). Because of the

previous discussion regarding track geometry behaviour (see 3.1.1.2), this is hardly surprising. However, the identification of damage types can be improved significantly by using fractal analysis.

5.2.2 GPR vs. fractal analysis

As explained above (see 3.1.2.2), fractal analysis of the vertical track geometry should permit identification of the various damage types in the track body. This raises the question of whether clearer trends for the different damage types are revealed in the context of correlation analysis as compared to track geometry behaviour. The results shown in Figure 70 may be interpreted as follows:

- The evaluation of the humidity content demonstrates that fractal analysis, as assumed, is capable of distinguishing between problems in the ballast bed and substructure rather well. While ballast humidity is strongly correlated with the medium wavelength dimension, there is a strong relationship between the humidity content in the intermediate layer and the long wavelength dimension.

- Clay fouling of the track body appears to be one of the relevant parameters of GPR evaluation, and correlates particularly well with the long wavelength dimension, as expected.

- The results relating to undulation confirm the possibilities of fractal analysis, since correlation with both the ballast bed and intermediate layer is limited to the long-wavelength range. Furthermore, it is perfectly comprehensible that a stronger correlation with the undulation of the track substructure occurs, since it is one layer higher, and thus has a stronger effect on track geometry.

- Recognised formation layers also tend to correlate more strongly with the medium than the long wavelength range. This is due to the fact that formation layer installation is a form of substructure enhancement, which means that the positive impact primarily pertains to the long-wave range.

- The contamination of ballast is correlated more strongly with the long-waved sector. This implies that GPR evaluations refer to contamination of the lower ballast bed, or rather, the mixing zone with the intermediate layer in this case. This corresponds with US studies [Sussman et al. 2003], which also regard the parameter *ballast fouling* as pertaining to this area.

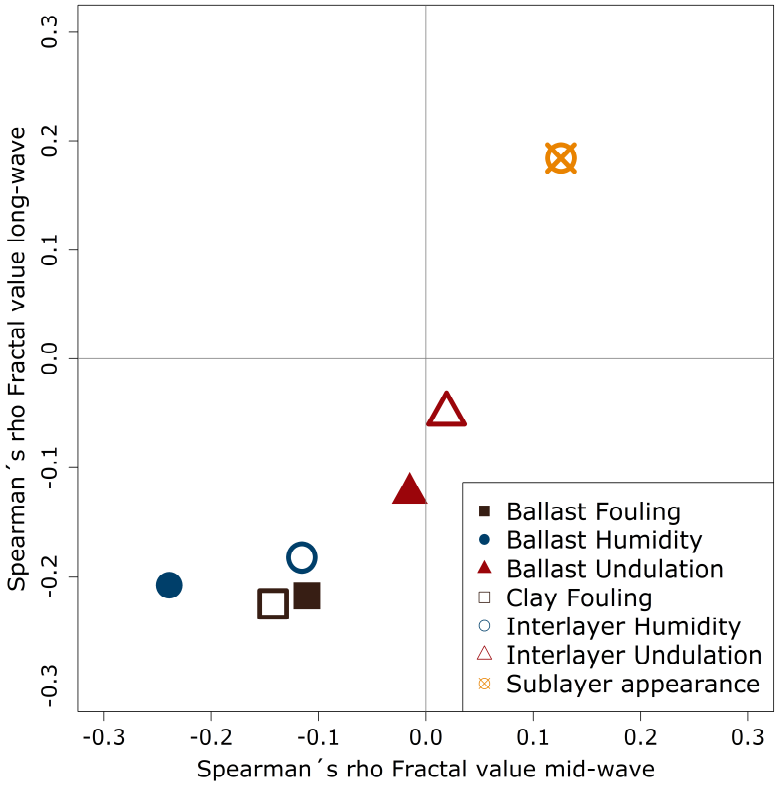

Figure 70 Correlation of GPR and fractal analysis, detail

The graphically illustrated results in Figure 71 are also listed in tabular form. This clearly shows that the minimum of ± 0.0104 required for Spearman's correlation coefficient is achieved throughout.

ρ_{SP}	Parameter	ρ_{SP}
-0,121	Ballast Fouling	-0,217
-0,240	Ballast Humidity	-0,196
-0,015	Ballast Undulation	-0,123
-0,142	Clay Fouling	-0,225
-0,114	Interlayer Humidity	-0,182
0,019	Interlayer Undulation	-0,050
0,123	Sublayer appearance	0,184

Figure 71 Correlation of GPR and fractal analysis, overview

In summary, it appears that it is indeed possible to identify different types of track damage by means of fractal analysis. This primarily confirms the assumption that the classification of wavelength ranges as medium and long-wave facilitates classifying issues as being in the ballast bed or in the substructure. The GPR may provide additional information with regards to contamination, evenness and humidity levels.

5.3 The individual parameters of fractal analysis

Since a significant and also logically comprehensible correlation of the outcomes of fractal analysis and GPR has been established, the following question arises: What are the mutual dependencies between the different wavelength ranges of fractal analysis? In answering this question, a correlation analysis of fractal analysis will be performed on the basis of the first longitudinal level measurements of 2014.

As previously suspected, this correlation analysis shows that the medium-wave range (Figure 72, centre) exhibits equally significant correlation with both the short and long wavelengths. The dependence of the short and long wavelength ranges, however, is significantly lower.

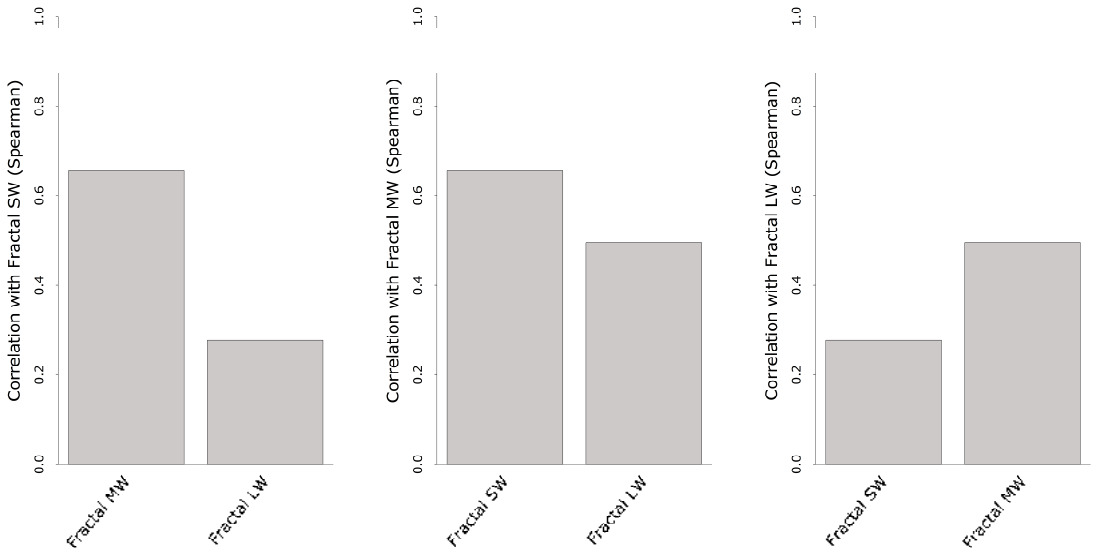

Figure 72 Correlation of the individual parameters of fractal analysis

This implies that the expression of the medium-wave range typically occurs jointly with either the short or the long-wave range. In addition to normal wear and tear, this can be explained in technical terms due to the fact that excessive ballast contamination is usually dominated by the following two factors:

- Deficient interaction between sleeper and ballast bed, resulting in unfavourable force transfer, and thus leads to excessive stress on the ballast bed.
- A subsoil with low loading capacity or failure of the separation effect between formation layer and ballast bed results in mixing of the ballast bed with rising fine subsoil particles.

Accordingly, it would seem entirely plausible that an expression of the medium-wave range of fractal analysis is typically not independent, but rather overlaps with either of the other two wavelength ranges. The moderate correlation between short- and long-waved ranges results from complete system failure of the entire track at the end of its service life. In such cases, the interactions between both sleeper and ballast, and ballast and formation layer, are typically defective.

Accordingly, track sections with issues occurring in the interaction between sleeper and ballast with near-perfect substructure condition would be expected to only exhibit correlations between the short and medium-wave range. This theory will be examined on the basis of a 50 km track section with an age of around ten years, which has been fitted with a bituminous formation layer. The superstructure consists of conventional concrete sleepers without under sleeper pads.

The exploratory analyses (Figure 73) show a significant correlation between the short and medium-waved fractal values. While the long wavelength range exhibits no abnormalities, an increase in the medium-waved fractal values is accompanied by an increase in the short-wave range in most cases. The individual fractal analysis parameters thus interact in accordance with the actual conditions on site, where faults in the ballast (if present) are caused by the inadequate interaction between conventional concrete sleepers and the upper ballast bed. The substructure, in contrast, does not exhibit any issues in either the *in-situ* behaviour, nor within the fractal analysis; any damage to the ballast bed was thus not caused by this component.

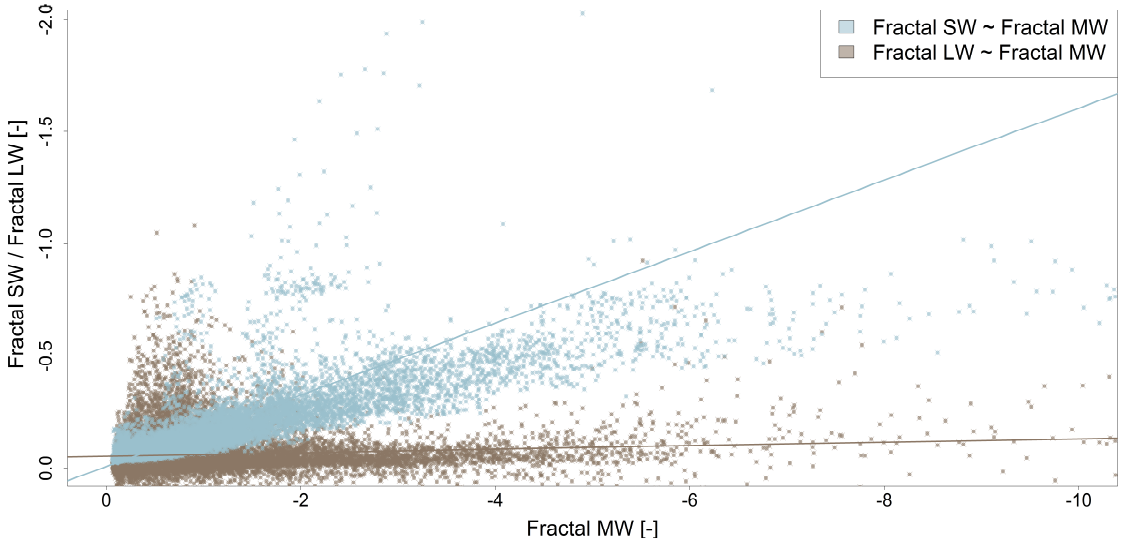

Figure 73 Fractal correlations for optimal substructure conditions

In order to prove the correlation result not just in graphic, but also in a statistical form, Spearman's correlation coefficient (Spearman's ρ) was also calculated (see 5.1.1). This rank correlation coefficient is a non-parametric measure of correlation. This means that it defines the strength of the relationship between two variables (Table 5).

Correlated variables	Spearman factor
Fractal medium-wave ~ Fractal short-wave	$\rho_{SP} = 0.8757$
Fractal medium-wave ~ Fractal long-wave	$\rho_{SP} = 0.1957$

Table 5 Spearman factor fractal analysis for optimal substructure conditions

Stochastic analysis thus also shows a very strong correlation between the medium-waved and short-waved fractal sector, while correlation with the long-wave sector is low.

5.4 SigModS vs. fractal analysis

The standard deviation of the modified gauge signal (SigModS) introduced in section 3.1.3 describes the noise or rather a low-frequency horizontal movement of one or both rails. This movement increases as soon as force transfer between rail and sleeper ceases to function optimally. On the one hand, any horizontal movement also entails a proportionate movement in the vertical direction. On the other, inadequate force transfer between rail and sleeper necessarily causes a disturbance of the interaction between sleeper and ballast. Accordingly, as Figure 74 shows, an expression in SigModS also causes elevated levels within fractal analysis. Due to the described method of calculation for SigModS, it seems likely that a correlation is indeed present, especially in the short-wavelength range of the fractal analysis.

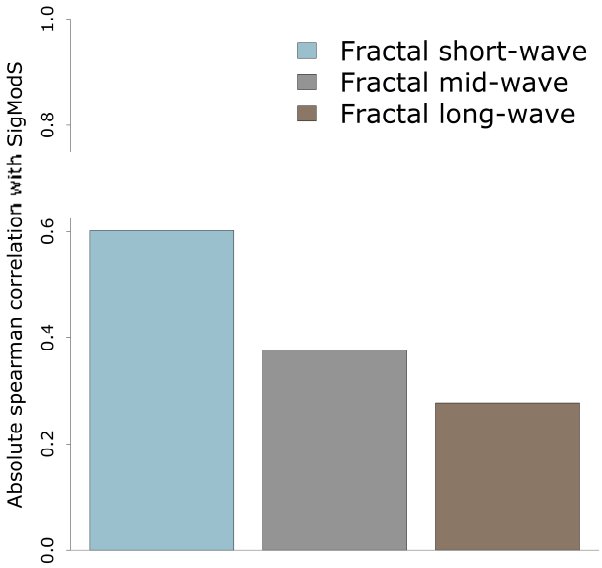

Figure 74 Correlation SigModS vs. fractal analysis

This assumption was confirmed by correlation analysis, which was again conducted using Spearman's factor (see 5.1). This shows that the present correlation between SigModS and the short-wave fractal range is significantly greater than with medium and long-waved fractal ranges. Accordingly, both parameters appear suitable for a condition evaluation of the sleepers, or rather their interaction with the rails and the ballast bed.

6

Aggregation for Description of the Infrastructure Condition

One of the major challenges in contemporary rail infrastructure asset management is formulating a holistic condition evaluation of the track. Nonetheless it should be capable of subdivision into various, component-specific levels of detail. This structure enables both a holistic condition evaluation, and an indication of the specific component(s) responsible for the relevant condition. The general evaluation of network quality therefore does not suffice; rather, maintenance planning must also be included. This work will now give an overview of the systems used to date, followed by a discussion of the methodology of the condition evaluation as formulated in the scope of the present work. This is primarily based on the methods of condition evaluation presented (see Figure 3), as well as the validation (see Figure 4) and correlation analyses (see Figure 5) used. The following questions are of particular relevance:

- Is the establishment of a component-specific condition evaluation feasible based on the assessed detection types or novel methods of analysis?
- Is the aggregation of this component-specific condition evaluation sense into holistic quality figures for the infrastructure (excl. rails) feasible?

6.1 Established quality figures

As early as in the 1960s, first models were formulated based on a weighted combination of different measuring signals at British Rail [Schramm 1967]. This system, which was called "Neptune", was based on the fact that deviations of the zero line were provided with different weighting factors for each measuring signal. This ultimately generates a comparable and holistic condition evaluation (Figure 75). The variables track twist, curvature line and slope line of the two rails are applied.

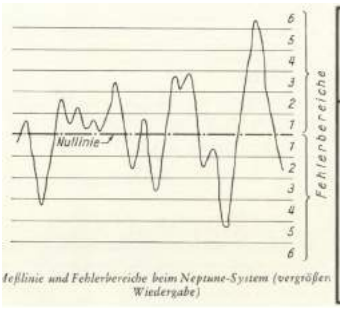

Meßlinien	Fehlerbereich-Nummer 1	2	3	4	5	6
	Fehlerbewertungszahlen					
Gleisverwindung	2	11	20	29	38	47
Krümmungslinie { linke Schiene	3	6	9	12	15	18
Krümmungslinie { rechte Schiene						
Senkungslinie { linke Schiene	2	4	6	8	10	12
Senkungslinie { rechte Schiene						

Figure 75 "Neptune" fault evaluation system [Schramm 1967]

As already explained (see 3.1.1), standard deviation of longitudinal level is used for maintenance planning in most countries. In recent years, however, TQIs (Track Quality Indices) have been developed to enable a holistic description of infrastructure. In this case, the input factors remain constant (vertical and horizontal track geometry, gauge and twist), with their standard deviations used as input. The various figures are differentiated by weighting factors of the respective parameters and the constraint length. The J coefficient [Madejski & Grabczyk 2002] and the Track Geometry Index (TGI) [Berawi et al. 2010] are examples (Formula 4) of methods based on a constraint length of 100 m or 200 m.

J - Koeffizient

$$J = \frac{S_z + S_y + S_w + 0{,}5 * S_e}{3{,}5}$$

$$S = \sqrt{\frac{1}{n}\sum_{i=1}^{n}(x_{i=1} - \bar{x})^2}$$

S_z	sd vertical
S_y	sd horizontal
S_w	sd twist
S_e	sd gauge

Track Geometry Index

$$TGI = \frac{2 * \mathrm{UI} + TI + GI + 6 * AI}{10}$$

$$GI, TI, AI, UI = 100 * e^{-\frac{(\sigma_{mes} - \sigma_n)}{(\sigma_{maint} - \sigma_n)}}$$

UI	sd uneveness (vertical)
AI	sd alignment (horizontal)
TI	sd twist
GI	sd track gauge
σ_{mes}	sd current value
σ_n	sd value after renewal
σ_{maint}	sd threshold value

Formula 4 Track Geometry Index and J-coefficient

A remarkable similarity of the two quality numbers becomes apparent upon closer consideration of the track gauge parameter. In comparison with the track position, this parameter is under-represented in both the J coefficient (S_e) and Track Geometry Index (TGI). The explanation is due to a phenomenon mentioned above: The gauge tends to take on larger values in curved sections. In some cases, a gauge widening is installed deliberately in curve areas for improved riding behaviour. A calculated standard deviation of the gauge signal is thereby affected significantly by this long-wave gauge widening. This value thus detects the presence of curve sections rather than track or specifically sleeper condition. In the scope of this work (see 3.1.3), this problem has already been solved by application of the modified standard deviation of track gauge (SigModS). In the context of the J coefficient and Track Geometry Index, this was remedied by allocating a lower weighting to the gauge signal to reduce distortion of the results for curve sections.

The latest amendment of EN 13484-6 [EN 13848-6 2014] also contains a proposal for a Track Quality Index. The specific method is called *Combined Standard Deviation* (CoSD), and is intended to permit "*evaluation of the entire track geometry quality for a track section*" [EN 13848-6 2014]. Again, the aforementioned parameters are employed; the infrastructure operators may define their own weighting factors.

$$CoSD = \sqrt{w_{\overline{AL}} * SD_{\overline{AL}}{}^2 + w_G * SD_G{}^2 + w_{CL} * SD_{CL}{}^2 + w_{\overline{LL}} * SD_{\overline{LL}}{}^2}$$

SD	Standard deviation of single parameters
w	Weighting factor for single parameters
$\overline{AL}$	Horizontal alignment (mean of both rails)
G	Track gauge
CL	Superelevation
$\overline{LL}$	Vertical alignment (mean of both rails)

Formula 5 Proposal TQI according to EN 13484-6

These Track Quality Indices enable a description of track geometry quality; the results will correspond to the track geometry behaviour to a greater or lesser extent depending on the choice of weighting factors. However, the infrastructure condition, and particularly the conditions of the individual components cannot be determined in sufficient detail. Accordingly, a component-specific condition evaluation will be formulated, based on the introduced analytical methods, as well as their validation and correlation, in the following section.

6.2 Component-specific condition evaluation

In the scope of this work, the evaluation of the infrastructure condition is conducted by application of a range of analytical methods (see Figure 3). Several of them were developed (further) at the Institute of Railway Engineering and Transport Economy. Also described are widely applied methods, which are, however, first being applied in the context of a component-specific condition evaluation of railway infrastructure. In the following, these methods of analysis are to be combined in a plausible manner to describe the component-specific condition of sleeper, ballast and substructure. This link is based on the results of the conducted validation process (see Figure 4) and stochastic correlation analyses (see Figure 5). The condition evaluation methodology employs historical measurement data to calculate deterioration rates, which are to account for the historical and future progression of the condition. Since GPR results represent an influencing parameter in the presented methodology, the aggregation methodology is applied to the condition in 2014, since GPR measurements are available for this period. The GPR evaluation was not conducted for the entire network; the developed methodology for condition evaluation thus refers to 1,200 km out of the 4,000 km of the TUG network (see 2.2). However, sensitivity analysis should indicate whether or rather how to expand this condition evaluation to the entire network purely based on measurement data and information that is available for the entire network, and in the form of time series.

6.2.1 Sleeper condition

In the present work, the sleeper condition is defined by the following parameters:

- Adhesion between rails and sleeper (rail fastening)
- Material condition and fatigue (cracks, crumbling, etc.)
- Condition and performance of the sleeper base and the associated load transfer between sleeper and ballast

As already demonstrated, these characteristics, and especially their behaviour over time, are materially dependent on the sleeper type (see 4.1.1 and 4.1.2.2). The validation process (see Figure 4) and correlation analysis (see Figure 5) indicate that the first two characteristics can be described using the modified standard deviation of the gauge (SigModS). For the latter parameter, the short-wave fractal value is confirmed to be the quality signal capable of describing excessive vertical movements of the sleepers, and thus primarily the interaction between ballast and sleeper (see 5.3 and 5.4). This behaviour is also referred to as hanging sleepers.

The description of sleeper condition SZ_m in the scope of the different evaluation methodologies is really self-evident, since the two evaluation methods use more than one parameter each. The condition according to the evaluation methodology is provided by value N, which is represented by the mean of the years 2010 to 2014, or since the last maintenance or renewal measure. This value is normalised to the maximum permissible value that is described by the 99th quantile of all values (Formula 6).

$$\boldsymbol{SZ_m} = \left(1 - \frac{N_m}{Max_m}\right) * 100 \qquad \boldsymbol{ZZ_{Sleeper}} = \sum_{m=1}^{n} SZ_m * \psi_m$$

SZ_m	*Sleeper condition based on methodology m*
N_m	*Value of methodology m*
Max_m	*Maximum value of methodology m*
ψ_m	*Weighting coefficient for holistic sleeper condition of methodology m*
ZZ	*Condition Figure*

Formula 6 Sleeper condition figure

The essential question relating to condition evaluation of the sleeper component thus pertains to the weighting factor ψ for the two quality signals or rather evaluation methodologies. This is calculated by means of the three aforementioned parameters for sleeper condition evaluation. As explained above, the first two values can be described by SigModS, and the latter by the short-wave fractal value. This results in a weighting ψ of two-thirds of the standard deviation of the modified track gauge (SigModS). Since the short-wave fractal value primarily describes one of three parameters, this quality signal is weighted with a third (Table 6).

Methodology Fractal Analysis	Max value
Fractal short-wave	-2,54 (99% Quantile)

Methodology Track Gauge	Max value
SigModS	2,16 (99% Quantile)

ψ = 33 %

ψ = 67 %

$\boldsymbol{ZZ_{Sleeper}}$

Table 6 Composition of sleeper condition figure

An assessment of the network-wide behaviour of the normalised quality signals reveals a left-skewed distribution in both cases (Figure 76). This distribution appears plausible in the light of the fact that the majority of cross-sections are, or can be expected to be, in safe and sound condition. These circumstances thus also necessarily cause a left-skewed distribution of values. The same effect would be expected for all other distributions of quality signals and condition evaluations subjected to network-wide analysis.

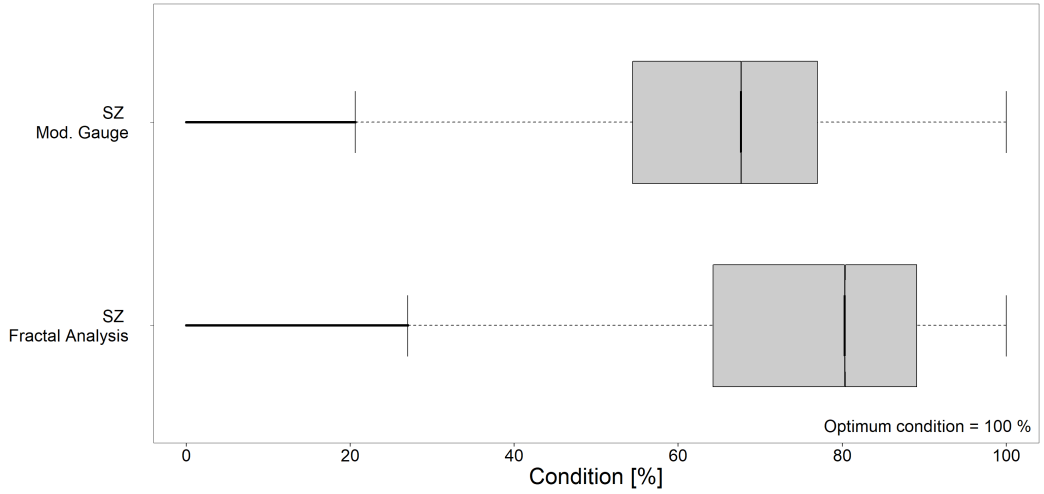

Figure 76 Distribution of sleeper quality signals

This results in a corresponding condition of the sleeper component for the entire track network, as shown in Figure 77. Naturally, the superposition of the two evaluation methods also yields a left-skewed distribution with a median of 71%. In the course of this work, the in-depth analysis of the sleeper condition is thereby performed by way of comparison with the two remaining components ballast and substructure.

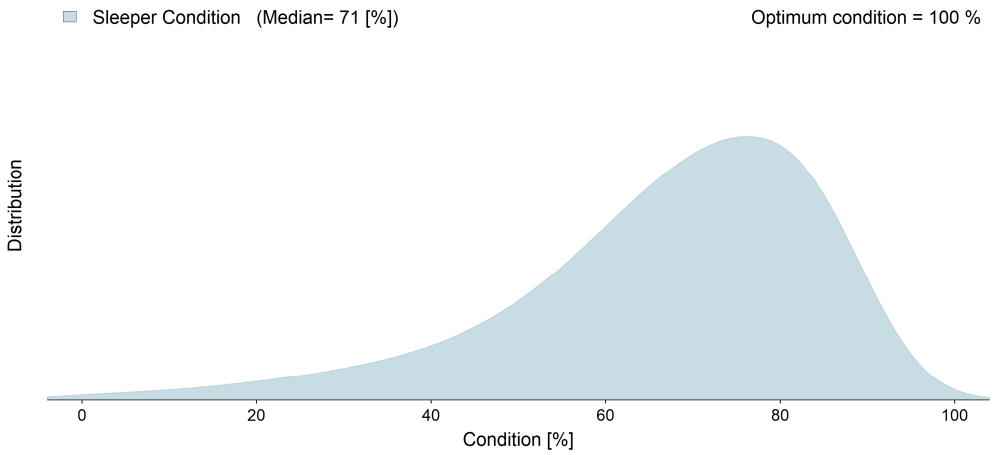

Figure 77 Sleeper condition figure

6.2.2 Ballast condition

The condition of this component is also generally determined according to the same algorithm. However, the different evaluation methods (GPR, fractal analysis, track geometry analysis) each employ several evaluation parameters. Accordingly, aggregation of the component condition proceeds in two stages (Formula 7). Initially, the ballast condition is determined with respect to the individual evaluation methods (BZ_m) based on the weighting parameter ε. Value N is represented by the values of the GPR parameters (see 3.2) on the one hand, and the deterioration rate b (see 3.1.1) on the other. In the case of fractal analysis (see 3.1.2) and the standard deviation of the vertical track position (see 3.1.1), a mean is calculated for the years 2010 to 2014, or since the last maintenance or renewal measure. This condition evaluation BZ_m is subsequently transferred into a component-specific condition figure by way of the weighting factors γ.

$$\boldsymbol{BZ_m} = (1 - \sum_{i=1}^{n} \frac{N_{m,i}}{Max_{m,i}} * \varepsilon_{m,i}) * 100 \qquad \boldsymbol{ZZ_{Ballast}} = \sum_{m=1}^{n} BZ_m * \gamma_m$$

BZ_m	*Ballast condition based on methodology m*
$N_{m,i}$	*Value of criterion i based on methodology m*
$Max_{m,i}$	*Maximum value of criterion i based on methodology m*
$\varepsilon_{m,i}$	*Weighting coefficient for ballast of criterion i based on methodology m*
γ_m	*Weighting coefficient for holistic ballast condition of methodology m*
ZZ	*Condition Figure*

Formula 7 Ballast condition figure

The weighting factors ε are calculated based on the validation process and correlation analyses. In the scope of evaluating the GPR, it was found that humidity and contamination levels of the ballast were the main figures for describing track ballast condition (see 4.2.3 and 5.2). It was also discovered that the assessment criterion *ballast contamination* primarily describes the transition layer (mixing zone) between ballast and substructure; this criterion is thus allocated a lower weighting. Overall, the GPR is more accurate in detecting the condition of the substructure than the ballast, which is reflected in the weighting factor γ (Table 7).

Evaluation methodology GPR		
Criterion	max value	Weighting $\mathcal{E}$ [%]
Ballast Fouling	4	28
Ballast Humidity	5	61
Ballast Undulation	6	4
Clay Fouling	2	8
Interlayer Humidity	5	0
Interlayer Undulation	6	0

γ = 25%

Evaluation methodology Fractal Analysis		
Criterion	max value	Weighting $\mathcal{E}$ [%]
Fractal mid-wave	-12 (99% Quantile)	80
Fractal long-wave	-1,5 (99% Quantile)	20

γ = 40%

Evaluation methodology Track Geometry		
Criterion	max value	Weighting $\mathcal{E}$ [%]
sigmaH	2,2 (99% Quantile)	60
b-rate (sigmaH)	0,73 (99% Quantile)	40

γ = 35%

$ZZ_{Ballast}$

Table 7 Composition of ballast condition figure

Regarding the evaluation methodology of fractal analysis, it was clearly established that the medium-wave fractal dimension describes the ballast condition, while the long-wave fractal dimension describes the substructure condition. The 80-20 weighting was selected since there is always a certain degree of interaction between the two components, which should not be neglected entirely. Conventional track geometry analyses (see 3.1.1) is also included in describing ballast condition, since it covers the vertical track geometry itself. In this context, the standard deviation of longitudinal level is classified as slightly more important than the rate of deterioration, which is more closely related to long-term subsidence [Holzfeind 2009].

Ballast condition exhibits the distributions for the evaluation methodologies BZ_m shown in Figure 78. Again, all box plots show the above-explained left-skewed distribution. The GPR evaluation, which is primarily defined by the humidity level of ballast, indicates a comparatively poor condition, while fractal analysis classifies the ballast condition as slightly better. This is due to the sensitivity of fractal analysis to ballast contamination, which worsens particularly towards the end of its service life, once the overall system is already defective.

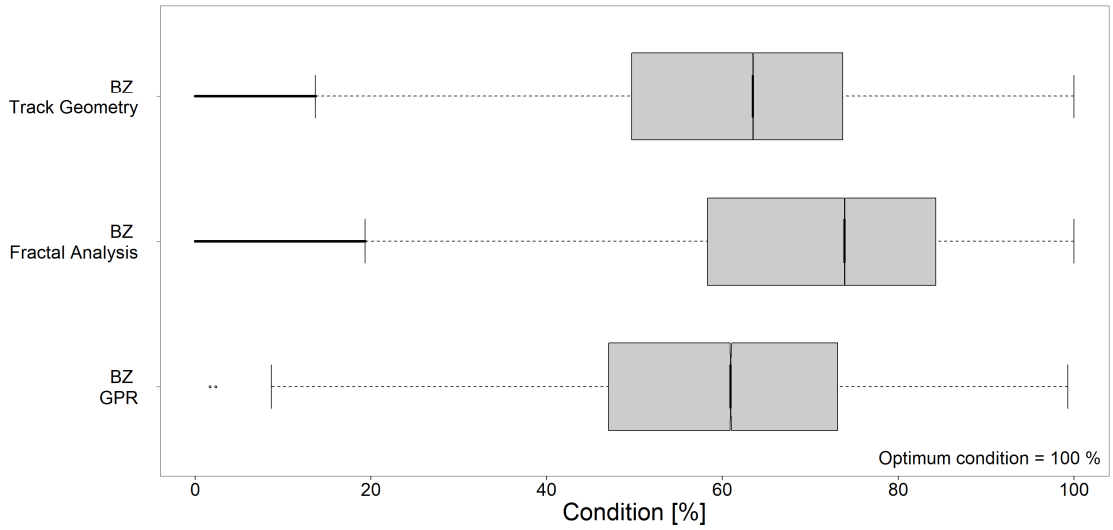

Figure 78 Distribution of ballast evaluation methodologies

The superposition of said three evaluation methodologies confirms the left-skewed distribution of the network-wide condition (Figure 79). However, the median of 63% indicates that the ballast condition is inferior to that of the sleeper.

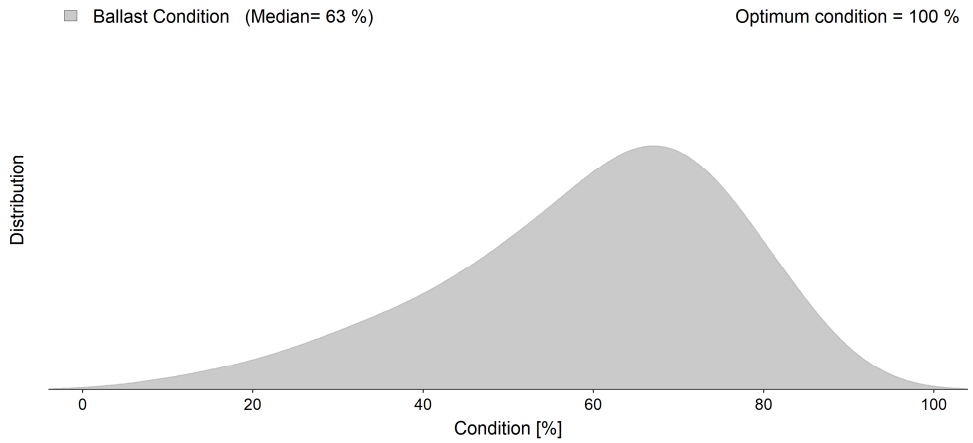

Figure 79 Ballast condition figure

6.2.3 Substructure condition

As is the case with the condition of the components sleeper and ballast, the substructure condition is also aggregated. The various evaluation methodologies each come with several valuation parameters, as is the case with ballast condition evaluation. Accordingly, aggregation of the component condition proceeds in two stages (Formula 8). Initially, the ballast condition is determined with respect to the individual evaluation methods (UZ_m) based on the weighting parameter δ. Value N is represented by the values of the GPR parameters (see 3.2) on the one hand, and the deterioration rate b (see 3.1.1) on the other. In case

of fractal analysis (see 3.1.2) and standard deviation of vertical track alignment (see 3.1.1), a mean is calculated for the years 2010 to 2014, or since the last maintenance or renewal measure. This condition evaluation UZ_m is subsequently transferred into a component-specific condition figure by way of the weighting factors β.

$$\boldsymbol{UZ_m} = \left(1 - \sum_{i=1}^{n} \frac{N_{m,i}}{Max_{m,i}} * \delta_{m,i}\right) * 100 \qquad \boldsymbol{ZZ_{Substructure}} = \sum_{m=1}^{n} UZ_m * \beta_m$$

UZ_m	Substructure condition based on methodology m
$N_{m,i}$	Value of criterion i based on methodology m
$Max_{m,i}$	Maximum value of criterion i based on methodology m
$\delta_{m,i}$	Weighting coefficient for substructure of criterion i based on methodology m
β_m	Weighting coefficient for holistic substructure condition of methodology m
ZZ	Condition Figure

Formula 8 Substructure condition figure

Particularly for the evaluation of GPR parameters, the weighting coefficients δ are derived from the previously conducted validation process (see Figure 4), and the correlation analysis (see Figure 5). For fractal analysis and track geometry analysis, weightings are inverted from values used for ballast. Primarily the long-wavelength dimension in the context of fractal analysis thus describes the substructure. Regarding track geometry analysis, the rate of deterioration is subject to a slightly higher weighting than the standard deviation of the longitudinal level (sigmaH) itself. As explained in detail above (see 3.1.1), the standard deviation of longitudinal level (sigmaH) is primarily influenced by the amplitudes of vertical track geometry. The significance of the latter is thus diminished, and particularly so in terms of the substructure condition, and they are allocated a correspondingly low weighting β (Table 8).

The GPR, however, particularly shines when it comes to railway substructure; the weighting β attributed to this evaluation methodology is thus higher than in the rating of the ballast condition. The validation and outcomes of the correlation analyses indicate that the parameters *clay fouling* and *humidity of the intermediate layer* have a major impact on substructure behaviour. The weighting coefficients δ were selected accordingly (Table 8).

Evaluation methodology GPR		
Criterion	max value	Weighting δ [%]
Ballast Fouling	4	19
Ballast Humidity	5	6
Ballast Undulation	6	16
Clay Fouling	2	29
Interlayer Humidity	5	23
Interlayer Undulation	6	6

β = 40 %

Evaluation methodology Fractal Analysis		
Criterion	max value	Weighting δ [%]
Fraktal MW	-12 (99% Quantile)	20
Fraktal LW	-1,5 (99% Quantile)	80

β = 40 %

Evaluation methodology Track Geometry		
Criterion	max value	Weighting δ [%]
sigmaH	2,2 (99% Quantile)	40
b-Rate (sigmaH)	0,73 (99% Quantile)	60

β = 20 %

$ZZ_{Substructure}$

Table 8 Composition of substructure condition figure

The condition evaluation for the substructure of the different evaluation methodologies UZ_m is summarised in Figure 80. As usual, there is a left-skewed distribution; track geometry analysis indicates a marginally worse condition than the fractal analysis and GPR.

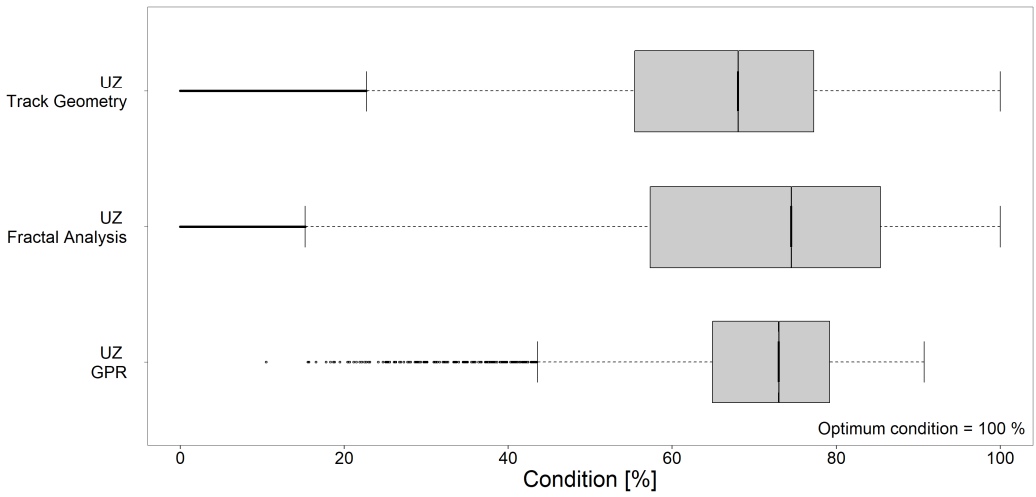

Figure 80 Distribution of substructure evaluation methodologies

The majority of the sections are in good condition, with a median of 69% (Figure 81). This appears to correspond to the actual, network-wide condition of the substructure, since substructure enhancement was conducted for around 20% of the 4000 track kilometres held in the TUG database in the last 20 years. Consequently, the majority of sections with

poor substructure in the main Austrian network should have already been renewed by now. Nonetheless, there are of course cross-sections where the substructure remains or has already returned to an inadequate condition. This particularly applies to the cross-sections that show a value of less than 50% in the scope of the present condition evaluations.

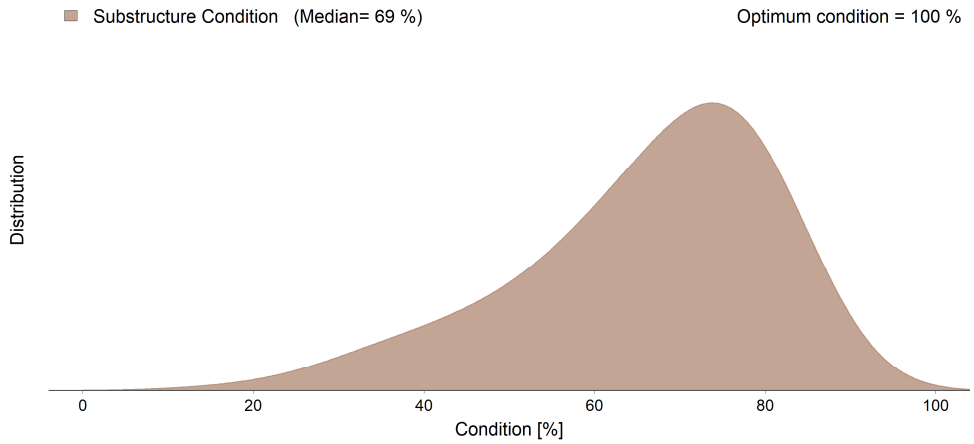

Figure 81 Substructure condition figure

6.2.4 Sensitivity analysis of the component-specific condition evaluation

After their aggregation, the component-specific condition evaluations will be subjected to a sensitivity analysis below. This is done to verify the robustness of the methodology, as well as to account for the fact that the population of the dataset has been reduced significantly by the inclusion of ground penetrating radar information. This is due to the lack of comprehensive GPR coverage (see 3.2), as the condition evaluation for the lowest common denominator of data is used in the aggregation algorithm. Nevertheless, the methodology of the condition evaluation includes the GPR data in this work, since the additional parameters for evaluation provide for more detail and improved results. Furthermore, the sample of more than 1,000 km (roughly a quarter of the total network) is more than enough for development of the methodology.

In any case, an examination of whether exclusion of the GPR data leads to comparable results will be conducted. This verifies the sensitivity of results, while also ensuring network-wide coverage of the condition evaluation. Since the GPR evaluations are used for evaluation of the components ballast and substructure, these two will also be subject to a closer look. First, the weighting factors for the respective methodologies of the component evaluation (Table 7 and Table 8) must be modified. To this end, the evaluation methodology GPR was set to 0 for each case. The other two evaluation methodologies were increased by equal measure until their sum was equal to 1 (Figure 82).

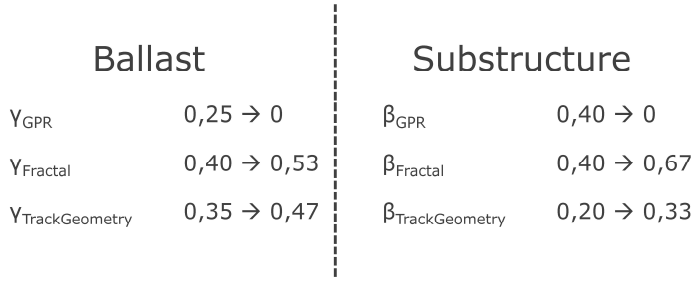

Figure 82 Modification of the weighting factors for sensitivity analysis

As part of the evaluation, the established and modified component condition were compared. The modified component condition was subjected to two different data filtering in this context. Dataset 1 refers to the same population as the conventional component condition, thus describing the sections that have been measured by GPR, but without consideration of the GPR data. Dataset 2, on other hand, refers to the entire TUG network (see 2.2), and thus describes a much larger data population (Table 9). This demonstrates that the developed methodology may be applied to the entire route network without GPR data in the future.

Dataset	Number Cross-sections	Median Ballast [%]	Median Substructure [%]
Component condition	212,742	63	69
Modified component condition (dataset 1)	212,742	64	68
Modified component condition (dataset 2)	731,600	66	71

Table 9 Sensitivity analysis results

The results of the conducted sensitivity analysis show that the methodology appears to be very robust. There is almost no difference, particularly between established component condition and the *modified component condition dataset 1*. This applies to both the components ballast and substructure (Table 9). Furthermore, the *modified component condition dataset 2* also shows only a marginal shift in results, even though the population is four times larger. It is also striking that use of dataset 2, i.e. application of the entire existing route network in the TUG database, somewhat increases the quality. This may be due to the fact that GPR runs tend to take place on routes that are known to have difficult boundary conditions. Nevertheless, the improvement only amounts to 2 %, and the variation in component condition (established, modified dataset 1 and modified dataset 2) may be regarded as similar.

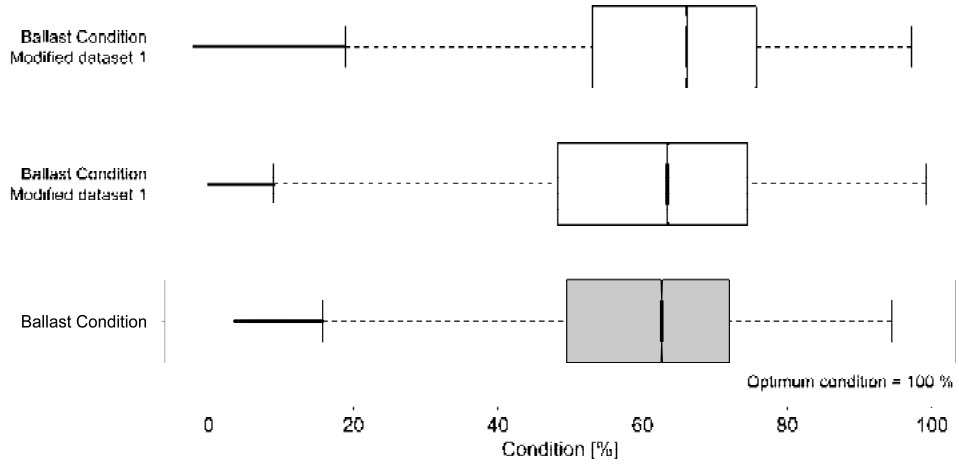

Figure 83 Sensitivity analysis, ballast condition

This similarity of the distributions is also reflected by a box plot analysis of the condition of the component ballast (Figure 83). This shows that the respective datasets also exhibit a similar distribution independently of the median value. The change due to modifying the weightings (Figure 82) is particularly limited for the ballast component, since the GPR data tend to be less relevant in this context than is the case with the substructure.

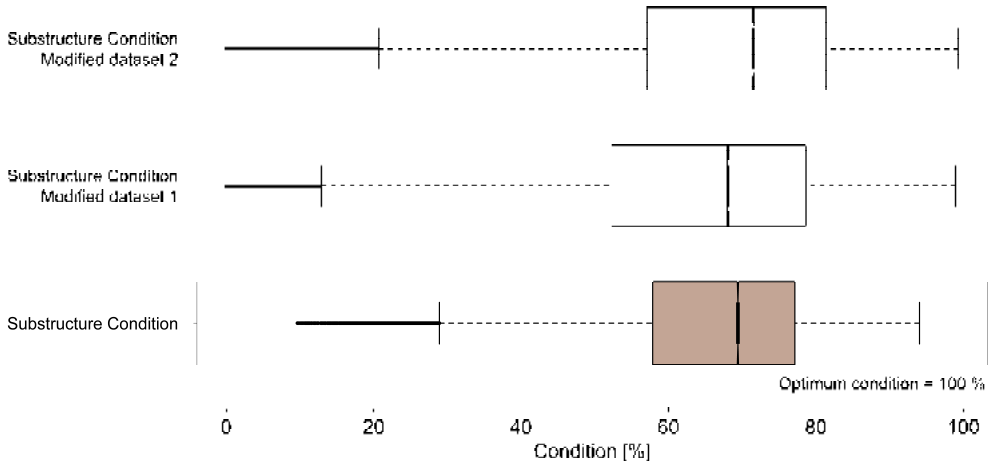

Figure 84 Sensitivity analysis, substructure condition

Accordingly, also the substructure condition shows only a slight change (Figure 84). While the median values remain almost identical, a higher level of scattering is apparent in the modified datasets. This is due to the fact that consideration of the GPR data provides greater accuracy, and a more certain result.

Accordingly, the sensitivity analysis has confirmed that the methodology is an extremely robust means for component-specific condition evaluation. The modification of datasets

and substantial increase in population only marginally affect the result of the respective component conditions. Consequently, this also demonstrates that the methodology may be employed for possible future applications without the (often non-existent) GPR data.

6.3 Aggregation of track quality figure

The first of the two questions raised earlier in this chapter can thus already be answered: It is indeed possible to establish a component-specific condition evaluation. Moreover, it is also possible to aggregate the outcomes into a holistic quality figure for railway infrastructure. The only remaining question: How to do it? This short and yet highly complex question will be dealt with in the following section.

6.3.1 Comparison of the component-specific condition evaluation

In considering the aggregation of component-specific condition evaluations, their mutual comparison must be analysed first. In this context, the median values (Table 10) clearly indicate that the ballast condition is worse than the condition of the sleeper or the substructure.

Condition figure	Network-wide median value [%]
Sleeper	71
Ballast	63
Substructure	69

Table 10 Comparison of the condition figures; median values

This result clearly reflects the circumstances caused by the change from wooden to concrete sleepers since the 1970s. In the majority of contemporary cases, the reason for track renewal is the condition of the ballast rather than that of the sleeper. This effect is caused by the properties of conventional concrete sleepers, which have very hard material characteristics, causing a greater load on the ballast. This phenomenon was mitigated by the introduction of the under sleeper pads. Nevertheless, almost two thirds (Figure 6) of the track network under consideration is currently equipped with conventional concrete sleepers without under sleeper pads. Moreover, it can be assumed that even concrete sleepers with pads will necessitate renewal of the ballast component - naturally with a corresponding delay. Generally, the ballast is the determining factor for service life, since this component passes through all wear conditions from optimal at installation to worn out at removal. Consequently, the network-wide condition is also worse than that of the sleepers (Figure 85).

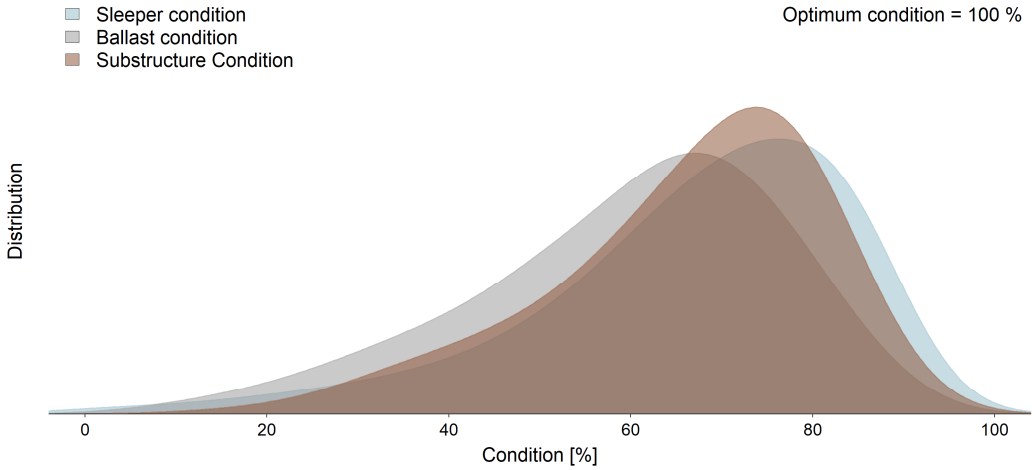

Figure 85 Comparison of component-specific condition figures

The condition of the substructure component exhibits a similarly positive network-wide condition to the sleeper component. The data also shows less scattering, which is reflected by the higher peaks in the distribution curve (Figure 85). This behaviour can be explained by the specific characteristics of the substructure component. As previously analysed (see 4.1.2.1), the substructure exhibits only very minor deterioration over time. This is especially true for solid substructure conditions with naturally grown soil, which do not change significantly over the service life, providing adequate drainage is ensured. In recent years, around 20% of the main Austrian network have already undergone substructure enhancement according to TUG database. Accordingly, it can be assumed that a majority of the sections affected by poor ground conditions have already been restored. This also explains the good network-wide substructure condition. Nonetheless, there are a few sections where the substructure remains in, or has already returned to, an inadequate condition. However, these may be located by way of the established component-specific condition evaluation.

6.3.2 Aggregation algorithm

The algebraic formulation of the aggregation of the individual component status data is logically derived from Formula 9. The crucial question, however, pertains to the choice of weighting coefficients α. Since this figure is to describe the quality of the entire infrastructure (excluding the track), the weighting factor is of corresponding importance. This is particularly the case when considering the sometimes strong variation in (temporal) behaviour of the individual condition evaluations for the various components.

$$\boldsymbol{Quality\ Figure_{Track}} = \sum_{k=1}^{n} ZZ_k * \alpha_k$$

ZZ_k *Condidion figure of component k (sleeper, ballast, substructre)*

α_k *Weighting coefficient for components*

Formula 9 Track quality figure

Naturally, the easiest way would be to attach the same importance to all components, and thus continuously adopt a weighting factor of 1. However, would this weighting correspond to reality? What is the single "most important" component to the infrastructure manager? On the one hand, of course, the components that are required for safe rail transport. The present work, as well as the asset management strategies of infrastructure operators, seeks to optimise the life of a component in terms of its economic service life. Accordingly, the optimisation is not concerned with the technical service life, which means that safety aspects should not be relevant. The safety evaluation of infrastructure components cannot be carried out properly on a network-wide basis in any case, since this issue can only be addressed by locally responsible parties for the relevant cross-sections. They are also ultimately responsible for the safe operation of trains. Thus, the infrastructure manager must define the importance of various infrastructure components based on cost. Minor maintenance activities are not suitable for sustainable improvement of the substantive condition of the components, even though it is clearly possible to remediate the track position and thus extend the service life of certain components. It therefore makes sense to state the replacement costs of the individual components. These costs are also the primary factors affecting the budget of an infrastructure operator. Any consideration of the renewal costs of individual components necessarily remains merely theoretical to some extent, since the economic objective should be to aim for track renewal for the entire track system as a whole. Nonetheless, this variant remains the best approach to recognise the "importance" of each component itself. The relative representation of the individual cost pools is shown in Figure 86: ballast bed cleaning is the cheapest, while substructure improvement, and consequently the substructure, is the most essential. Weighting coefficients α therefore emerge of 0.36 for the sleepers, 0.2 for the ballast, and 0.44 for the substructure condition.

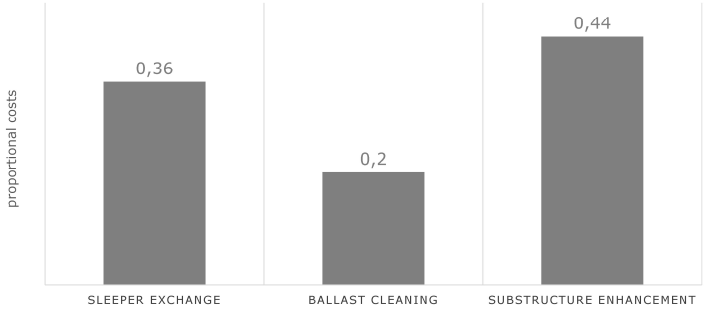

Figure 86 (Theoretical) Costs of component replacement

The immense importance of the substructure corresponds to calculations previously performed at TU Graz [Veit 2006] showing that this component is the most essential cost driver of railway infrastructure. Life-cycle costs of infrastructure may rise by a factor of eight in extreme cases for poor substructure conditions.

Another possibility of aggregation would involve consideration of the costs incurred by due maintenance measures in lieu of the replacement value. This quality figure would not solely focus on the residual value, but also on the current condition of the asset. It would also be conceivable to use both aggregation methods in parallel to have two different results on hand: Namely, an indication of the substantial condition (residual value), as well as of the current condition of the asset for short-term improvements. The latter would require a more detailed consideration of the different maintenance measures at different times of the service life and for different superstructure types or boundary conditions. For instance, the maintenance costs differ widely if the superstructure of the section is equipped with wooden or concrete sleepers, since this results in different maintenance options and cycles.

The superstructure components merely play a subordinate role in the aggregation algorithm selected for the present work, which is based on the costs of renewal. This is partly because the renewal costs are affected by the expenses for materials installed in the future, and thus mostly correspond to a uniform standard. On the other hand, the relationship between sleeper and ballast installation as well as substructure improvement only changes marginally for different materials.

6.3.3 The track quality figure

The track quality figure from network-wide aggregation is generated as illustrated in Figure 87. The left-skewed distribution is also apparent when it comes to the overall condition, as was the case with the condition evaluations of the individual components. This is due to the inert characteristics of railway infrastructure, which may be explained by the standard deviation of the longitudinal level. This may take on values of up to 4.5 mm in extreme

cases, while the attention threshold [13848-5 2008 EN] for maintenance measures starts between 1.2 mm and 1.4 mm, depending on the track speed. Accordingly, the network-wide median value amounts to around 1.0 mm, meaning that a symmetrical distribution of values is impossible. The example of this quality signal may also serve to illustrate why achievement of the best possible condition of 100% is virtually impossible. Even immediately after the installation of a track system, a best-case standard deviation of the longitudinal level of 0.3 mm (median of 0.5 mm) can be achieved for ballasted track [Hansmann 2015]. This behaviour is due to certain tolerances of track materials (eg. straightness of rails, ballast granulation, loading capacity of the substructure); this behaviour is referred to as inherent track geometry [Rießberger 1997].

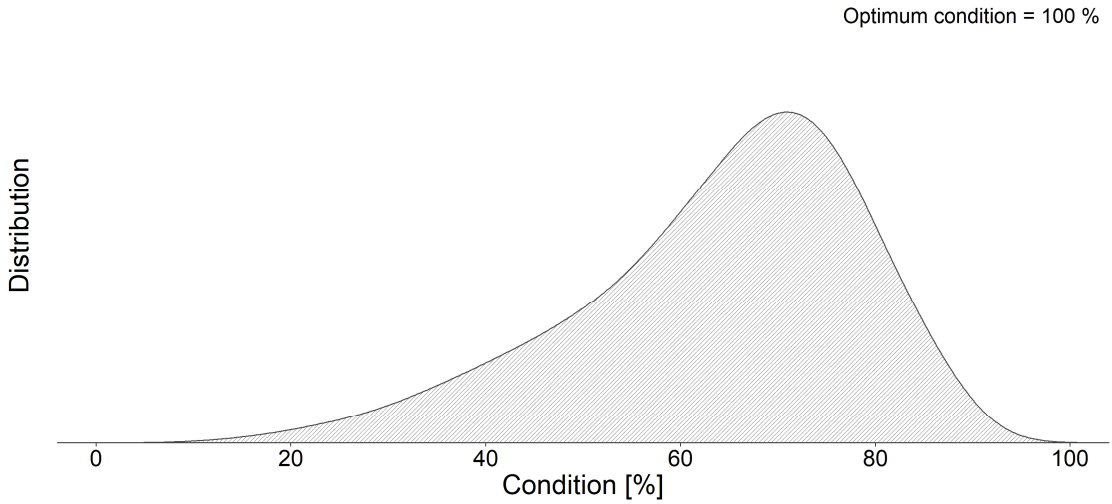

Figure 87 Track quality figure

This behaviour also applies to GPR and fractal analysis evaluation (see 4.1.3), as well as the standard deviation of the modified gauge (see 4.1.2.2). This aggregation permits quantification of the network-wide quality of the infrastructure (Figure 87). However, this raises the following question: Does this figure describe a good, a poor, or an appropriate network quality?

This question should be answered by an attempt to compare the distribution of the established track quality figure with the remaining service life on the basis of the standard elements. As previously explained, this is based on the fact that this quality figure describes the substantial condition of the asset. Accordingly, the figure should also correspond to or at least approximate the age distribution of the track network. An ageing network should thus show below-average condition. A network, however, where the average section has not yet reached 50% of its expected service life, should thus indicate an above-average condition. This comparison requires two measures to ensure meaningful comparability of

the datasets: First, sections that have already exceeded the strategic service life according to the standard element, which would thus have a negative residual life, are to be filtered from the dataset. Secondly, the distribution of the track quality figure must be modified, since 95% of the cross-sections are classified with a condition between 34% and 92% as a result of the previously discussed distribution characteristics. Accordingly, meaningful comparisons are not feasible with data approximating a normal distribution, as is the case with remaining service life. Therefore, the distribution of the track quality figure is stretched to a scale of 0% - 100%, based on the upper and lower whiskers.

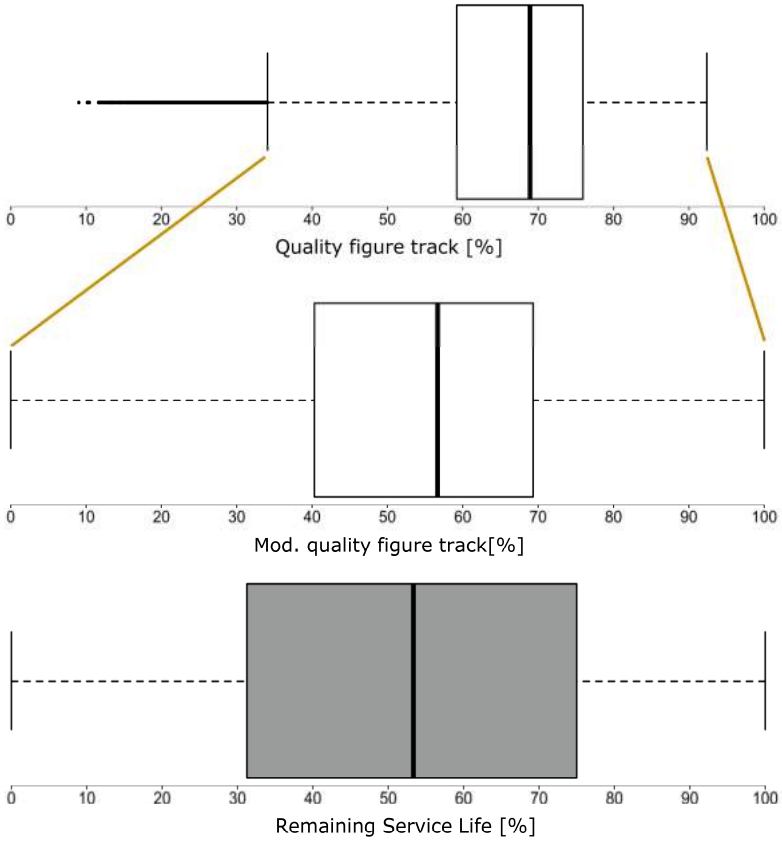

Figure 88 Strategic remaining service life and track quality figure

The modified (normalised) distribution shows that the remaining service life is subject to comparable distribution. In both cases, the resulting median amounts to a value between 50% and 60%. On the one hand, this means that the network under consideration (excluding ageing route cross-sections!) has a remaining service life of 54%. On the other hand, this indicates a slightly above-average quality of 56%. Consequently, the initially formulated question of whether the track quality figure describes the actual quality of the network as good, poor or appropriate, can be answered that the network-wide quality condition is as would be expected considering the age distribution, or even marginally better.

7

From Condition Evaluation to Asset Management

The International Union of Railways [UIC 2010] has defined "cost-optimised life-cycle decision-making for inspection, maintenance, renewals and improvement of assets" as the primary goal of asset management. Accordingly, detection of the system condition and planning of maintenance and renewal measures constitute two essential components of asset management. The corresponding plans always ought to be cost-optimised for the life-cycle, and thus under consideration of the cost required over the entire lifetime of the asset. All of these considerations must be made in the context of the budget available to the infrastructure manager. Accordingly, utilisation of available resources is to be optimised, and the right measures must be executed at the right time. However, even if the available budget is used efficiently, its size remains the limiting factor in many cases. This results in the following, slightly provocative question:-

"You have to ask yourself if you're going to adapt the budget to the network or the network to the budget." (Veit)

The latter, namely adaptation of the network or rather condition to the existing budget has already become a reality for many railway infrastructure managers, since available budgets are decreasing. Accordingly, operators are trying to avoid maintenance and renewal measures unless absolutely necessary for safety reasons. This degrades the network-wide condition of the infrastructure continuously, which results in the bulk of these "saved" renewal measures becoming necessary concurrently at a later date, entailing a delayed

increase in the reinvestment rate that is by then all the more necessary. Moreover, maintenance measures that were not performed in a timely manner have a negative effect on the service life of the track, causing an increase in the required reinvestment rates in the long term [Marschnig 2016]. On the other hand, the railway infrastructure manager may also elect to close certain (minor) routes, if the condition of the route is already poor, requiring a range of measures.

Adaptation of the budget to the network would naturally be the preferred solution from the perspective of the railway infrastructure manager; the desired condition of the present network would simply be defined, and the budget adapted accordingly. This approach, however, is largely dependent on the provider of funds. The possibility of implementation particularly depends on how well the infrastructure manager can demonstrate the necessity of the funding. For this purpose, the need for a similar or even larger budget to ensure adequate quality must be demonstrated based on the development of the network condition.

The condition evaluation established in this research was designed to determine the most efficient use of existing resources in terms of scale of renewals (see 7.2), as well as the representation of network, track or cross-section condition (see 7.1). One of the advantages of this methodology is in fact that this condition evaluation is cross-section specific. Consequently, all generated component conditions, as well as the track quality figure, can be calculated for the network, or a certain region, track, or route kilometre.

The evaluation of the network condition and the determination of renewal amounts should always be effected for a specific asset. Accordingly, the analyses presented in this chapter are performed on the basis of datasets that were previously filtered by valid lengths (see 2.2).

7.1 Network-wide condition evaluation

The presentation and interpretation of the network-wide asset condition can be conducted by means of different variants. The "single, perfect" variant does not exist; rather, all methods of determining the detected asset condition have both advantages and disadvantages. In this context, the choice of a methodology, and updating it annually, is of crucial importance. This ensures the viability of time series analysis, since the interpretation of the asset condition is based on the same methodology throughout. Regardless of the selected methodology, however, an objective and comprehensive condition evaluation must be established, as implemented in the scope of the present research.

Three possible approaches to representation, classification and interpretation of the network condition are discussed below. Two of them particularly consider the track age, and thus do not focus solely on current quality, but rather the quality that would be expected for the relevant age. A poor condition at the end of the service life would thus be weighted far more lightly than a similarly poor condition (in absolute terms) at the start of its service life.

7.1.1 Classification on the basis of age-specific distribution of values

A relatively simple method for classifying the network condition is a classification based on the age-specific distribution of values. This involves division into box plots of 25 million gross tons (MGT) per day and track each based on the cumulative load, which are used to generate values for the track quality figure for each range. Then, a deterioration curve of the upper whisker, the third quartile, the median, the first quartile and the lower whisker is calculated by linear regression. This permits a comparison of the quality of each cross-section with its specific cumulative gross tons against these deterioration curves. The linear time course of the median value describes the quality expected at the respective age. If it is above the median value, the quality is better than would be expected for the volume of cumulative gross tons. Accordingly, the cross-sections are divided into the classes A to E depending on quality (Figure 89).

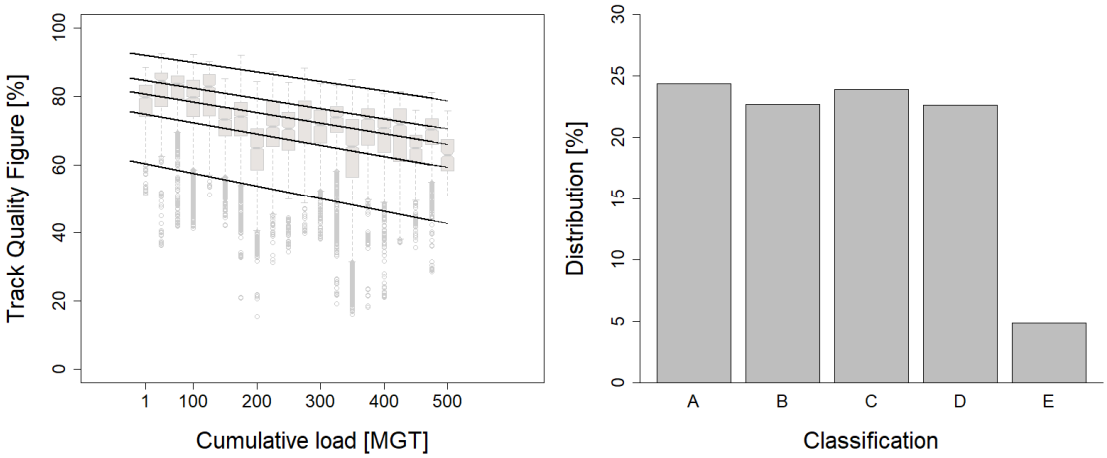

Figure 89 Classification on the basis of age-specific distribution of values

The quality of the individual cross-sections can be interpreted very well by way of this method, since it also permits representation of the effects of track age. For class A grading, a cross-section may exhibit a far poorer value of the track quality figure after 500 million

gross tons (MGT) per day and track than at the beginning of the service life. This corresponds to the considerations of the infrastructure operator, since a new asset is expected to be in perfect condition and exhaust the intended service life optimally.

The disadvantage of this system is in the interpretation of the classification (Figure 89, right). Due to the properties of a box plot, the classes are always distributed in the same way. This is particularly the case when recalibrating the stochastic boundary value definition for the classes for every input of current measurement data. Accordingly, this calibration could be performed once only, and to boundary values then defined as a fixed value. In this manner, the development of the classification over time would become apparent.

7.1.2 Condition classification

Another option for condition classification is the conversion of the cross-section specific track quality figure to a so-called track index. This code already takes into account the age of the asset by way of an age coefficient (K_{Age}), which is calculated by way of the quotient of the current cumulative load to the cumulative load at the end of the expected service life (Formula 10). This expected end of service life is based on the assumptions of the standard elements (see Figure 1). The age coefficient values may assume a range from zero to one, which also undergoes a linear change over the service life. Since the value range of the condition code primarily varies between 85% and 60%, the different deltas are converted using influencing factor C (Formula 10). This is made up of the absolute difference between the 95% quantile and the 5% quantile of the track quality figure.

$$\text{Track Index} = \frac{(Quality\ Figure_{Track} + C * K_{Age})}{1 + C}$$

$$K_{Age} = \frac{Cl_{cur}}{Cl_{EOL}}$$

$$Influence\ \text{Factor}\ C = abs(Quality\ Figure_{Track_{95}} - Quality\ Figure_{Track_5})$$

$\text{Quality Figure}_{\text{Track}}$	Established Track Quality Figure at each cross-section
$kumBel_{cur}$	*Cumulative load at current state*
Cl_{EOL}	*Cumulative load at the End of expected servife life*
$\text{Quality Figure}_{\text{Track 95\%}}$	*95% Quantile of net-wide Track Quality Figure*
$\text{Quality Figure}_{\text{Track 5\%}}$	*5% Quantile of net-wide Track Quality Figure*

Formula 10 Track index

This algorithm transposes the quality values for all cross-sections into a code corresponding to the age. Naturally, this distorts the actual condition of the cross-section, however, it does enable an age-independent comparison of all cross-sections. This is manifested by

the fact that the introduced track index is subject to virtually zero deterioration over time (Figure 90, right).

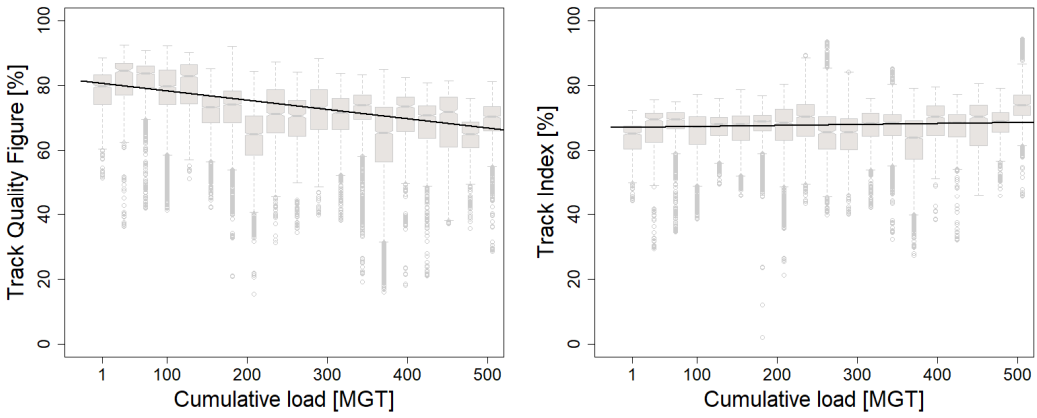

Figure 90 Transposition of infrastructure condition into track index

The inclusion of the effects of age now permits conversion of the track index into any grading or classification system. In choosing the classification scale, the aforementioned need for coherence is of primary importance. Once introduced, it must not be changed in any case, since the classifications would cease to be comparable. In the scope of the present work, an individual scale was formulated to demonstrate this methodology (Table 11).

Class	Percentage	Interpretation
A	100 – 79	Condition very good for the age
B	78 – 71	Condition good for the age
C	70 - 63	Condition corresponds to age
D	62 - 54	Condition poor for the age
E	53 - 0	Condition very poor for the age

Table 11 Custom classification of track index

However, this raises the question of which class railway infrastructure managers should actually strive to achieve. One would certainly be inclined to favour Class A, i.e. the best condition. However, it must be considered that shifting the bulk of the network-wide cross-sections to Class A would be extremely costly, in terms of both renewal and maintenance measures. In the light of limited budgetary possibilities, this approach is neither feasible nor sensible. As already explained, the asset management particularly entails using the available budget resources efficiently with a view to the life-cycle. Accordingly, as many maintenance activities as necessary are carried out, but also as few as possible. In this context, it would seem logical to aim for Class C, i.e. a "condition appropriate for the age".

This is particularly true when considering the definition for this class: Namely, very high initial quality of the components, which declines continuously until the end of their service life. This corresponds to the definition of an efficient use of available resources, and is also clearly the most prevalent class in the observed network (Figure 91).

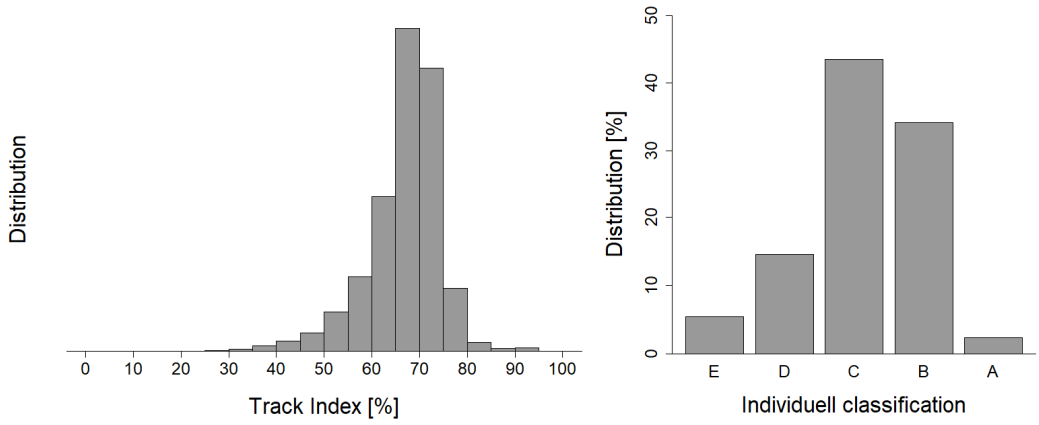

Figure 91 Distribution of track index; distribution for custom classification

However, this classification is always subject to a certain degree of subjectivity, particularly in the choice of class limits. This can be illustrated with reference to several examples, which are all based on the same dataset (Figure 91, left) as well as their own custom classification scales (Figure 91, right). For this purpose, the official school grading scales of Austria, Germany, Brazil, Great Britain, Estonia [Kultusministerkonferenz – Zentralstelle für ausländisches Bildungswesen 2016] and those of the United States [House of Representatives Florida 2001] are used as a basis. This demonstrates the variations that may arise due to different classification scales. The basic statement, namely that the peak of the frequency distribution tends to be at the centre of the classification scale, nonetheless applies to a certain extent for all systems.

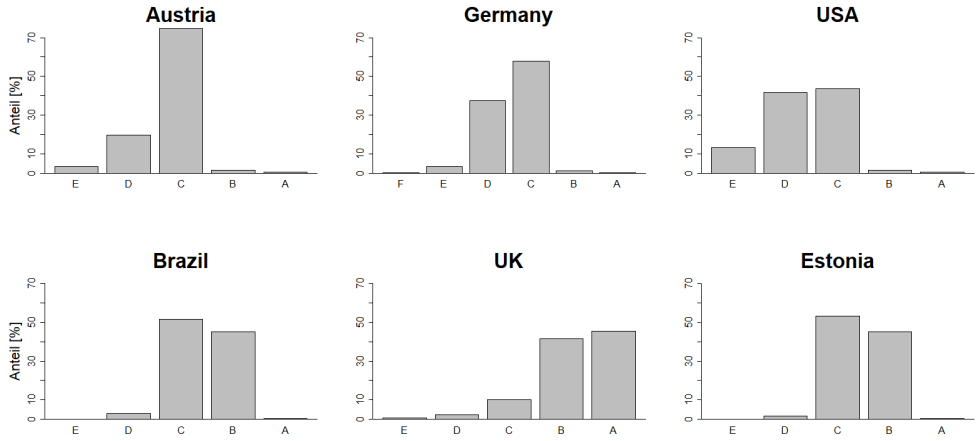

Figure 92 Classification based on school grading systems

This fact must be taken into account especially when conducting international comparisons between various infrastructure operators. This requires the creation of conversion tables (equivalent to the school system) to ensure comparability.

7.1.3 Mean value

The easiest solution is formation of the mean value of the various parameters. In the present example, the track quality figure (see 6.3.3), the track index (see 7.1.2), and the individual component status (see 6.2) were chosen (Figure 93). This is to provide the technical condition, while at the same time considering the asset age of the respective cross-sections by way of the track index.

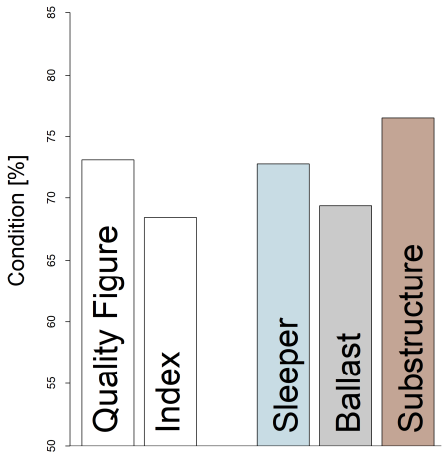

Figure 93 Network-wide condition; mean value

This application is as easy to understand as it is to implement, and the risk of errors in the scope of creation and updating are low; this ensures that the condition evaluations remain coherent and thus comparable.

7.2 Budget-relevant aspects

Infrastructure operators spend a significant part of their budget on asset renewal. The early and adequate assessment of renewal requirements thus plays a vital role. The following discussion is to determine whether or how the condition evaluation as established in the present work may describe current renewal requirements. The methodology, in turn, is applied to open track sections (filtered for valid lengths, see 2.2).

7.2.1 Estimating the scope of renewal

The identification of track cross-sections requiring renewal first requires an analysis of the condition in which renewals become necessary. Information from a long-term cooperation project between the ÖBB and the Institute of Railway Engineering and Transport Economy was sourced for this purpose. The Institute has evaluated a range of reinvestment projects once annually for a period of four years, and has calculated the optimum reinvestment from both a technical and economic point of view. Towards the end of the track service life, the condition deteriorates, requiring more frequent maintenance measures to ensure the minimum level of quality for the safe movement of trains. The goal is to establish the point where the cost savings from declining depreciation are equal to the cost increase due to maintenance requirements. This requires a definition of the maintenance work required to extend the service life of track. Maintenance requirements for coming years can thus be quantified, and the ideal point in time for the renewal of the railway infrastructure determined accordingly. The most significant and expensive maintenance measures are single sleeper replacements (ESW) and ballast bed cleaning (REI). These maintenance activities are identified in the scope of project evaluation based on all available data, the opinion of regional ÖBB managers, and track inspections. Moreover, detailed geotechnical investigations are conducted for the aforementioned reinvestment projects to determine the route sectors requiring substructure enhancement (USan). Based on this information, the component condition that requires renewal of the respective component can now be determined. The sections used for this study are listed in Table 12 below.

Planned measure	Number of sections	Total length
Single sleeper replacement (ESW)	47	13.11 km
Ballast bed cleaning (REI)	39	9.16 km
Substructure enhancement (USan)	10	3.22 km

Table 12 Sample planning of measures for identification of critical condition

Now, these sections are to be compared with the established condition evaluation. However, one fact should be borne in mind: The maintenance procedures formulated in the

scope of the project review were designed to ensure that the measure covers a plausible length of track (i.e. not too short). Accordingly, not all of the cross-sections within the maintenance sections required renewal. Rather, short sections in good condition may be present throughout these sections, which are also renewed for economic reasons and to promote a homogeneous track condition. For this reason, the first quartile, rather the median value, is the appropriate boundary value of the individual component condition evaluations. The outcome shows that renewals are to be carried out for all components in a condition of around 30% (Figure 94).

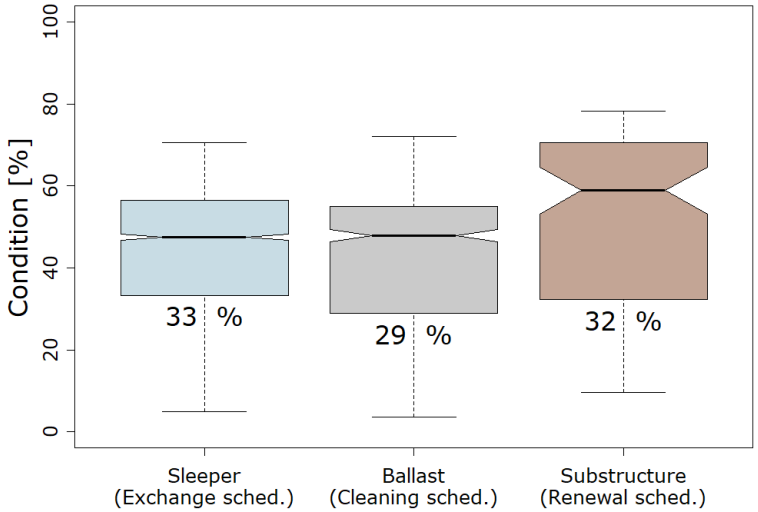

Figure 94 Determination of critical condition

The renewal requirements can now be calculated under consideration of the established boundary values. The results are illustrated by a scatter diagram showing the ballast condition on the ordinate and the sleeper condition on the abscissa (Figure 95, left), since both of these components constitute a direct trigger for track renewal. The individual cross-sections are thus represented in terms of their sleeper and ballast condition. Furthermore, critical substructure condition (< 32%) is illustrated by brown rectangles in a third dimension. It is readily apparent that there are individual cross-sections that are due for renewal either due to the sleeper condition (Area I) or due to the ballast condition (Area III). Naturally, there are also areas requiring renewal both due to the sleeper and the ballast (Area IV). The individual cross-sections due to substructure enhancement are clearly almost entirely in areas III and IV. These are the quadrants in need of ballast renewal. This seems plausible, and thus confirms the established methodology, since there is a very strong interaction between the components ballast and substructure. Technically, it is just about impossible for poor sleeper condition to occur in combination with poor substructure condition, while the ballast is in very good condition. This case may theoretically arise immediately after ballast cleaning, which would, however, not be sensible, since poor condition of the other two components would certainly suggest track renewal.

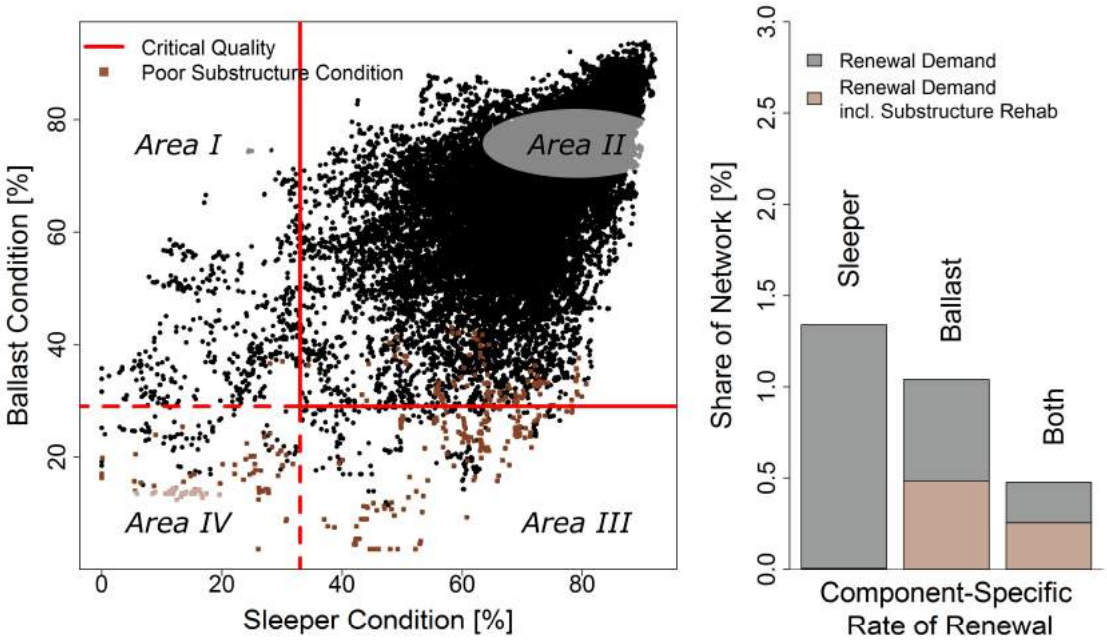

Figure 95 Estimating the scope of renewal

This analysis now permits determination of the overall renewal requirements according to the triggering components (Figure 95, right). In the reference network, around 2.7% of the individual cross-sections require renewal measures. This annual renewal rate would correspond to an average track service life of 37 years in this rail network. It should be considered that the TUG database (see 2.2) covers the Austrian main network, and thus does not include any secondary lines with light loads. The ratio of cross-sections requiring substructure enhancement (20%) corresponds to the prevailing conditions in Austria (see 3.2.3.1). It may thus be stated that the established methodology provides plausible results, and is apparently capable of detecting the actual condition of the infrastructure.

The issue of budget shortages and the increasing importance of efficient utilisation of existing resources has already been discussed in the present research project. Within the framework of the established methodology, gradation of boundary values may be employed as an additional aid to decision-making. This would permit identification of the worst sections requiring urgent renewal. For sections that are close to the critical condition (Figure 94), the renewal measure may possibly be delayed briefly.

7.2.2 Distribution to regions/routes

As mentioned above, the formulated methodology constitutes a cross-section specific condition evaluation, which can be applied to any segment of the route network. Accordingly, the methodology for determining the scope of renewal as presented in 7.2.1 may also be applied to individual routes or regions (Figure 96). This permits the identification of regions

that are in worse condition than the remainder of the respective network, thus requiring a greater scope of renewal. Naturally, this also applies to the required scope of substructure enhancement measures.

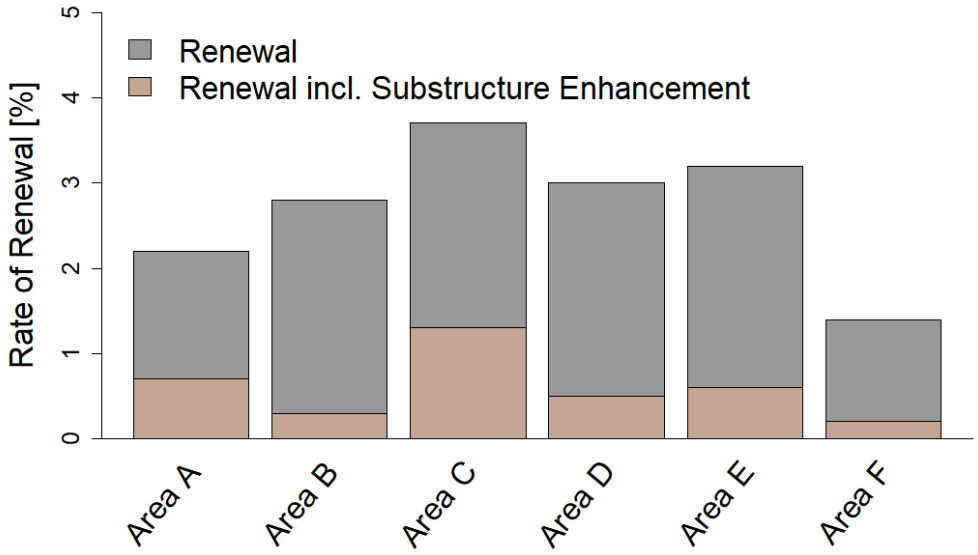

Figure 96 Example of region-specific distribution

The infrastructure operator can use this information to distribute the renewal budget appropriately to the different areas or routes on the network.

8

Summary and Outlook

This work presents a method for measurement-based, component-specific asset condition evaluation as a basis for sustainable asset management for railway infrastructure. The methodology was formulated for the assessment of individual track sections, as well as the condition of entire networks. The condition evaluation includes a range of specific parameters, which provide a highly detailed insight into the infrastructure condition. These parameters are then aggregated into a component-specific condition evaluation for sleeper, ballast and substructure, as well as a holistic track quality figure. The methodology thus permits a more detailed and thus more complex, or alternatively an overview condition evaluation, depending on the application.

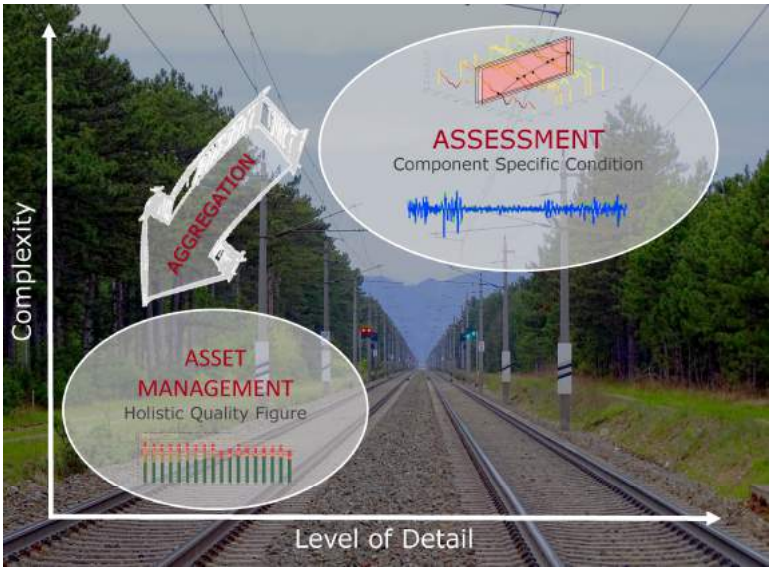

Furthermore, the findings show the benefits of the presented methodology for the asset management of a railway infrastructure manager. Firstly, this may take the form of a network-wide, regional, track or cross-section specific condition evaluation, which describes the past and future development of the network. Secondly, it also enables the formulation of component-specific maintenance and the scope of necessary renewal measures. The methodology also enables for distinguishing whether sleeper or ballast condition triggers track renewal. The substructure condition evaluation serves to identify the areas that require substructure enhancement as well as track renewal.

This methodology was developed by creating innovative indicators, which are derived from different measurement signals for improved interpretation of signal characteristics. At the same time, known measurement signals are analysed and processed further. All evaluation parameters are then subjected to a comprehensive validation process to check whether they are suitable for utilisation in component-specific condition evaluation.

In-depth correlation analysis between the various parameters is then conducted to identify how they could be aggregated into a component-specific condition evaluation.

The aggregation process takes place in two steps: First, the evaluation parameters are compiled into a component-specific condition for sleeper, ballast and substructure based on the results of the validation process and correlation analyses. Next, the track quality figure, which provides a comprehensive description of the holistic infrastructure condition, is derived from these component condition evaluations.

The developed methodology was thus validated adequately, and its contribution to infrastructure asset management was clearly demonstrated. In spite of answering raising questions in track asset management, the results also point to further research in this subject area, which should not remain unmentioned at this point.

One of the first further goals should be an amendment of the condition evaluation methodology to permit optional inclusion of GPR data. In the scope of the present work, it was decided to include this information in its entirety, since this increases the depth and certainty of the outcomes. However, the network length covered by the condition evaluation was thereby reduced, since the GPR data is not available for the entire route network. The sensitivity analysis, however, clearly demonstrated that formulation of a component-specific condition assessment for the entire network without the need for GPR data is clearly feasible. Depending on data availability, the future adaptation of the underlying algorithm should therefore be capable of generating an automated condition evaluation with or without GPR data to extend coverage to the entire route network.

Furthermore, it must be considered that the formulated evaluation methodology is structured in a cross-section specific manner. This constitutes an enormous advantage, since it enables description of the entire route network, any route segments, or even a single cross-section. The resulting scope of renewal accordingly relates to segments that were compiled by the purely technical sequence of individual cross-sections which have already reached a critical condition. However, this does not imply that these segments automatically result in a economic viable section for improvement works. Currently, the determination of work sections takes place mostly on a manual to semi-automatic basis in the course of the project. However, it would be conceivable and useful to develop a methodology that converts segments requiring renewal or maintenance into economically sensible work sections on an automated basis.

In science, there's no reaching of goals.
In science, there are only milestones. (according to Henning M. Beier)

Bibliography

Audley, M. & Andrews, J.D. 2013, *The effects of tamping on railway track geometry degradation,* Journal of Rail and Rapid Transit, 227, no. 4, pp. 379-391.

Auer, F. 2014, Berührungslos arbeitende Gleismessfahrzeuge und Auswertung der Messdaten [Non-contact track measurement vehicles and analysis of measurement data], Eisenbahn Ingenieur Kalender EIK, pp. 53-66.

Auer, F. 2010, Zur Verschleißreduktion von Gleisen in engen Bögen, Technische Universität Graz [On wear mitigation of tracks in tight curves].

Auer, F. 2004, Gleislagequalitätsanalyse zur Instandhaltungsoptimierung [Track quality analysis for maintenance optimisation], ETR Eisenbahntechnische Rundschau, no. 01, pp. 838-844.

Auer, F., Zuzic, M., Schilder, R. & Breymann, H. 2007, 13 Jahre Erfahrung mit gleisgebundener Untergrundsanierung im Netz der ÖBB [13 years of experience with track-bound substructure enhancement in the ÖBB network], Eisenbahntechnische Rundschau, no. 12, pp. 817-827.

Balfour Beatty Rail 2010, Service Anlagenmanagement [Asset management services], Balfour Beatty Rail GmbH, Germany.

Berawi, A., Delgado, R., Calçada, R. & Vale, C. 2010, *Evaluating track geometrical quality through different Methodologies,* International Journal of Technology, no. 1, pp. 38-47.

Berghold, A. 2016, Wirkungsweise von unterschiedlichen Gleisschotterarten mit und ohne Schwellenbesohlung [Mode of action of different ballast types with and without sleeper pads], ZEVRail, 140, no. 1-2, pp. 45-52.

Bundesministerium für Wissenschaft und Verkehr 1971-2001, Eisenbahn- und Seilbahnstatistik [Rail and cableway statistics], Austria, Vienna.

Clark, M., Gillespie, R., Kemp, T., McCann, D. & Forde, M. 2001, *Electromagnetic properties of railway ballast,* NDT & E International, 34, no. 5, pp. 305-311.

Daniels, D.J., Gunton, D.J. & Scott, H.F. 1988, *Introduction to subsurface radar,* Radar and Signal Processing, IEEE Proceedings F, 135, no. 4, pp. 278-320.

De Bold, R. 2011, *Non-Destructive Evaluation of Railway Trackbed Ballast*, University of Edinburgh.

EN 13848-1 2009, Bahnanwendungen, Oberbau - Qualität der Gleisgeometrie, Teil 1: Beschreibung der Gleisgeometrie [Railway applications, superstructure - Track geometry quality, Part 1: Description of track geometry], ÖNORM, Österreichisches Normungsinstitut, 1020, Vienna.

EN 13848-2 2004, Bahnanwendungen, Oberbau - Qualität der Gleisgeometrie, Teil 2: Messgeräte - Gleismessfahrzeuge [Railway applications, superstructure - Track geometry quality, Part 2: Measurement devices - Track geometry vehicles], ÖNORM, Österreichisches Normungsinstitut, 1020, Vienna.

EN 13848-5 2008, Bahnanwendungen, Oberbau - Qualität der Gleisgeometrie, Teil 5: Geometrische Qualitätsstufen [Railway applications, superstructure - Track geometry quality, Part 5: Geometric quality levels], ÖNORM, Österreichisches Normungsinstitut, 1020, Vienna.

EN 13848-6 2014, Bahnanwendungen, Oberbau - Qualität der Gleisgeometrie, Teil 6: Charakterisierung der geometrischen Gleislagequalität [Railway applications, superstructure - Track geometry quality, Part 6: Characterisation of track geometry quality], ÖNORM, Österreichisches Normungsinstitut, 1020, Vienna.

ENV 13005 1999, Leitfaden zur Angabe der Unsicherheiten beim Messen [Guide to the statement of measurement uncertainty], ÖNORM, Österreichisches Normungsinstitut, 1020, Vienna.

Enzi, M. 2011, Optimaler Re-Investitionszeitpunkt für den Oberbau von Streckenabschnitten [Optimum timing of reinvestments in the superstructure of route sections], Technische Universität Graz.

Eriksen, A., Venables, B., Gascoyne, J. & Bandyopadhyay, S. 2006, *Benefits of high speed GPR to manage trackbed assets and renewal strategies,* PWI Conference, Brisbane, 19th June.

Esveld, C. 2001, *Modern Railway Track,* 2nd MRT-Productions, Netherlands.

Fahrmeir, L., Künstler, R., Pigeot, I. & Tutz, G. 2007, Statistik [Statistics], 7th Springer, Heidelberg.

Freudenstein, S., Iliev, D. & Ahmad, N. 2011, Die Kontaktspannung zwischen elastisch besohlten Schwellen und Schotter [Contact stress between elastically sleeper pads and ballast], ETR Eisenbahntechnische Rundschau, no. 05, pp. 13-20.

Gallagher, G., Leiper, Q. & Forde, M. 2000, *Ballast Evaluation using Ground-Penetrating-Radar,* Railway Gazette International, 02, pp. 101-102.

Hansmann, F. 2015, Innovative Data Analysis a contribution to sustainable railway asset management, TU Graz.

Hansmann, F. & Landgraf, M. 2013, Wie fraktal ist die Eisenbahn? [How fractal are railways?] ZEVRail, 137, no. 11-12, pp. 462-470.

Holzfeind, J. & Hummitzsch, R. 2008, Qualitätsverhalten von Gleisen [Quality behaviour of tracks], ZEVRail, Glasers Annalen 132, no. 6-7, pp. 212-224.

Holzfeind, J. 2009, Zur Prognostizierbarkeit des Qualitätsverhaltens von Gleisen - Analyse des Qualitätsverhaltens am Einzelquerschnitt [On the predictability of the quality behaviour of tracks - analysis of the quality behaviour based on individual cross-sections], Technische Universität Graz.

House of Representatives Florida, [Online]*, High School Grading Scale - Fact Sheet*. Available: [2016, 17.05.].

Hummitzsch, R. 2009, Zur Prognostizierbarkeit des Qualitätsverhaltens von Gleisen - Statistische Analyse des Gleisverhaltens zur Erstellung eines Prognosemodells [On

the predictability of the quality behaviour of tracks - statistical analysis of the track behaviour for a prognostic model], Technische Universität Graz.

Hyslip, J. 2002, *Fractal Analysis of Geometry Data for railway track condition assessment*, University of Massachusetts.

Hyslip, J. & Vallejo, L. 1997, *Fractal analysis of the roughness and size distribution of granular materials,* Engineering Geology, 48, pp. 231-244.

Kohler, M. 2002, Der Bettungsmodul für den Schotteroberbau von Meterspurbahnen [Bedding modulus for ballasted track of metre gauge railways], Eidgenössische Technische Hochschule Zürich.

Koppe, P. & Stozek, A. 1999, Kommunales Abwasser [Municipal waste water], 4th Vulkanverlag, Essen.

Auswärtiges Amt, Germany, [Online], anabin - Infoportal zu ausländischen Bildungsabschlüssen [Infoportal for foreign qualifications]. Available: http://anabin.kmk.org/no_cache/bildungswesen.html [2016, 17.05].

Landgraf, M. 2015, *From track data to asset management,* European Railway Review, 21, no. 2, pp. 58-61.

Landgraf, M., Hansmann, F., Marschnig, S. & Veit, P. 2014, *Track Geometry and Substructure - a Provable Correlation?* ACTGEORAIL 14, ed. Librairie Ifsttar, 978-2-7208-2621-4, Paris, 07.11.2014.

Lunne, T., Robertson, P.K. & Powell, J.J.M. 1997, *Cone Penetration Testing in Geotechnical Practice,* E & FN Spon, New York.

Luomala, H., Peltokangas, O. & Nurmikolu, A. 2014, *Stiffmaster - a continuous Track Stiffness Measurement Device,* ACTGEORAIL 14, ed. Librairie Ifsttar, Paris, 07.11.2014.

Madejski, J. & Grabczyk, J. 2002, *Continuous geometry measurement for diagnostics of tracks and switches,* Delft University of Technology, Netherlands.

Mandelbrot, B. 1967, *How long is the coast of Britain?* Science, 156, pp. 636-638.

Marschnig, S. 2016, iTAC - innovative Track Access Charges, Postdoctoral Thesis, Technische Universität Graz, Graz.

Niessen, J. 2005, Einsatz des GeoRail-Verfahrens [Application of the GeoRail process], Eisenbahningenieur, 56, no. 8, pp. 48-53.

ÖBB Holding AG 2016 Annual Report 2007-2015, Vienna.

ÖBB Infrastruktur AG 2015, Annual Report 2014, Vienna.

ÖBB-Infrastruktur AG 2014, Regelwerk 09.02 – Tragschichten, Gestaltung der Randbereiche einschließlich Kabeltroganlagen [Rulebook 09.02 - Formation layers, design of the peripheral areas including cable trays], Vienna.

Oberweiler, G. 1987, Vom Gleisrevisionswagen zur Oberbau-Meßwageneinheit (OMWE) [From track revision vehicles to the superstructure measurement unit], Eisenbahntechnische Rundschau ETR, 36, no. 01+02, pp. 73-79.

Olhoeft, G.R. 2000, *Maximizing the Information Return from Ground Penetrating Radar,* Journal of Applied Geophysics, 43, no. 2, pp. 175-187.

Piazolo, M. 2011, Statistik für Wirtschaftswissenschaftler: Daten sinnvoll aufbereiten, analysieren und interpretieren [Statistics for Economists: Practical preparation, analysis and interpretation of data, 2nd Verlag Versicherungswirtschaft GmbH, Karlsruhe.

Rießberger, K. 1997, Gleisgeometrie und Wirtschaftlichkeit - oder - wie gut muss ein Gleis sein? [Track geometry and economics - or - how good does a track really have to be?] Österreichische Verkehrswissenschaftliche Gemeinschaft, Graz.

Rießberger, K. 1975, Das Verhalten der Meß- und Fehlerverkleinerungssysteme der Gleisbaumaschinen in periodischen Gleisfehlern bei Arbeiten im Ausgleichsverfahren [The behaviour of measurement and error reduction systems of track-laying machines in periodic track errors when working on the compensation process], Eisenbahntechnische Rundschau ETR, 24, no. 11, pp. 417-424.

Roberts, R. & Rudy, J. 2006, *Railroad ballast fouling detection using ground penetrating radar: A new approach based on scattering from voids,* ECNDT 2006–Th.4.5, 1,.

Röhsler, M. Annual Report 2005 - 2013, Schienen-Control GmbH, Vienna.

Schilder, R. & Piereder, F. 2000, Planumsverbesserung mit der Aushubmaschine AHM 800-R [Substructure remediatio with the excavating machine AHM 800-R], Eisenbahntechnische Rundschau ETR, 49, no. 9, pp. 577-586.

Schilder, R. Übergangskonstruktionen Feste Fahrbahn - Schotter: Neue Entwicklungen [Transition zones slab track - ballast: New developments], Paper presented at the lecture "superstructure", Technische Universität Graz, 2013, Graz.

Schramm, G. 1967, Fortschritte in der Gleismessung [Advances in track measurement], Eisenbahntechnische Rundschau ETR, no. 4, pp. 124-127.

Schultheiß, H. & Schulz, G. 1985, Schwellen für die Deutsche Bundesbahn [Sleepers for the German railways], Eisenbahntechnische Rundschau, no. 10, pp. 723-728.

Soldati, G. Den Geheimnissen der Einsenkung auf der Spur [Uncovering the secrets of track subsidence], Paper presented at the Annual Meeting, Interessensgemeinschaft Unterbau, 2013, Bern.

Sussmann, T.R., Selig, E.T. & Hyslip, J.P. 2003, *Railway Track Condition Indicators from Ground Penetrating Radar,* NDT & E International, 36, no. 3, pp. 157-167.

UIC 2010, *Guidelines for the Application of Asset Management in Railway Infrastructure Organisations*, International Union of Railways, Paris.

Veit, P. 2006, Qualität im Gleis - Luxus oder Notwendigkeit [Track quality - luxury or necessity], Eisenbahningenieur EI, 57, no. 12, pp. 32-37.

Veit, P. 2002, *Infrastructure Maintenance Strategies,* Rail International, no. 6, pp. 2-10.

Vidovic, I. 2016, Das Gleislageverhalten nach Einbau einer Tragschicht [Track geometry behaviour after installation of a formation layer], Technische Universität Graz.

Wolter, U., Neubert, J. & Erhard, F. 2013, Inspektion der Gleislage nach der EN 13848 mit Sehnenmessverfahren [Inspection of track position according to EN 13848 with the chord measurement method], Eisenbahntechnische Rundschau ETR, no. 1+2, pp. 28-30.

Monographic Series TU Graz

Railway Research

Vol. 1 Stefan Marschnig

iTAC – innovative Track Access Charges
2016
ISBN 978-3-85125-493-8

Vol. 2 Fabian Hansmann

The Missing Link between Asset Data and Asset Management
2018
ISBN 978-3-85125-567-6

Vol. 3 Matthias Landgraf

Smart data for sustainable Railway Asset Management
2018
ISBN 978-3-85125-569-0